STUDIES TOWARD THE SYNTHESIS OF NOVEL 1,4-OXAZEPAN-5-ONE AND COUMARIN DERIVATIVES

A Thesis Submitted to
the Graduate School of Engineering and Sciences of
İzmir Institute of Technology
in Partial Fulfillment of the Requirements for the Degree of

DOCTOR OF PHILOSOPHY

in Chemistry

by
Tuğçe AKBAŞ

December 2022
İZMİR

ACKNOWLEDGEMENTS

First of all I would like to express my appreciation to Prof. Dr. Ali Çağır for giving me the great opportunity to carry out my graduate study in his research laboratory, for his encouragement, patient, endless attention, and scientific guidance throughout this study. It was an invaluable experience for me to work with him.

I would also like to express my appreciations to my thesis committee, Prof. Dr. Yeşim Gül Salman and Assoc.Prof. Ümit Hakan Yıldız for their kindly help and advice. Besides this, I would also like to thank to my examining committee members, Prof. Dr. Canan Varlıklı and Prof. Dr. Yurdanur Akgül for accepting to evaluate my thesis and their valuable suggestions.

I would also like to thank to Scientific and Technical Research Council of Turkey for financial support for this project (116Z591 and 119Z096). Next, I would like to thank my labmates Fikrican Dilek, Hülya Bozoğlu, Ezgi Vural, Mustafa Erdoğmuş, Başak Çetin for their invaluable help and kind mess in the laboratory.

I am grateful to my sister in IYTE, Derya Mete my biggest chance in life, Nehir Nalıncı Barbak, Erman Kıbrıs and C301 family for their good friendship, encouragements, and constructive comments.

My special thanks go to my mother Minever Kanbur, my father Sebahattin Kanbur, my sister Büşra Kanbur, and my husband Emre Akbaş. They provided the greatest support in my education life, who never spared their love and support and always encouraged me. It would not have happened without them.

ABSTRACT

STUDIES TOWARD THE SYNTHESIS OF NOVEL 1,4-OXAZEPAN-5-ONE AND COUMARIN DERIVATIVES

In this study it is aimed to synthesize potential novel MDM2 inhibitor which has 1,4-oxazepan-5-one skeleton. For this purpose (R)-(4-chlorophenyl)glycine was used as a starting material. Reduction of that with $LiAlH_4$ and the protection of amine by Trt group was performed. After oxidation to aldehyde, direct or stepwise installation of glutaconic to the structure by either Michael type addition or coupling with amine by using HATU was quite problematic and all attempts were failed toward the preparation of this skeleton.

Besides, synthesis of 1,4-oxazepan-5-one was also tried starting from chiral aminoalcohol and protected 5-hydroxy-2-pentanoic acid in two steps, first coupling then oxa-Michael addition. However this did not work well too. It seems that presence of activated methylene group might be the main problem in the addition of glutaconic acid reactions.

In the second part of this thesis it was aimed to synthesize the 1,2,3-triazole substituted coumarin in order to investigate the potential antiproliferative properties of these over cancer cells. Acetylsalicilic acid was used as starting material in these syntheses. That was transformed 4-acetylene substituted coumarin derivatives as key intermediates then their transformations to corresponding final products was performed by click chemistry.

ÖZET

YENİ 1,4-OKSAZEPAN-5-ON VE KUMARİN TÜREVLERİNİN SENTEZİNE YÖNELİK ÇALIŞMALAR

Bu çalışmada 1,4-oksazepan-5-on iskeletine sahip potansiyel yeni MDM2 inhibitörünün sentezlenmesi amaçlanmıştır. Bu amaçla başlangıç maddesi olarak (R)-(4-klorofenil)glisin kullanılmıştır. Bunun $LiAlH_4$ ile indirgenmesi ve aminin Trt grubu ile korunması hedeflenmiştir. Aldehite oksidasyondan sonra, glutakonik asitin yapıya doğrudan veya kademeli olarak, Michael tipi ekleme veya HATU kullanılarak amin ile birleştirilmesi amaçlanmıştır. Ancak bu tepkime oldukça sorunlu gerçekleşmiş ve bu iskeletin hazırlanmasına yönelik tüm girişimler başarısız olmuştur.

Ayrıca kiral aminoalkol ve korumalı 5-hidroksi-2-pentanoik asitten başlanarak önce kupling sonra oksa-Michael ilavesi olmak üzere iki aşamada 1,4-oksazepan-5-on sentezi de denenmiştir. Ancak bu da iyi çalışmamıştır. Glutakonik asit reaksiyonlarının eklenmesinde aktif metilen grubu varlığı ana problem gibi görünmektedir.

Bu tezin ikinci bölümünde, çeşitli 1,2,3-triazol ikameli kumarinin sentezlenmesi ve kanser hücreleri üzerinde potansiyel antiproliferatif özelliklerinin araştırılması amaçlanmıştır. Bu sentezlerde başlangıç maddesi olarak asetilsalisilik asit kullanılmıştır. Anahtar ara ürünler olarak 4-asetilen ikameli kumarin türevlerine dönüştürülmüş ve ardından bunların karşılık gelen ürünlere dönüşümleri amaçlanmıştır.

TABLE OF CONTENTS

LIST OF FIGURES

Figure **Page**

Figure **Page**

LIST OF TABLES

Table **Page**

ABBREVIATIONS

d	Doublet
dd	Doublet of doublets
dt	Doublet of triplets
ddd	Doublet of doublet of doublets
m	Multiplet
δ	Chemical shif
Hz	Hertz
DMP	Dess-Martin periodinane
DCM	Dichloromethane
DMF	Dimethylformamide
THF	Tetrahydrofuran
Et_3N	Triethylamine
Eq.	Equivalent
HATU	Hexafluorophosphate azabenzotriazole tetramethyl uronium
TMSCI	Trimethylsilylchloride
Boc	Tert-butyloxycarbonyl
Trt	Trityl
mL	Mililiter
mg	Milligram
g	Gram
μM	Micromolar

CHAPTER 1

INTRODUCTION

1.1.P53 - MDM2 Pathway and Cancer

p53 is a short-lived transcription factor that plays an important role in preventing the production of tumors. Activated p53 binds to DNA and enhances the transcription of many genes involved in cell cycle arrest, DNA repair, senescence, and apoptosis (Wade, Li, and Wahl 2013). Consequently, loss of p53 activity in tumor cells provides a significant selective growth advantage, and it has been suggested that failure in the p53 pathway may be a necessary stage in the progression of tumors. Multiple studies have shown that a lack of p53 activity relates to the growth of tumors. In addition, restoring endogenous p53 function in established tumors resulted in tumor regression in vivo and may be an useful anti-cancer therapy strategy. (Shinohara and Uesugi 2007).

Approximately fifty percent of human malignancies contain p53 mutations that render it ineffective. In the remaining 50% of malignancies, the wild-type p53 is inhibited by the MDM2 (human murine double minute 2) oncoprotein through a direct protein-protein interaction (Ding et al. 2013) . Due to the fact that MDM2 is primarily responsible for the suppression of p53's tumor suppressor function and directly antagonizes p53 through their contact. Blocking the protein-protein connection between MDM2 and p53 would release p53 from MDM2, restoring the tumor suppressor function of wild-type p53 (Graves et al. 2012). Agents designed to inhibit the interaction between MDM2 and p53 may have therapeutic potential for the treatment of human malignancies with wild-type p53 (H. Wang and Yan 2011).

MDM2 suppresses p53 function by preventing p53-mediated transactivation, inducing nuclear export of p53, and acting as an E3 ubiquitin ligase that targets both itself and p53 for proteasomal degradation (Hsieh et al. 1999). Since all of these pathways can be blocked by blocking the MDM2-p53 interaction, disruption of the protein-protein interaction with small molecule MDM2 inhibitors has been regarded a promising strategy for reactivating the p53 pathway in wild-type p53 malignancies

for the past two decades. Several studies with small molecule MDM2 inhibitors have demonstrated inhibition of tumor growth in vitro and in vivo, and several small compounds have recently entered clinical trials (Figure 1.1).

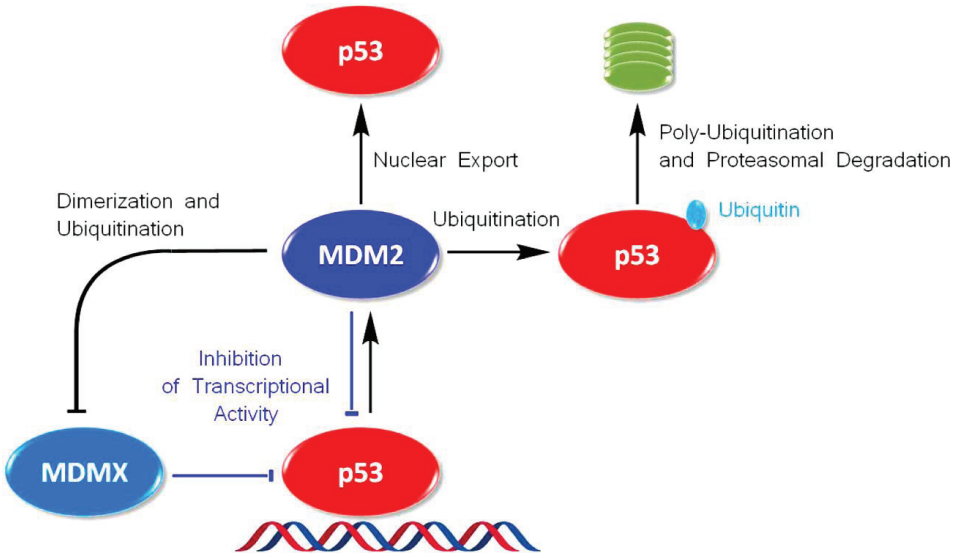

Figure 1.1. Inhibition of p53 by MDM2 and MDMX (Source:Wang, 2020).

The interaction between MDM2 and p53 has been localized to the first 120 N-terminal amino acids of MDM2 and the first 30 N-terminal amino acids of p53. As depicted in Figure 1.2, the cocrystal structure reveals that the MDM2-bound p53 peptide adopts a -helical conformation and interacts with MDM2 primarily via three hydrophobic residues, Phe19, Trp23, and Leu26 (Shaomeng Wang et al. 2017). This hydrophobic region enables the development of small, non-peptide-based molecules to reactivate the p53 protein. Due to their inability to permeate through the cell membrane, it has been discovered that peptide-based drugs are ineffective (Graves et al. 2012).

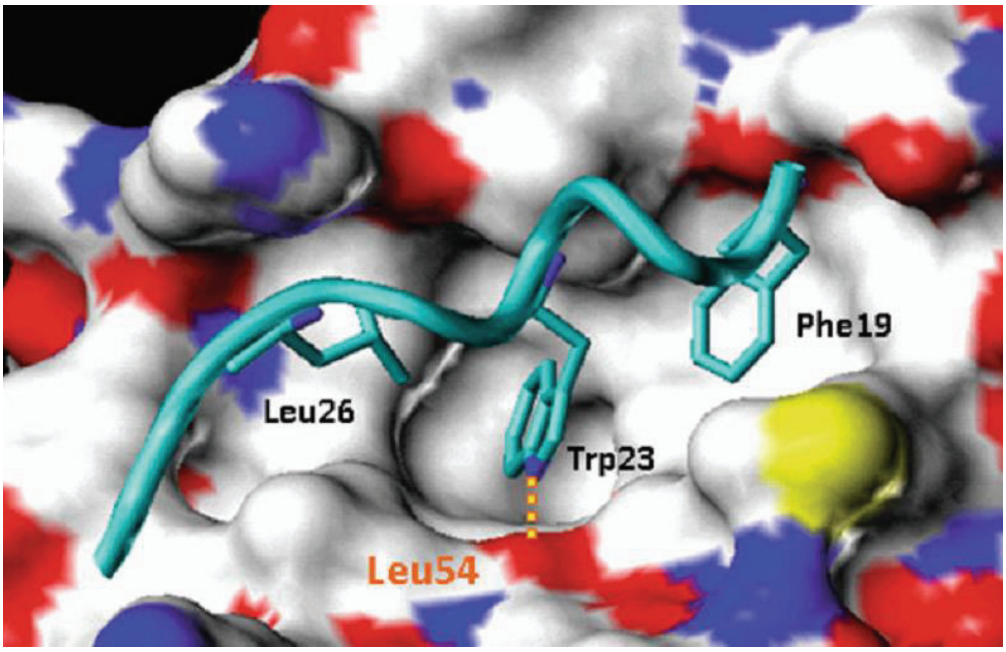

Figure 1.2. Crystal structure of MDM2 bound to p53 (Source: Wang, 2020)

1.2.P53-MDM2 inhibitors as anticancer agents

1.2.1.Chalcone derivatives

Chalcones are natural products with a common chemical scaffold of 1,3-difesilli-2-propen-1-one. These natural products are common in plants as pioneers of flavonoid classes. Natural departures attracted the attention of the science community due to their wide and effective biological activities. They have anticancer, cancer advantageous, anti-inflammatory, antidiabetic, antioxidant, antimicrobial and neuroprotective activates properties (Luthar, Cicchetti, and Becker 2000).

Isoliquiritigenin 1 was the first naturally occurring chalcone reported to induce cell cycle arrest and apoptosis in cancer cell lines, potentially through the interference with p53 pathway. When A549 cells (Human non-small cell lung cancer) were treated with 20 μM isoliquiritigenin (1), more than 46% of the cells were arrested in G1 phase, and this percentage increased to 60% when treated with 40 μM isoliquiritigenin (1) (Moreira et al. 2021).

When human non-small cell lung cancer A549 cells were treated with 20 μM isoliquiritigenin (1), over 46% of cells were arrested in G1 phase, with this

percentage increased to 60% with 40 μM of compoud 1. A more recent study published by Kim et al. showed that isoliquiritigenin (1) produces ROS in human renal carcinoma Caki cells. This production of Ros stabilized and activated p53, increasing its levels. In addition to that, it downregulated MDM2, which contributed to the increased expression of p53 (Kim et al. 2017).

Isolespeol (2) is a natural prenylated chalcone and has been isolated by Fang et al. It is obtained from the leaves of Artocarpus communis (a plant grown in tropical and subtropical regions). We reported that Isolespeol (2) showed a promising in vitro growth inhibitory effect in human liposarcoma SW 872 cancer cells, showing an IC of 3.8 μM, and this effect was associated with increased p53 levels at 3 μM after 3 hours of treatment. In addition, isolespeol (2) induced apoptosis in SW872 cells via Fas and mitochondria-mediated pathways (Fang et al. 2008).

Treatment of lung adenocarcinoma A549 cells with prenylated chalcone xanthohumol (3) induction of apoptotic cell death and G1 cell cycle arrest was achieved by treatment of lung adenocarcinoma A549 cells with prenylated chalcone xanthohumol. Induction of apoptotic cell death and G1 cell cycle arrest was achieved by treatment of lung adenocarcinoma A549 cells with prenylated chalcone xanthohumol (3). Induction of apoptosis was associated with activation of caspase-3, while upregulation of key cell cycle regulators p53 and p21, as well as downregulation of cyclin D1 (Sławińska-Brych et al. 2016).

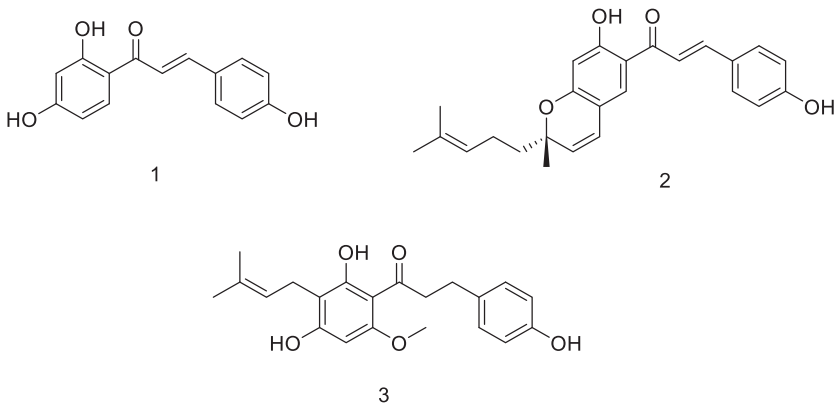

Figure 1.3. Small molecules of MDM2 inhibitors

1.2.2.Imidazole derivatives

In the past few decades, numerous classes of drugs candidates that inhibit the interaction between p53 and MDM2 have been discovered. Among these nultins, also known as 2,4,5-triphenyl imidazoline derivatives, are a class of anti-proliferative drug candidates aimed for the inhibition of p53–MDM2 interaction. The Nutlins were discovered to be the first potent and selective small molecule antagonists of the p53–MDM2 interaction (Klein and Vassilev 2004).

In cancer cells, stimulation of the p53 pathway resulted in cell cycle arrest in the G1 and G2 phases and caspase-dependent death. Nutlins displayed great selectivity for the interaction between p53 and MDM2. Their antitumor impact was detected only in cells with wild-type p53, but not in cells with mutant or deleted p53, indicating that Nutlin activity is derived from p53 pathway activation. Excitingly, it appears that occupation of the p53-binding pocket on MDM2 by the Nutlins is sufficient to disrupt the complex of full-length p53 and MDM2 in vitro and in vivo, independent of the recently proposed additional interaction site between the two proteins.

Nutlin-2 compounds with the p53 binding site via exploiting hydrophobic contacts on MDM2. Nutlin-3a powerful chemical, has shown potential in vitro and in vivo bioactivity. It can bind to MDM2 in the p53-binding pockets and reactivate the p53 pathway in cancer cells, causing cell cycle arrest, death, and growth suppression in nude mice bearing human tumor xenografts (Hu et al. 2011).

Nutlin-3 inhibits the formation of tumors in 90% of mouse models, according to studies. Roche has conducted Nutlines optimization experiments. Among the compounds optimized as a result of these investigations is RG7112, which has an IC_{50} of 18 nM. Additionally, clinical trials for this medication were initiated . (Figure 1.4) (Vu et al. 2013).

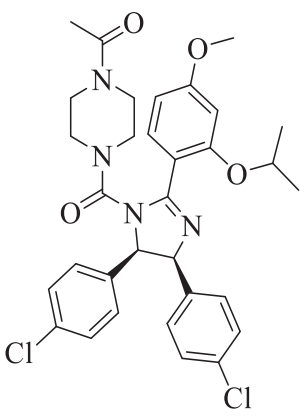

4
Nutlin-1

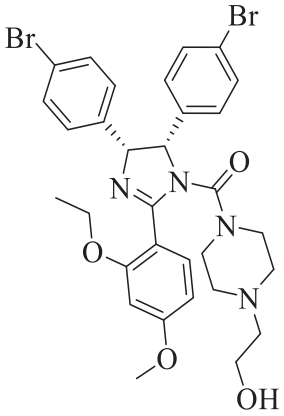

5
Nutlin-2

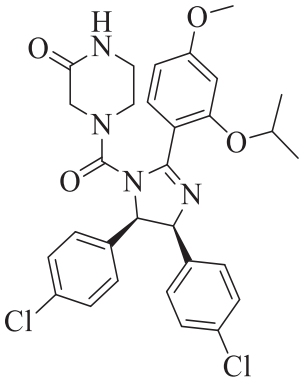

6
Nutlin-3

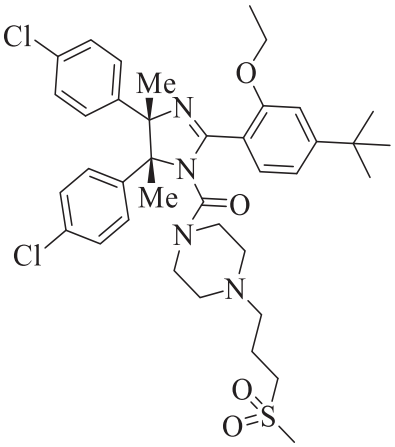

7
RG7112

Figure 1.4. Imidazol based small molecules of MDM2 inhibitors

1.2.3.Piperidinone derivatives

Compound 10, discovered and developed by Amgen, entered phase I clinical trials for the treatment of human cancer in 2012. This compound was obtained through structure-based design and extensive optimization of a new class of MDM2 inhibitors containing piperidin-2-one. The piperidinone-containing compound 8 was designed as an MDM2 inhibitor based upon a structural analysis of known MDM2 inhibitors. Compound 8 inhibits MDM2 with IC_{50} = 34 nM and served as an excellent lead compound for further optimization.

Upon the basis of the NMR and cocrystal structures of 8 or its analogues complexed with MDM2 furtheroptimization of two sites of compound 8 yielded compound 9 (AM 8553), which has an IC_{50} value of 1.1 nM against MDM2 (Kd = 0.4 nM to MDM2). Compound 9 effectively activates wild-type p53 in vitro and in vivo and dose-dependently inhibits tumor growth in the SJSA-1 xenograft model in mice. At 150 and 200 mg/kg daily oral dosing for 2 weeks, it achieves partial tumor regression (27%) after 2 weeks of treatment (Rew et al. 2012). It was further optimized for potency, pharmacokinetic properties, and in vivo efficacy. This yielded a series of potent and orally active MDM2 inhibitors including 10, whereas the latter was selected for clinical development.

Compound 10 binds to MDM2 with IC_{50} = 0.6 nM in a competitive binding assay and has a Kd value of 0.045 nM for MDM2, determined by surface plasmon resonance (SPR). It potently inhibits cell proliferation with IC_{50} values of 9.1 and 10 nM in an BrdU proliferation assay in the SJSA-1 and HCT-116 cell lines, respectively, and demonstrates over >1000-fold selectivity over the HCT-116 p53 knockout (p53−/−) cell line (Rew and Sun 2014a).

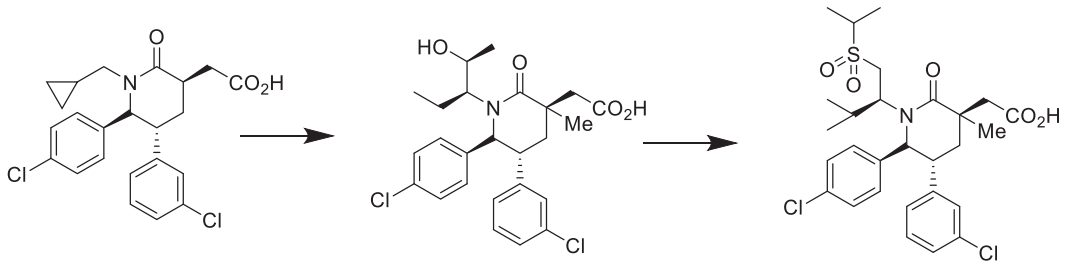

8
IC_{50}=34 nM

9 (AM 8553)
IC_{50}=1.1 nM

10 (AMG 232)
IC_{50}=0.6 nM

Figure 1.5. Structures of piperidinone-containing MDM2 inhibitors

1.2.4.Morpholinone derivatives

AMG 232, a highly powerful and selective piperidinone inhibitor of the MDM2-p53 interaction, was discovered before. Novel morpholinone MDM2 inhibitors were identified as a result of our ongoing hunt for powerful and varied analogues (Gonzalez et al. 2014). Compared to the piperidinone series, modification to a morpholinone core has a considerable effect on both potency and metabolic

stability. AM-8735 emerged as an inhibitor with outstanding biochemical potency, cellular potency, and pharmacokinetic features within this morpholinone class (Gonzalez et al. 2014) (Chunyuan Guo1, Guie Dong1, Xinling Liang2, Zheng Dong1 2017).

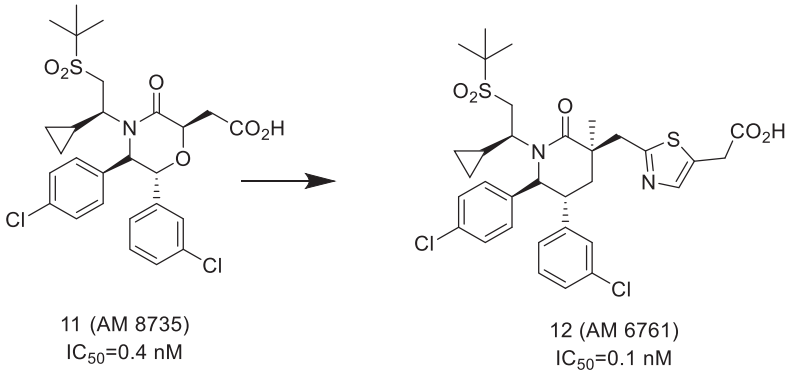

Figure 1.6. Structures of 11 and 12

Compound 11 binds to MDM2 in the SJSA-1 cell line (IC_{50} = 0.4 and 0.1 nM respectively). SJSA-1 female athymic nude mice xenografts exhibited partial tumor regression at the conclusion of therapy when given 11 orally at 100 mg/kg per day. Intriguingly, the rat clearance of 11 is slower and its hepatocyte stability is greater compared to the corresponding piperidinone-containing analogue (Gonzalez et al. 2014).

The metabolic oxidation and glucuronidation of 11 are significantly slower than those of its piperidinone-containing analogue, as revealed by metabolite profiling. These data suggest that morpholinone-containing MDM2 inhibitors, such as 11, have a more advantageous drug metabolism and pharmacokinetics (DMPK) profile than piperidinone-containing MDM2 inhibitors, such as 10 (Rew et al. 2012).

Additional modification of the molecule 10 focused on the substitution of its carboxylic acid component with isosteres. It was fascinating to discover that heterocycles, such as the thiazole group, are a suitable alternative for the carboxylic acid group and establish hydrogen bonds with the imidazole NH of His96 with the nitrogen atom (Gonzalez et al. 2014). This modification resulted in the development of compound 12 (AM 6761), which exhibits high MDM2 binding affinity (IC_{50} = 0.1 nM), high cellular potency (SJSA-1 IC50 = 16 nM), and favorable pharmacokinetic features. 5.6% tumor reduction was observed in SJSA-1 female athymic nude mice

xenografts following 12 days of treatment with 12 at a daily dose of 50 mg/kg (Gonzalez et al. 2014).

The metabolite profiles of 12 in mouse, rat, dog, monkey, and human hepatocytes indicate that 12 is largely eliminated via oxidative pathways, thereby differing from 11's predominant glucuronidation-mediated metabolism (Gonzalez et al. 2014) (Rew and Sun 2014).

1.3.Morpholinone derivatives as MDM2-P53 Inhibitors

Compounds 13 and 14 were placed in three critical binding sites (Leu26 $_{(p53)}$, Trp23 $_{(p53)}$, and Phe19 $_{(p53)}$ packages in MDM2 protein) and the molecules of alcohol and carboxylic acid ends were directed out of the binding package (Figure 7). Note that most MDM2 inhibitors have vicinal benzene groups. When designing molecules 13 and 14 the conformers and energies of structures that can mimic these molecules have been determined while using B3LYP/6-31G* (Figure 1.7.). In the piperidinone derivative 13 while there were two substituents at the C-3 position, the energy difference between the cross-units (gauche) and the anticonformation of the benzene rings was calculated as 2.4 kcal / mol and the ratio of the cross / anti isomers was 1:46. Indeed, the presence of two substituents at gauch conformation increases the MDM2 inhibition effect (Gonzalez et al. 2014) (Rew et al. 2012) (Sun et al. 2014).

On the other hand, when the morpholinone structure of 13 has a single substituent at C-2 carbon, the energy difference between cross/anti-conformers is 0.6 kcal / mol and it was sufficient for the only substituent at C-2 in benzene rings to stay crosscorrelation. The cross (gauche) conformation of the benzene rings which is taken with MDM2, is also apparent in the x-ray crystallography of the molecules. Similarly, new molecules with benzene rings in the gauche conformation may exhibit similar MDM2 inhibitory properties (Gonzalez et al. 2014).

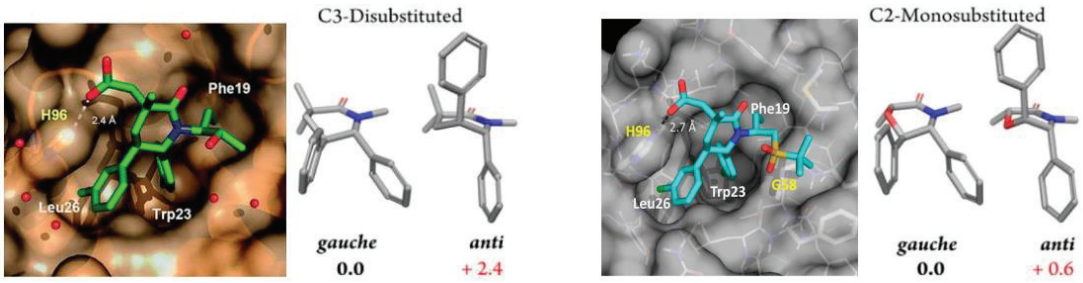

Figure 1.7. Bounding of 13 and 14 to the MDM2 protein and their conjugate energies which is calculated B3LYP/6-31G* method (Gonzalez et al. 2014).

1.4.Synthesis of morpholinone and piperidinone based MDM2-P53 Inhibitors

AMG 232 discovered and developed by Amgen, entered phase I clinical trials for the treatment of human cancer in 2012. This compound was obtained through structure-based design and extensive optimization of a new class of MDM2 inhibitors containing piperidin-2-one (Rew and Sun 2014).

In summary, a robust process to manufacture AMG 232 was developed to deliver drug substance of high purity. The commercial process development efforts have resulted in several significant outputs, including the following: i. the use of a novel bench-stable Vilsmeier reagent, methoxymethylene-N,N-dimethyliminium methyl sulfate, for selective in situ activation of a primary alcohol intermediate; ii. the isolation of crystalline intermediate DHO which enhances the process capacity to reject impurities; iii. the use of The novel process was shown to produce 18 kg of medicinal material (99.9 LC area%) with an overall yield of 49.8 percent from DLAC (1). This is a considerable improvement in comparison to the first-in-human process, which produced 32 percent of an overall yield (Cochran et al. 2019) (Figure 1.8).

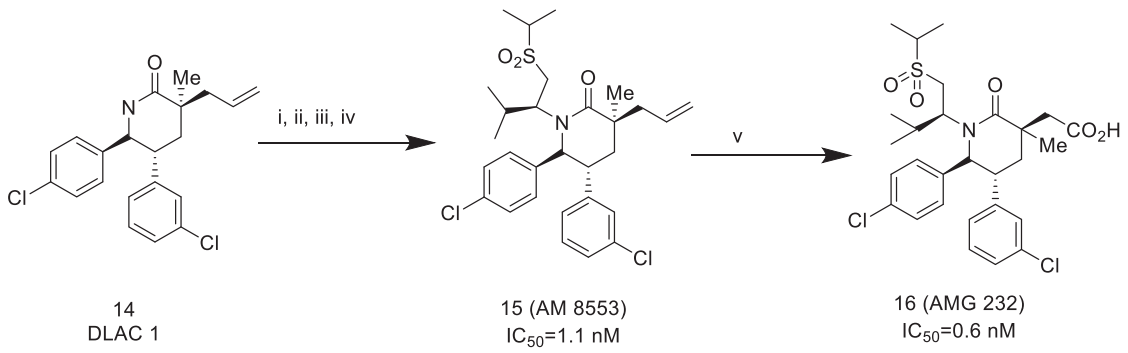

Figure 1.8: Sythesis of AMG 232

The discovery of AMG 232, a highly powerful and selective piperidinone inhibitor of the MDM2 p53 interaction, was published before. Novel morpholinone MDM2 inhibitors were discovered as a result of continuing research into various and powerful analogues. Compared to the piperidinone series, this modification to a morpholinone core has a significant effect on both potency and metabolic stability. AM-8735 emerged as an inhibitor with outstanding biochemical potency (HTRF IC50 = 0.4 nM) and cellular potency (SJSA-1 EdU IC50 = 25 nM), as well as pharmacokinetic features, within this morpholinone series (Gonzalez et al. 2014).

Amgen's discovery of the AM-8735 production pathway gives significant information for our research (Silva et al. 2020). Gonzalez and coworkers, beginning with (R)-4- chlorophenylglycine, synthesized enantioselectively (R,R) amino alcohol 24. $LiAlH_4$ is first used to reduced the (R)-4-chlorophenylglycine to produce amino alcohol 18, then the amino group is protected by a Boc group. Dess Martin Periodinanone (DMP) was then used to convert alcohol to aldehyde. The stereoselective addition of 3-chlorophenylmagnesium bromide to aldehyde yielded protected N-Boc amino alcohol 22. Acid induced deprotection reaction of Boc group and neutralization gave the product compound 24. Under basic conditions, the amino alcohol interacted with chloroacetyl chloride to produce compound 25 as a morpholinone (Figure 1.9.). Due to the chiral amino alcohol, the N-alkylation of morpholinone to compound 28 with ethyl 2-bromo-2-cyclopropylacetate yielded diastereomers 28a and 28b. With superhyride, compound 28a might be converted to primary alcohol. In the subsequent stage, alcohol is transformed to tioether via the Mitsunobu reaction and further oxidation processes, yielding compound 11, also known as AM-8735 (Gonzalez et al. 2014) (Figure 1.10.).

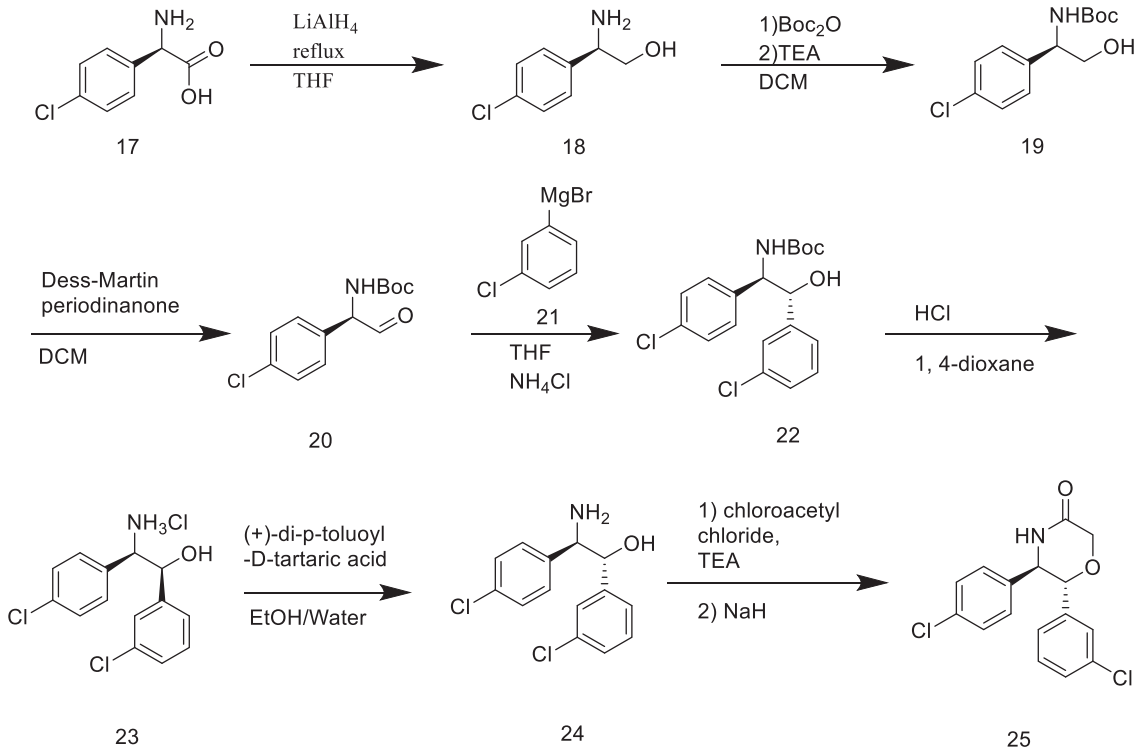

Figure 1.9. Preparation of chiral morpholinone precursor compound 25 reported by Gonzales and co-work

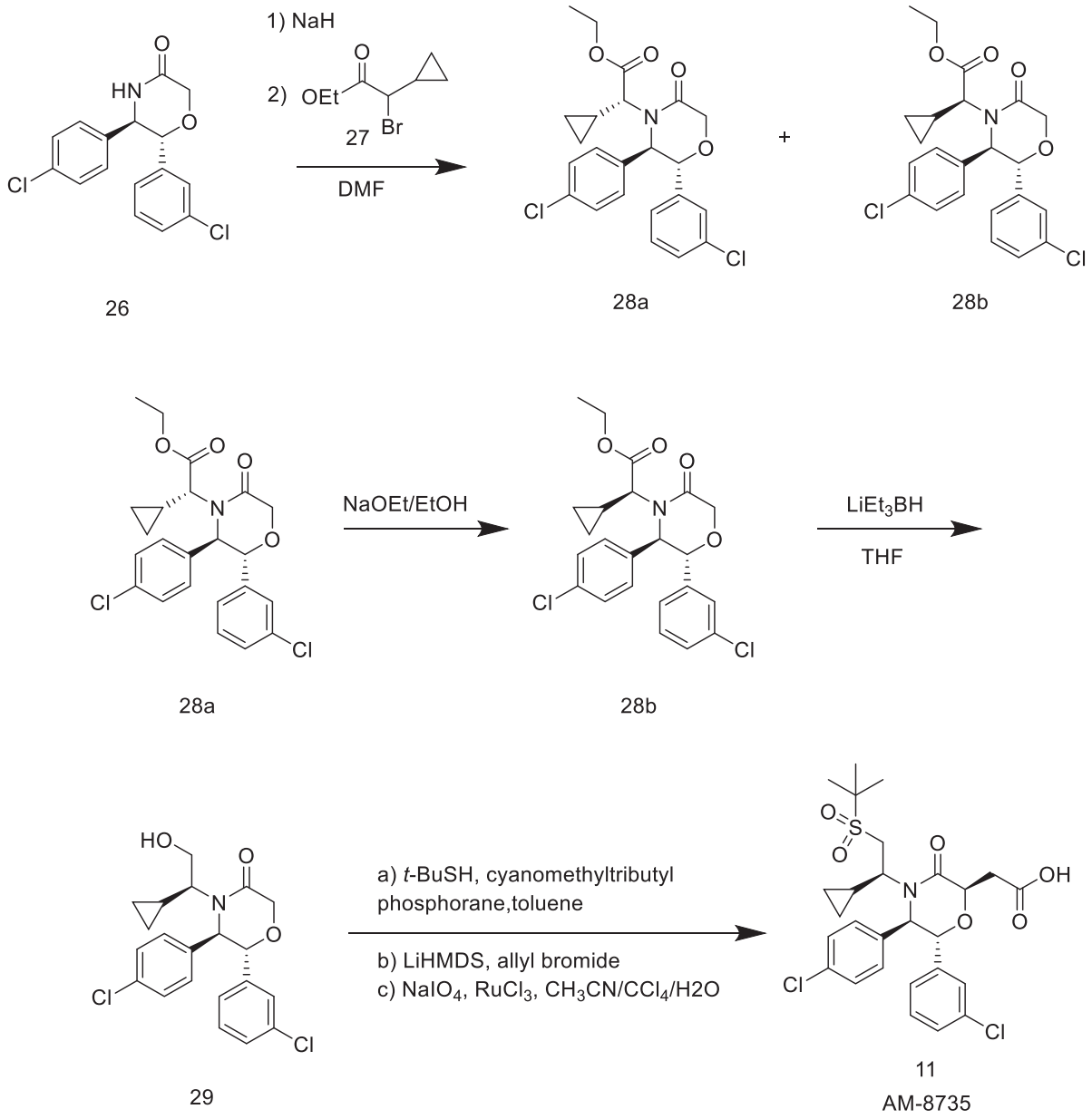

Figure 1.10. Synthesis of AM-8735 which is the best morpholinone derived MDM2 inhibitor.

1.5.Design of novel 1,4-oxazepan-5-onederivatives as potential MDM2-P53 inhibitors

Conformer distribution and energies were calculated by using B3LYP / 6-31G * for a series of final 1,4-oxazepane-5-one derivatives in our molecular modeling study (Figure 1.11). The methyl groups that are shown in model compound

are only designed to facilitate the calculation; actually different R groups will be in these positions. A similar approach was used by Daqing Sun and his team, and the results were parallel to the calculations (Gonzalez et al. 2014). A total of 99.9% of these 1,4-oxazepan-5-one isomers consist of three conformers. Only one of these conformers of the (2R,3R,7S) -isomer has a gauche conformation with percentage ratio 47.3%. On the other hand, two of the conformers of the (2R,3R,7R) -isomer have a gauche conformation and have a total percentage of conformers of 99.0%. It is expected that the (2R,3R,7R)-isomer may have much higher MDM2 inhibitory property than the (2R,3R,7S) -isomer.

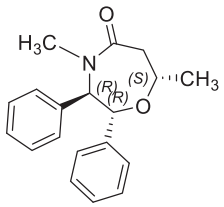

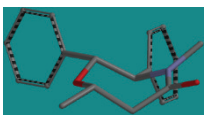

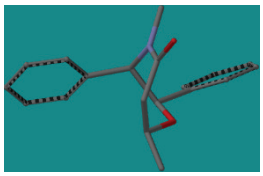

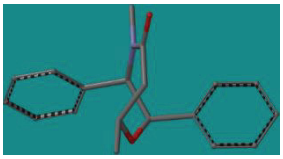

(2R,3R,7S)-isomer			
Relative energy (kcal/mol)	0.00	0.04	1.02
Conformer ratio (%)	0.473	0.441	0.085

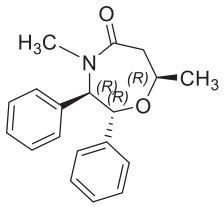

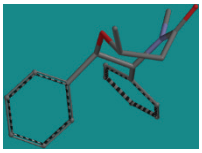

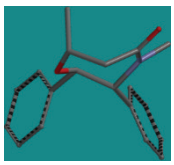

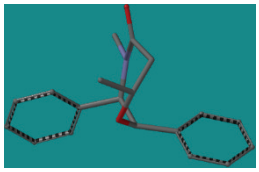

(2R,3R,7R)- isomer			
Relative energy (kcal/mol)	0.00	1.67	2.73
Conformer ratio (%)	0.934	0.056	0.009

Figure 1.11. Calculations of conformer distribution and energies for 1,4-oxazepane-5-one skeleton by using B3LYP/6-31G*

In previous studies, it has been shown that the morpholinone-based MDM2 inhibitors which include an acetic acid near the oxygen atom in the ring contributes great MDM2 inhibition activity. For this reason, it is thought that, an acetic acid

group will be added to the carbon adjacent to the oxygen atom of the 1,4-oxazepane-5-one ring show greater activity. On the other hand, it would be more appropriate to modify the substituents on the nitrogen atom of the ring in accordance with the activity.

Since we do not have sufficient (strong) computer equipment, we have performed the docking of MDM2 enzymes with AutoDock 4.2.6 and AutoDock Vina, of the morpholinone derivative having the same substituent as 31a, 31b and 32. The conformal distributions were determined using the Spartan'14 program and the MMFF force field, and the conformers with the highest ratios were subjected to MDM2 enzymes. Since only the conformational analysis for the morpholinone derivative here did not reveal the gauche conformation for the phenyl groups, the mapping was carried out by using the molecule Spartan'14 program to provide phenyl groups in the gauche conformation. The AutoDock Vina program is newer than AutoDock 4.2.6 and has been reported to provide more accurate results. However, while AutoDock 4.2.6 can calculate the binding energy and inhibition constant, the AutoDock Vina program only shows the result of the binding energy.

If we look at MDM2 binding profiles obtained with AutoDock 4.2.6 program, the conformers with the highest population of all molecules are linked to MDM2 enzyme. It is evident that alcohol derivatized 31b has a stronger inhibitory effect than the reference morpholinone derivative. In addition, the molecule 32 obtained from the replacement of alcohol with triazole appears to have an inhibition constant at low nanomolar concentrations. When the same docking procedure is carried out with the AutoDock Vina program, the reference morpholinone derivative appears to have a stronger MDM2 inhibition than the alcohol-derivatized 31a and 31b isomers, whereas the triazole derivative 32 binds to the MDM2 enzyme at the competing level with the morpholinone derivative.

It is useful to add something at this point, assuming that the protein is a static structure that does not move while the proteins are being donated. However, in reality, moveable side chains in the active region may also provide for stronger binding of the proteins to the inhibitors by taking appropriate conformations.

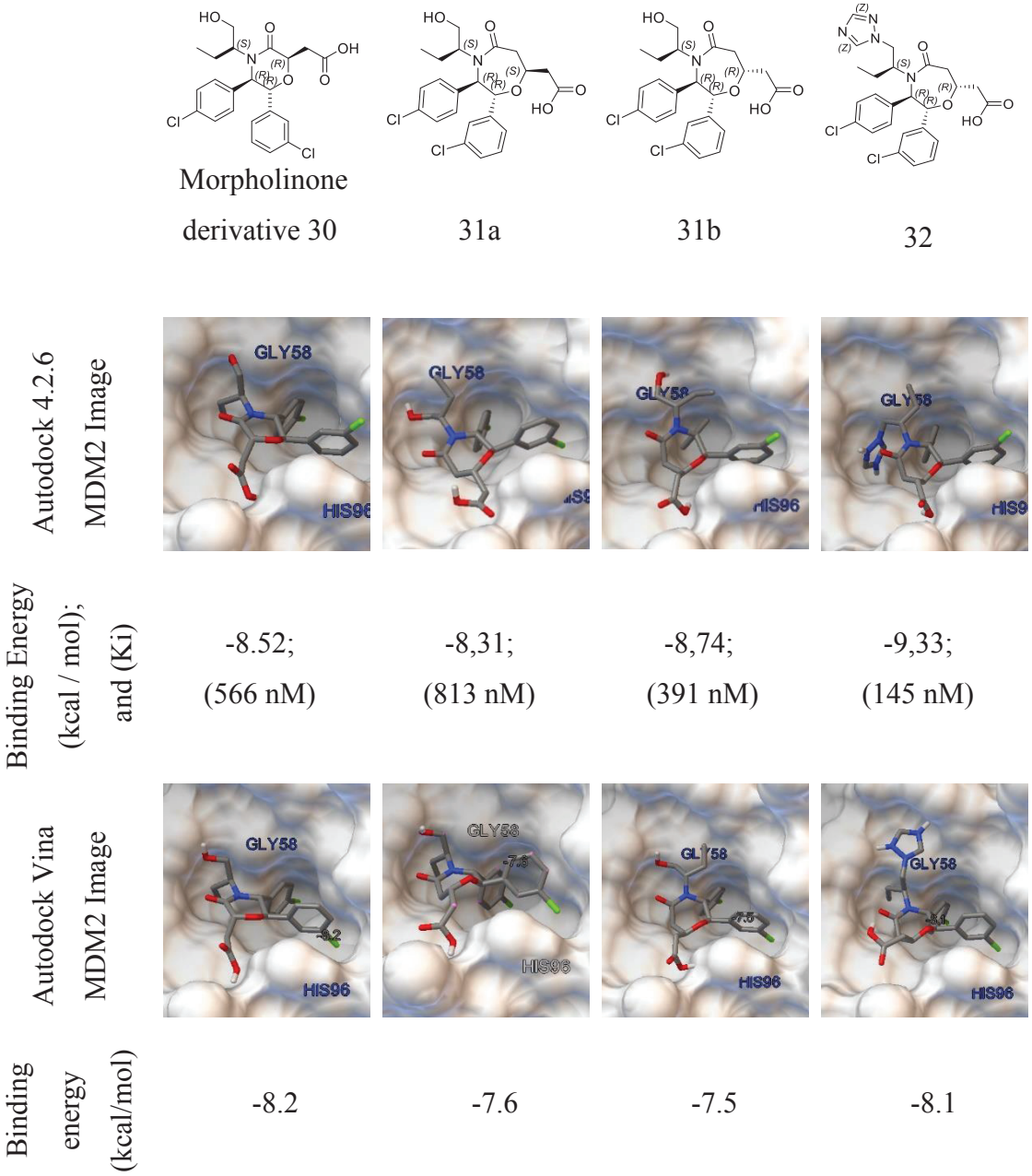

Figure 1.12. Packing scores of compounds 30, 31a, 31b and 32 to MDM2 (PDB Code) performed by Autodock vina and Autodock 4.2.6.

1.6.Sythetic routes for the the synthesis of 1,4-oxazepan-5-one scafold

Because of its potentially useful biological effects, such as anticancer, anti-HIV, depressive, and antitumor properties, fused oxazepanone compounds have

attracted a significant amount of research in recent years (Binaschi et al. 2010). In addition, they exhibit a wide range of pharmacological and neurochemical effects as possible medicines for the central nervous system, potential atypical antipsychotics, -secretase inhibitors, histone deacetylase inhibitors, and muscarinic cholinergic receptors. Sintamil I and its analogues have been reported as effective antidepressants. Properties similar to clozapine have been reported for ioxapine (Liu et al. 2011) .

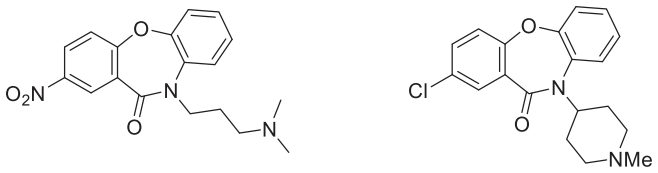

33
Sintamil I

34
Ioxapine

Figure 1.13. Structure of Sintamil I and Ioxapine

As a consequence of this, a number of different methods have been developed in order to synthesize fused oxazepanone scaffolds. These techniques include the intramolecular aromatic substitution in 2-hydroxyanilines of ortho substituted benzoic acids (X = F, Cl, NO2), (Smits et al. 2006) the reaction of 2-(2-halophenoxy)- phenylamines and 2-(2-halophenoxy)pyridine-3-amines with carbon monoxide under pressure using palladium catalysts (Yang et al. 2010). The heating of xanthen-9-one oximes with phosphorus pentachloride through the Beckmann rearrangement and the intramolecular cyclocarbonylation of substituted 2-(2-iodophenoxy)anilines (Lu and Alper 2005) are other examples. However, these procedures are not optimal since they require numerous stages or a transition metal catalyst.

A very useful improvement would be a way to make something in just one step, without a transition metal catalyst. In pharmaceutical, biomedical, and optical chemistry, the Smiles rearrangement has become an useful technique (Liu et al. 2011).

It has been shown that the Smiles rearrangement tandem reaction is a good way to prepare fused oxazepanone scaffolds by reacting commercially available N-

substituted salicylamides with substituted benzenes or pyridines (Liu et al. 2011) (Figure 1.14).

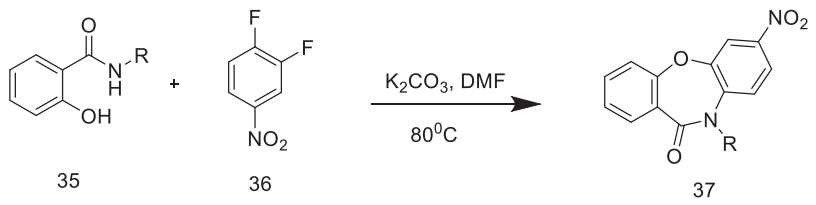

Figure 1.14. Synthesis of compound 37

1.7.Proposed synthetic scheme for the synthesis of novel 1,4-oxazepan-5-one derivatives

In this study compounds 38a and 38b were proposed as MDM2 inhibitors (Figure 1.15). Proposed synthetic route for these skeletons was summarized in Figure 16. In this synthesis the study reported by Gonzales and coworkers was used as guide and started by the reduction of (R)-4-chlorophenylglycine to produce chiral aminoalcohol 18. After protection of amine with Boc group, primary alcohol will bw oxidized to aldehyde 20. Addition of 3-chlorophenylmagnesium bromide should yield chiral amino alcohol 22, which is achiral intermediate than can be reacted further with trans-glutaconic acid to produce the desired 1,4-oxazepan-5-one derivatives (38a and 38b) (Figure 1.16).

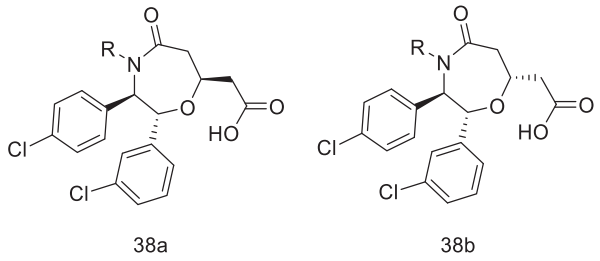

Figure 1.15. The proposed structure of chiral 1,4-oxazepan-5-one derivatives as MDM2 inhibitors.

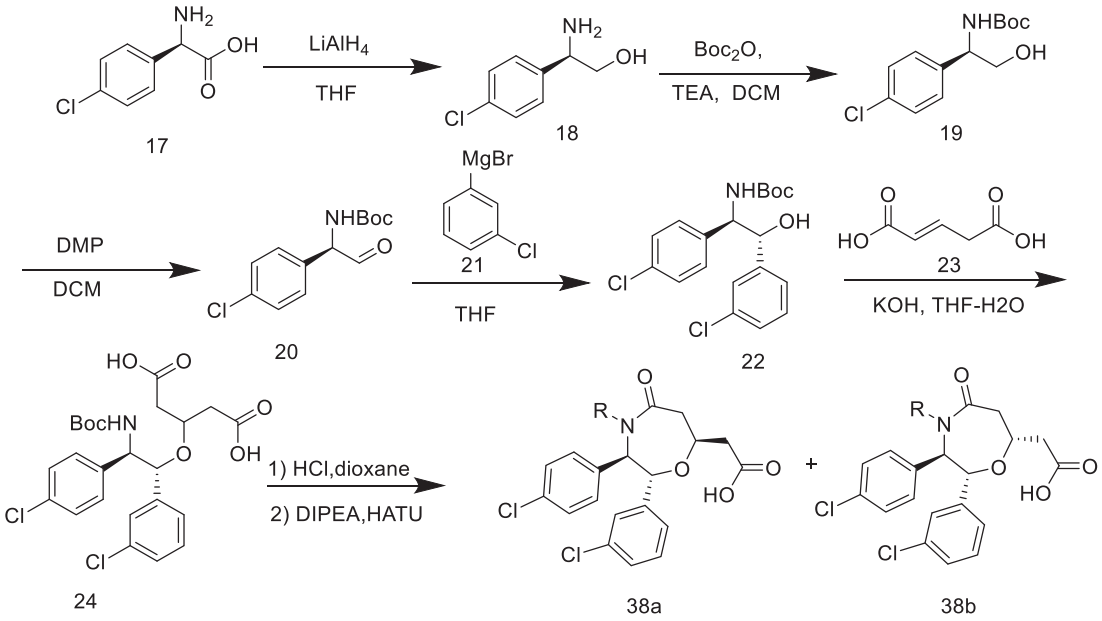

Figure 1.16. Assymetric synthesis of 1,4-oxazepane-5-on skeleton

In the next step, the nucleophilic addition reactions of benzyl alcohol 40 (or 1,2,4-triazole) to the chiral epoxide 39 will be carried out to produce benzyl ether 41 and triazole 42 derivatives (Mugunthan, Mcguire, and Glasziou 2011). Afterwards 4-bromobenzenesulphonyl chloride will be added to the alcohol to form a good leaving group (42 and 46) (Figure 1.17) (Gonzalez et al. 2014).

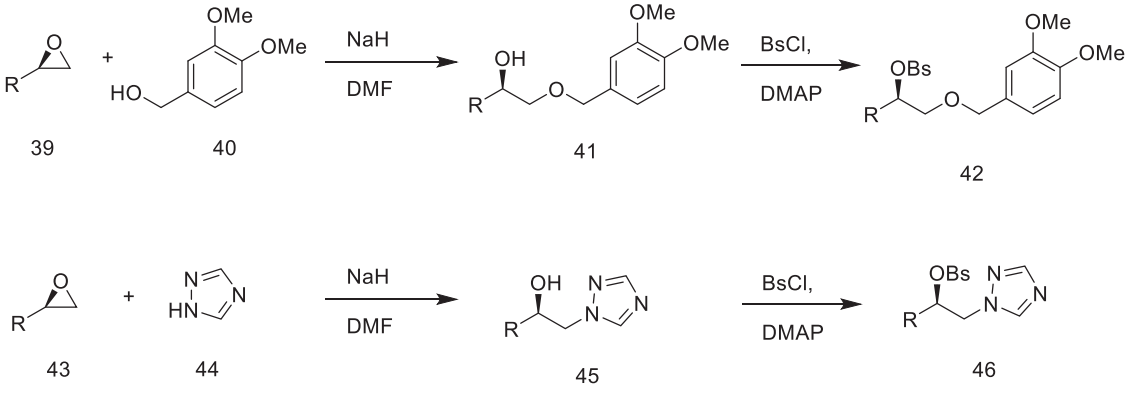

Figure 1.17. Synthesis of important ether and triazole intermediates

Before derivatizing the amide nitrogen of resulting 1,4-oxazepane-5-one derivatives (47a and 47b), the carboxylic acid group will be converted to the tert-

butoxide ester using DCC and t-BuOH (Nahmany and Melman 2001). After that it will be reacted with compound 42 by nucleophilic substitution reaction under basic condition. Removal of the tert-butyl ester by TFA would produce target compound 50a.

On the other hand, reaction of 42a with chiral oxazepan-5-one derivative (48a) under basic condition followed by the deprotection of dimethoxy benzyl alcohol ether by DDQ and ester group by TFA would produce second target product 49a, as shown in Figure 1.18.

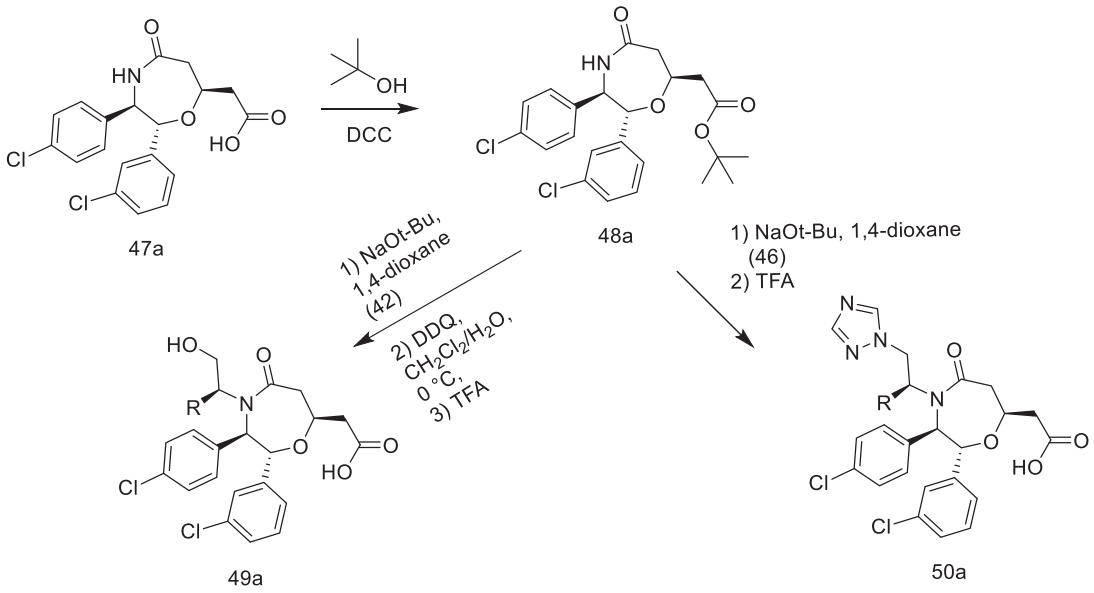

Figure 1.18. Synthesis of desired MDM2 inhibitors

1.8.Structure of Coumarin and its derivatives as anticancer agents

Cancer is one of the most common diseases that lead to death around the world. Even though many chemotherapeutic drugs have been found that stop uncontrolled cell division to treat cancer, these drugs have serious side effects that are a significant disadvantage. Additionally, multidrug resistance is a significant issue in cancer treatment. Due to issues such as cytotoxicity and drug resistance, several studies are done to discover and develop efficient anticancer drugs. Researchers have focused on the anticancer action of coumarins in recent years due to their high biological activity and minimal toxicity. Coumarin derivatives (Figure

1.19) are frequently used for the treatment of prostate cancer, renal cell carcinoma, and leukemia, and they can also reduce the negative effects of radiotherapy. Due to its photochemotherapy and cancer therapeutic potential, both natural and synthesized coumarin derivatives attract attention (Emami and Dadashpour 2015).

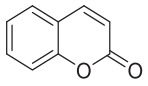

51

Figure 1.19. Structure of coumarin

Polyphenolic chemicals known as coumarins are members of a category of oxygenated heterocyclic compounds that are colorless and crystalline. They were initially identified from a plant known as Dipteryx odorata Willd (Fetzer et al. 2022). (Fabaceae) locally known as "coumaroun" (Vogel, 1820) Coumarin (1,2-benzopyrone or 2H-1-benzopyran-2-one) and coumarin derivatives are often found as heterosides or free chemicals in plants. To date, scientists have collected around 800 coumarin derivative chemicals from roughly 600 genera across 100 families. Many plant species, especially those in the families Rutaceae and Apiaceae, in the class Dicotyledonae of the division Spermatophyta, contain coumarin or a derivative thereof in their seeds, roots, or leaves. Some coumarins, like novobiocin, coumermycin, and aflatoxin, are obtained from microorganisms rather than vascular plants. (Akkol et al. 2020)

According to research on the anticancer properties of coumarin and its derivatives, the mechanism of action of these substances is typically caspase-dependent apoptosis. Some of the coumarin derivatives also affect the destiny of normal cells by altering GTP-binding protein-containing signal transduction pathways and decreasing Bcl-2 expression. The Bcl-2 protein family comprises of apoptotic Group 1 (Bcl-2 and Bcl-XL) and pro-apoptotic Group 2 (Bax, Bad, Bid, and Bak). The Bcl-2 protein family members BH1, BH2, and BH3, and their dimerization, affect the susceptibility of a cell to negative stimuli (Elinos-Báez, León, and Santos 2005).

Inhibition of the Hsp90 protein is another cancer treatment method. Novobiocin (Nvb) and other analogs with coumarin moiety interact with an ATP-linked

molecular chaperone that affects the folding of several proteins, including cancer-related kinases and transcription factors. Novobiocin and its analogs inhibit Hsp90 by inducing Hsp90 protein breakdown via the ubiquitin proteasome pathway (52-59) (Figure 1.20) (Akkol et al. 2020).

p53 is a transcription factor that inhibits cell proliferation and plays a crucial role in apoptosis. However, apoptosis can also be activated by the binding of the target genes to the DNA sequence and the activation of the subgenes' promoters, p21 and Bax. 7,8-Dihydroxy-4-methylcoumarin promotes apoptosis through the downregulation of p53, Bax, p21, and COX-2, the upregulation of c-Myc protein, and the reduction of ERK1/2. Figure 7 indicates the general structure-activity relationship (SAR) and anti-cancer activity of coumarins. (Akkol et al. 2020).

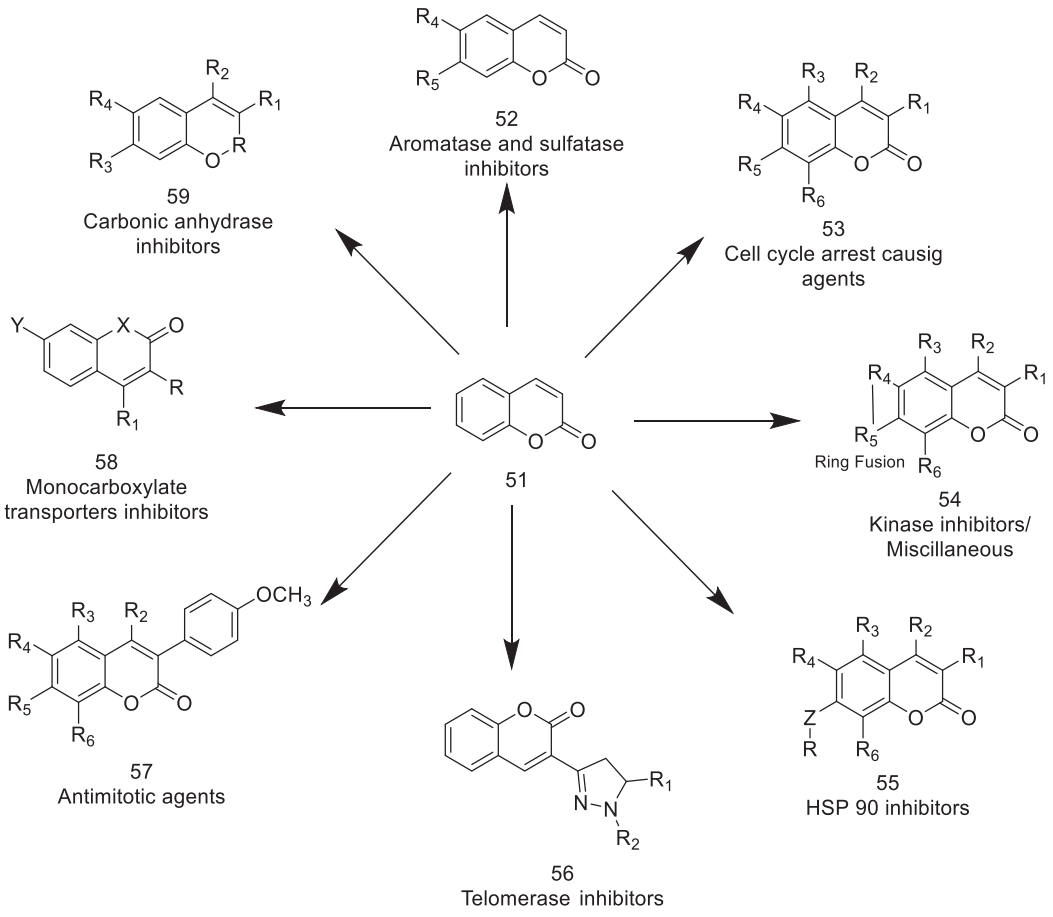

Figure 1.20. Coumarins showing anticancer activity with structure activity relationship(Akkol et al. 2020)

Neopeucedalactone 60, was isolated from the roots of Peucedanum praeruptorum Dunn as a novel coumarin of the xanthyletin class (Li et al. 2020). The anticancer study revealed that neopeucedalactone exhibited moderate in vitro cell growth inhibitory activities (MTT [3(4,5dimethylthiazol2yl)2,5diphenyl tetrazolium bromide] assay) against the human leukemic HL60, THP1 cell lines, and the human prostate cancer PC3 cell line, with IC50 values of 9.97, 27.80 and 48.68 μM, respectively (Figure 21).

All seven coumarin derivatives derived from Saposhnikovia divaricata (Turcz.) Schischk. were sensitive to MEL8, U937, DU145, MDAMB231, and VT474 cancer cell lines, with 50% growth inhibitory concentration (GI_{50}) values ranging from 8.76 to 51.08 μM (Urbagarova et al. 2020). Compound 61 (GI_{50}: 8.76 μM; MTT assay) was comparable to doxorubicin (GI_{50}: 7.91 μM) against MDAMB231 cells, whereas 62 (GI_{50}: 9.42 μM) was 2.1 fold more effective than cisplatin (GI_{50}: 19.82 μM) against DU145 cells.

Esculetin 63 (IC50: 20 μM; CCK8 [Cell Counting Kit8] assay), isolated from the seeds of Euphorbia lathyris L., inhibited HL60 leukemia cells through numerous mechanisms, including apoptosis, autophagy, and G0/G1 cell cycle arrest. In addition, esculetin was able to disrupt the Raf/MEK/ERK signaling cascade in leukemia cells in a concentration-dependent manner, demonstrating its anticancer potential (Z. Wang et al. 2020).

The coumarin derivative 64 (IC_{50}: 25.69–49.13 μM; MTT assay) obtained from Daphne oleoides was active against A549, HBL100, and HeLa cancer cells, however psoralidin 65 (IC_{50}: 9 μM ; MTT assay), a natural furanocoumarin isolated from Psoralea corylifolia L., shown potential action against HepG2 (Lin et al. 2021). Multiple mechanisms, including apoptosis, autophagy, and cell cycle arrest, were identified in the study demonstrating that psoralidin inhibits the proliferation of human liver cancer cells. In a xenografted mouse model, psoralidin (40 mg/kg) dramatically suppressed the volume and weight of xenografted tumors by around 80%.

Ferulin C 66 (IC50: 19.8 and 15.6 μM; MTT assay), a natural sesquiterpene coumarin isolated from the roots of Ferula ferulaeoides (Steud.) Korov.et al, demonstrated potent activity against MCF7 and MDAMB 231 breast cancer cells as well as a remarkable tubulin polymerization inhibitory activity (IC50: 9.2 μM). Further research revealed that ferulin C disrupted the integrity and structure of

microtubules, stimulated considerable cell cycle arrest in the G1/S phase via p21Cip1/Waf1 CDK2 signaling, promoted classical cell death, and inhibited metastasis by downregulating Ras–Raf–ERK and AKT–mTOR signaling. Notably, ferulin C could induce autophagy via ULK1 signaling to enhance the suppression of cell growth and metastasis. In the MCF7 xenograft mouse model, ferulin C (100 mg/kg) strongly inhibited the proliferation of cancer cells and suppressed approximately 50% of the tumor's volume and weight without causing mice to lose weight. This compound's potential in vitro and in vivo activity and superior safety profile made it a suitable candidate for further preclinical research (Yao et al. 2020).

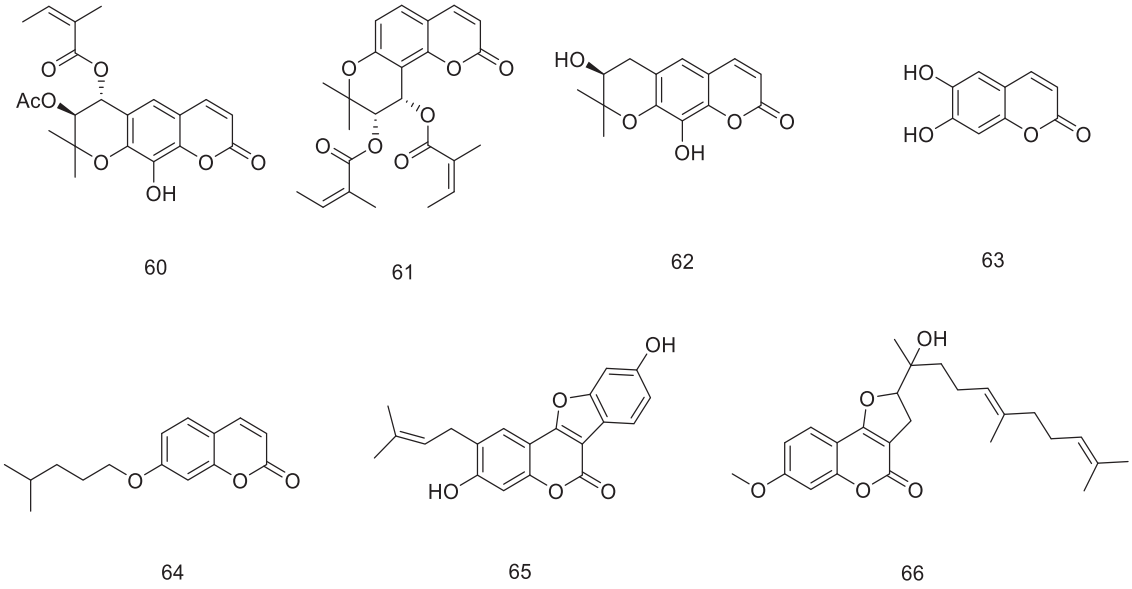

Figure 1.21. Chemical structures of the naturall products having derived coumarin functional group

1.9.Synthetic routes for Coumarin Scaffold

Compounds having the coumarin nucleus (2H-1-benzopyran-2-one) are an important class of heterocycles that play a significant role in natural products and synthetic organic chemistry. They are found as benzopyrene derivatives in a number of plant sources. Coumarins have significant biochemical and physiological impacts on plants (Molnar, Lončarić, and Kovač 2020). Organic compounds with the coumarin moiety have also been found to have many useful properties, such as

antibacterial, antifungal, antimicrobial, antioxidant, analgesic, antimutagenic, anticancer, anti-HIV, anti-inflammatory, antibiotic, anticoagulant, antitumor, tumor necrosis factor-a inhibitory, serine protease inhibitory, and steroid 5a-reductase inhibitory activities, as well as being used as fluorescence sensors (Vekariya and Patel 2014).

Organic chemists are interested in the synthesis of coumarin and its derivatives due to their wide range of applications. Numerous techniques, including the Pechmann condensation, the Perkin reaction, the Knoevenagel condensation, the Wittig reaction, and the Baylis–Hillman reaction etc. have been developed for their synthesis. Nonetheless, the Pechmann and Knoevenagel reactions are generally used for the synthesis of coumarins due to their simple reaction conditions and high product yields (Kumar, Nagamallu, and Govindappa 2015).

1.9.1.The Perkin reaction

The Perkin reaction, also known as the Perkin condensation or the Perkin synthesis, typically involves the condensation of aromatic aldehydes and carboxylic acid anhydrides or carboxylic derivatives in a base-catalyzed reaction, which results in the formation of cinnamic acid derivatives. This type of reaction is also known as the Perkin condensation. Heating salicylaldehyde sodium salt 67 with acetic anhydride 68 is the first step in the Perkin reaction, which is used to synthesize coumarin 69 (Kumar, Nagamallu, and Govindappa 2015). (Figure 1.22)

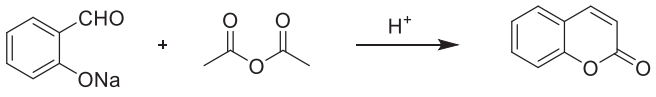

67 68 69

Figure 1.22.Coumarin synthesis by Perkin reaction

1.9.2.The Peckman reaction

Pechmann and Duisberg were the ones who initially described the Pechmann condensation reaction in the year 1883. Because of the simplicity with which it can be prepared and the low cost of the starting material, it has found widespread

application in the synthesis of coumarins. This technique calls for the reaction of phenol 70 andketo 71 ester in the presence of an acid catalyst (Kumar, Nagamallu, and Govindappa 2015) (Figure 1.23).

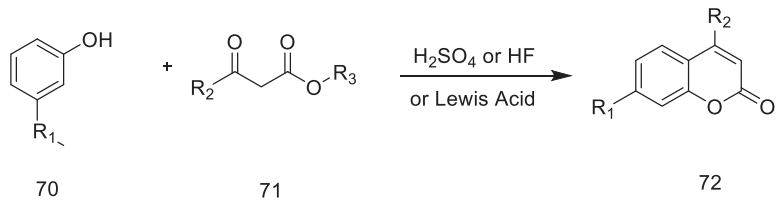

Figure 1.23.Coumarin synthesis by Peckman reaction

1.9.3.Knoevenagel condensation

In the process of Knoevenagel condensation, an active methylene molecule is nucleophilically added to aldehydes or ketones in a reaction that is catalyzed by a weak base. This is typically followed by the removal of water from the system. In most cases, Lewis acids or weak bases serve as the catalysts for the Knoevenagel condensation reaction, which converts salicylic aldehydes into coumarins during the course of a reaction that begins with salicylicaldehyde and malonic acid or esters. With the presence of at least one electron-drawing group, activation of the methylene group can be accomplished (nitro, cyano, carbonyl, sulfonyl) (Molnar, Lončarić, and Kovač 2020).

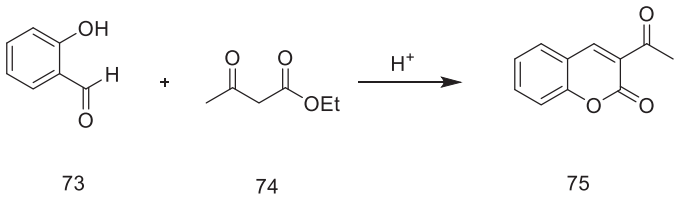

Figure 1.24.Coumarin Synthesis by Knoevenagel condensation

1.9.4.Wittig reaction

The Wittig reaction is initiated by carbonyl compounds, which combine with ylides containing phosphorus to produce alkenes. Using various catalysts, substituted

salicylaldehydes, methyl or ethyl chloroacetate, and triphenylphosphine are used to produce substituted coumarins via the Wittig reaction (Valizadeh and Vaghefi 2009) (Figure 1.25).

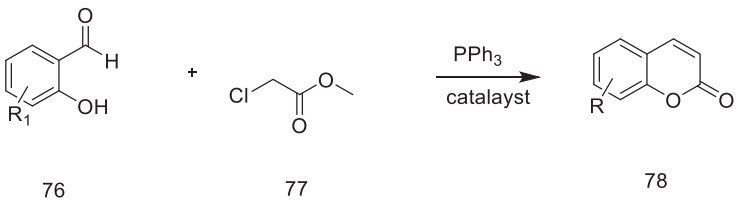

76 77 78

Figure 1.25.Coumarin synthesis by Wittig reaction

1.10.1,5-disubstituted 1,2,3-Triazol derivatives as anticancer agents

Due to their numerous biological properties, which include anticancer activity, 1,2,3-triazoles are a significant class of five-membered heterocyclic molecules. Since they may be produced synthetically, 1,4-disubstituted 1,2,3-triazoles are still the most researched triazole derivatives. At the same time, 1,5-disubstituted triazoles are becoming more and more popular as cis-amide bond bioisosteres. In particular, it has recently been demonstrated that certain 1,5-disubstituted 1,2,3-triazoles inhibit Rac and Cdc42 GTPases, whose hyperactive expression or overexpression is one of the mechanisms of cancer signaling and metastasis and which play a significant role in hyperproliferative and neoplastic diseases (Synthesis 2022).

A hydrogen atom and an amino group, respectively, were substituted for the lead compound's 30-hydroxyl group in compounds 79 and 80, which demonstrated cytotoxic effects with IC_{50} values of 27 and 11 nM. Triazole 81, which has a hydroxyl group at position 3 on ring B, was less active than both 79 and 80 (IC_{50} = 35 nM). The fact that triazoles 79 and 80 were more active than their regioisomers 82 and 83 suggests that the location of the 1,2,3-triazole moiety is significant (Odlo et al. 2008) (Figure 26).

The capacity of the triazoles to inhibit tubulin assembly was further examined in those compounds that demonstrated notable lethal effects in the K562 cell

experiment. Triazoles 79 and 80 inhibited the assembly of tubulin with IC_{50} values of 7.0 and 4.8 nM, respectively (Odlo et al. 2008) (Figure 1.26).

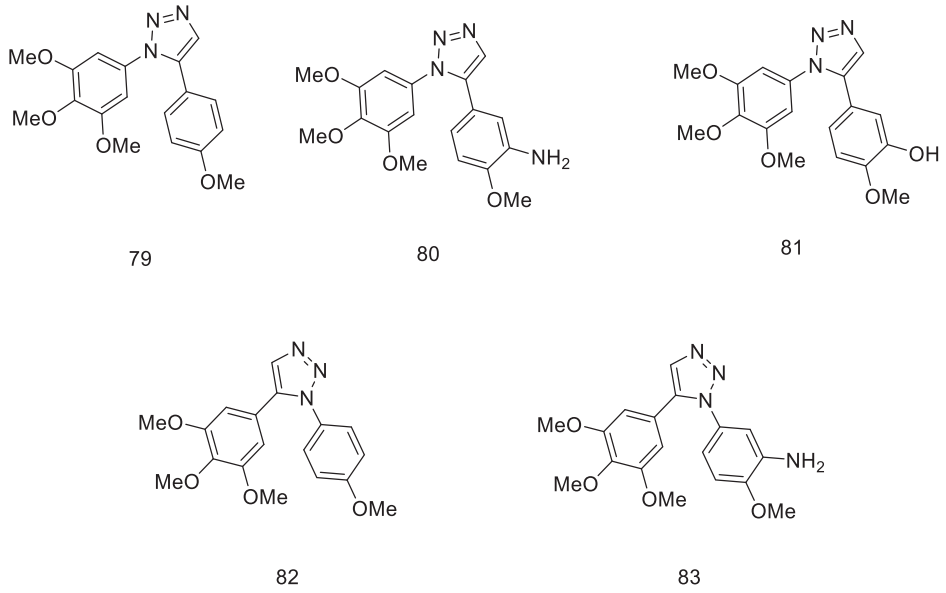

Figure 1.26. 1,5-disubstituted 1,2,3-Triazol derivatives

It is of particular significance that, out of all the cell lines that were studied, this one showed the most promising cytotoxicities. It was discovered that hybrids with an epiquinidine skeleton and a 1,5-disubstituted triazole linker (85a and 85b) are more effective than their epiquinine equivalents, 84a and 84b, respectively. indicating that the relative arrangement of the cinchona residue plays an important role in the production of the antiproliferative action. In addition, in accordance with the substitution pattern indicated previously, the 3,4,5-trimethoxybenzoyl derivative 85a was determined to be the most potent model among the series of hybrids. The exceptional activity of 85a may be attributable in part to its relatively stiff molecular structure, in which the entire rotation of the 1,5-disubstituted triazole ring is impeded by the surrounding, highly interfering chalcone- and quinuclidine units. There is a good chance that the fact that this skeletal structure has a limited conformational space gives it a strong potential to selectively attach to a target biomolecule that is involved in a signal-transferring pathway that is associated with cell proliferation. The fact that the 3,5-dimethyl-4-hydroxybenzoyl derivative 85b, which essentially adopts the same skeletal conformation, displays a substantially decreased activity exclusively against the PANC-1 cell line points to an increased importance of the

substituents at the chalcone terminal in the evolution of the tumour-selective cytotoxic effect induced by the cinchona-chalcone hybrids studied in this work. This is an important finding, and it should be noted (Figure 1.27).

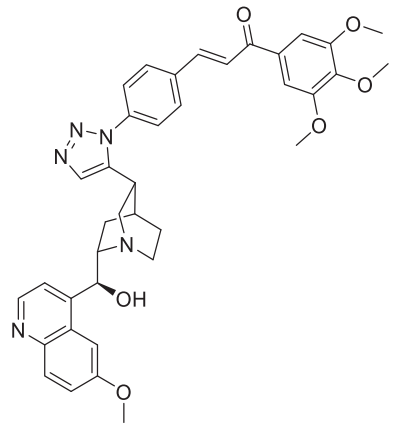

84a

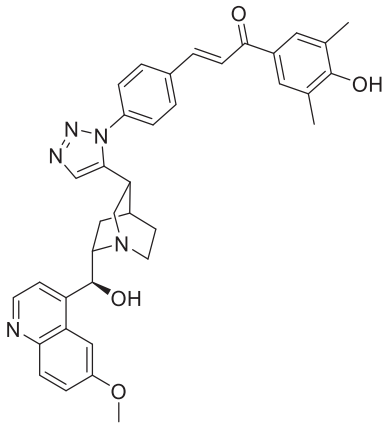

84b

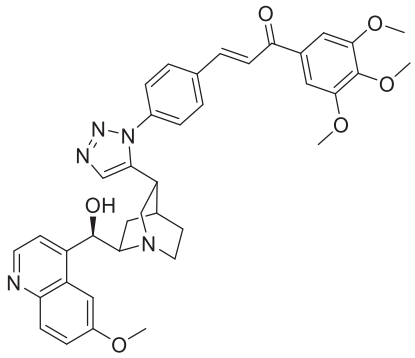

85a

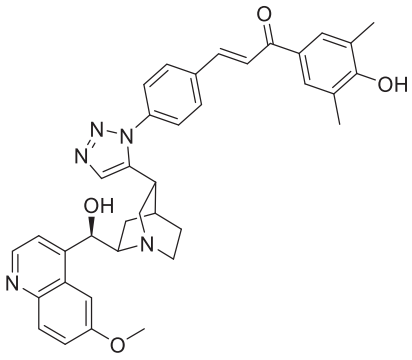

85b

Figure 1.27. Structures of the biologically active 1,2,3-triazole substituted chalcone structures (84a-b and 85a-b)

1.11.Synthetic routes for 1,2,3-Triazol derivatives

1.11.1.Synthesis of 1,2,3-triazoles by using Cu(I)-catalyzed azide-alkyne cycloaddition (CuAAC) reaction

A well-known regioselective approach for producing 1*H*-1,2,3-triazole containing building blocks for use in pharmaceutical and material chemistry applications is the Cu(I)-catalyzed azide-alkyne cycloaddition (CuAAC) process. This reaction is catalyzed by the copper ion. The ease of use, wide range of functional groups that it is compatible with, eco-friendliness, and great selectivity of this approach have contributed to its widespread adoption. Good yields were achieved during the synthesis of 1,2,3-triazoles hybrids based on ferrocene (Haque et al. 2017) (Figure 1.28).

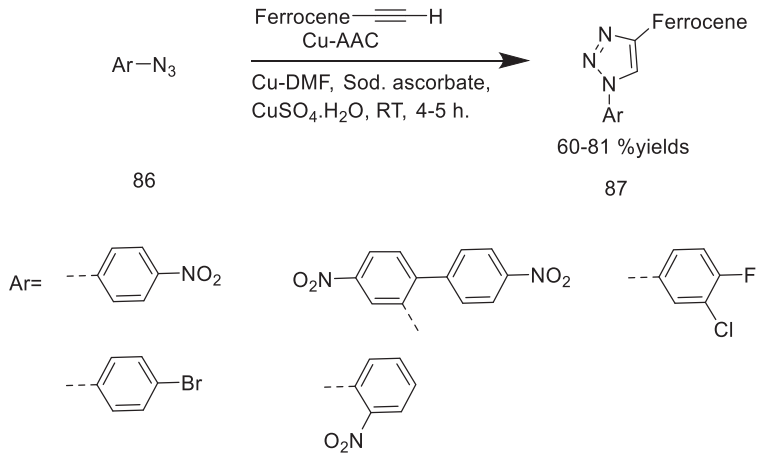

Figure 1.28. Cu(I)-catalyzed azide-alkyne cycloaddition (CuAAC) reaction for the synthesis of 1,4-disubstituted 1,2,3-triazoles

1.11.2.Synthesis of 1,2,3-triazoles by using microwave enhanced sequence through Knoevenagel condensation

Using non-conventional energy sources such as microwave heating, ultrasonic waves, and light-induced click reactions has emerged as a potent strategy for speeding up the rate of various chemical transformations. Several microwave-Cu(I)-coupled click chemical techniques have been reported in recent times (Nemallapudi et al. 2020).

The most common cycloaddition reaction involving an azide and an alkyne offers a route to triazoles. However Yulin Lam offered a nice alternative by talking about the cyclo addition of vinyl sulfones and azides (Figure 1.29). The work is

directly applied to a solid-phase method, which makes it easy to access triazoles. It is reported that sulfinate can be turned into a sulfone with the help of a microwave, which is followed by Knoevenagel condensation and then azide cyclo addition. It's important to note that each step works better when heated in a microwave (Nemallapudi et al. 2020).

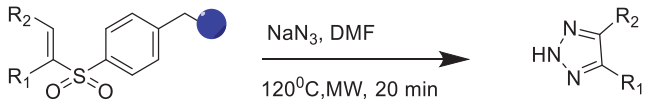

88 89

Figure 1.29. Preparation of 2H-1,2,3-triazole derivatives by adding sodium azide to vinyl sulfones

1.11.3.Synthesis of 1,2,3-triazoles by using CuSO4.5H2O/1-(4-methoxyphenyl)-3-phenylthiourea through green chemistry aproach

For the copper (I)-catalyzed azide–alkyne cycloaddition reaction, also known as CuAAC, an extremely effective and efficient catalytic system, $CuSO_4.5H_2O$/1-(4-methoxyphenyl)-3-phenylthiourea, has been developed. Within the catalytic system described in the previous paragraph, substituted thiourea serves a dual role, first as a reductant and then as a ligand. For the CuAAC process, a catalyst consisting of $CuSO_4.5H_2O$/1 (4-methoxyphenyl)-3-phenylthiourea is one that is both economical and effective. The new catalytic system also offers desirable traits including mild and green chemistry reaction conditions and a wide range of substrate compatibility. A variety of 1,4-disubstituted 1,2,3-triazoles have been produced in aqueous solution using the $CuSO_4.5H_2O$/1-(4-methoxyphenyl)-3-phenylthiourea catalytic system by Yuan and coworkers with good to excellent yields (Siyu Wang et al. 2017) (Figure 1.30).

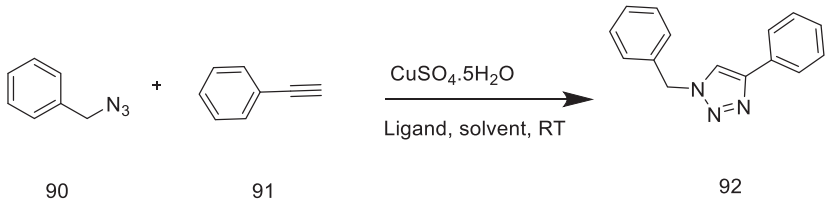

Figure 1.30. Synthesis of 1,2,3-triazoles by using CuSO4.5H2O/1-(4-methoxyphenyl)-3-phenylthiourea

1.12.1,2,3-Triazol Substituted Coumarin Derivatives and their Biological Activities

Coumarin derivatives are found in many plants and have been studied a lot as antiviral, anti-inflammatory, antibacterial, and anticancer agents. Another promising group known as 1,2,3-triazole has emerged as one of the most important heterocycles in contemporary medicinal chemistry. Additionally, its applications have been expanded to include a wider range of disorders (Malini et al. 2000). In recent years, a library of coumarin derivatives conjugated with 1,2,3-triazole has been synthesized. These coumarin derivatives have been shown to possess different level of bioactivity. In terms of their anticancer potential, H.M. Liu and his colleagues found that 4-((1,2,3-triazol-1-yl)methyl)coumarin derivatives induced apoptosis in cancer cells, which is a good reflection of their ability to induce the disease. In addition, novobiocin analogues containing 1,2,3-triazole at the C-3 position of coumarin shown significant cytotoxic action against two different breast cancer cell lines (SKBr-3 and MCF-7) (Peterson and Blagg 2010). A family of 3-(1,2,3-triazol-1-yl)coumarins were synthesized and proved to reduce neutrophils in the LPS-inflamed subcutaneous tissue. On the other hand, through inhibiting 5-lipoxygenase, a triazole connected to the C-7 position of coumarin by a methene can also cause remarkable anti-inflammatory activity. Both of these classes of compounds have been shown to have anti-inflammatory properties (Ouellet et al. 2012). In addition, compounds having 1,2,3-triazol-1-yl attached to the C-3 position of coumarin (95) shown the ability to block the aggregation of amyloid-, a process that is thought to have a causative role in the progression of Alzheimer's disease (Soto-Ortega et al. 2011).

Figure 1.31 provides a summary of the compounds discussed in the previous paragraphs (Zhang et al. 2014) (Figure 1.31).

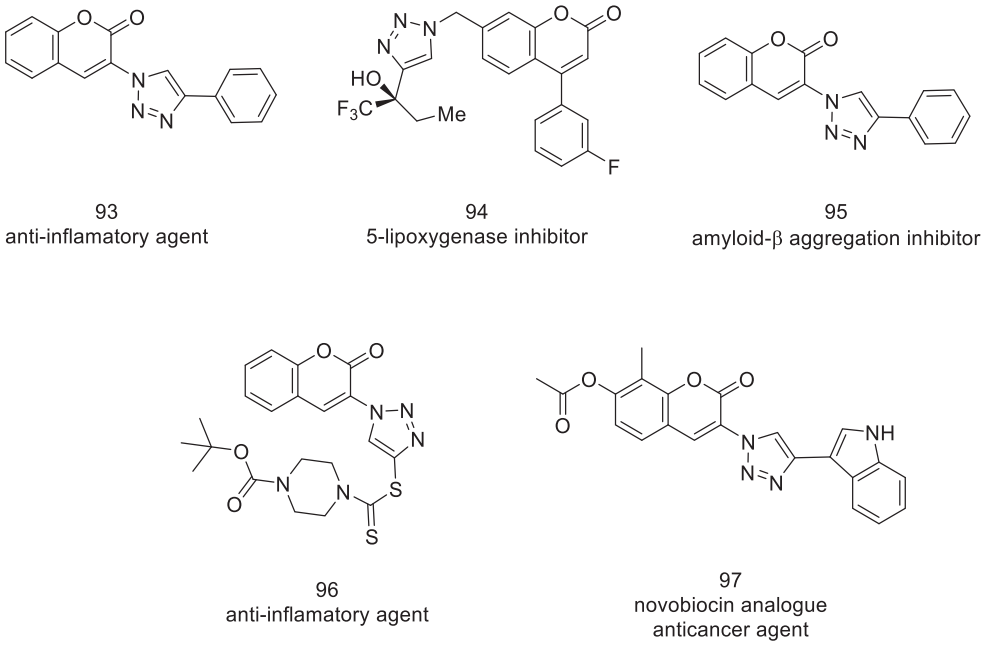

Figure 1.31. Structures of biologically active coumarin derivatives conjugated with 1,2,3-triazole.

The antitumor activity of a novel compounds combining coumarin, 1,2,3-triazole, and benzoyl-substituted arylamine was evaluated in vitro. Under both normoxic and hypoxic circumstances, the compound 100 showed significant antiproliferative action against MDA-MB-231, a human breast cancer cell line. Moreover, the 4-substituted coumarin linked to benzoyl 3,4-dimethoxyaniline via 1,2,3-triazole (compound 100) exhibited the most potent antiproliferative activities with an IC_{50} value of 0.03 M, approximately 5000 times more potent than 4-hydroxycoumarin (IC50 > 100 M) and 20 times more potent than doxorubicin (IC50 = 0.06 M). Docking study revealed that compound 100 could inhibit carbonic anhydrase IX (CA IX) (An et al. 2018).

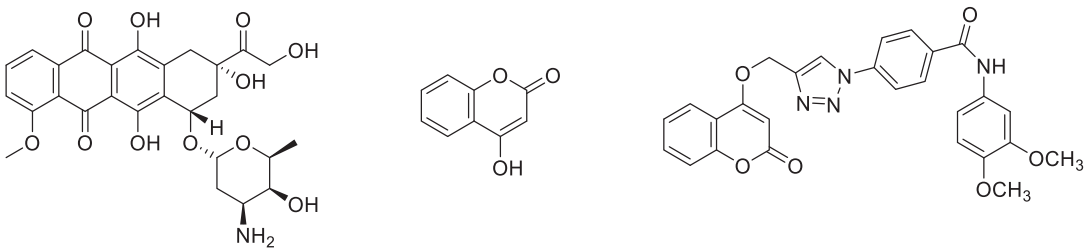

98
Doksorubicin

99
4 Hydroxycoumarine

100

Figure 1.32. Structures of doxorubicin, 4-hydroxycoumarin hybrid and compound containing 1,2,3-triazole coumarin

CHAPTER 2

RESULT and DISCUSSION

2.1. Studies carried out by using N-Boc protected chiral aminoalcohol (22) and glutaconic acid (23) to prepare 1,4-oxazepan-5-one skeleton

It was mentioned that 1,4-oxazepan-5-one skeleton has similar functional group with morpholinone based MDM2 inhibitors reported by Gonzales et al (Gonzalez et al. 2014). In that study they reported the preparation of N-Boc protected chiral aminoalcohol (22) as precursor for the preparation of morpholinone structure. Because of that this synthetic route was used in order to produce target 1,4-oxazepan-5-one skeleton.

According to the referred study (R)-4-chlorophenyl glycine (17) was used as starting material and reduced by using $LiAlH_4$ in dry THF to produce aminoalcohol (18). Then nitrogen atom was protected by Boc group by using Boc anhydride under basic condition. Afterwards primary alcohol was oxidized to aldehyde by using Dess-Martin Periodinone. The oxidation reaction of N-Boc protected aminoalcohol with Dess-Martin periodinan reagent to aldehyde was carried out repetitively even in gram order. These steps are quite reproducible and yields are quite good for each step as summarized in Table 2.1.

Table 2.1. Preparation of compound tert-butyl (R)-(1-(4-chlorophenyl)-2-oxoethyl)carbamate (20)

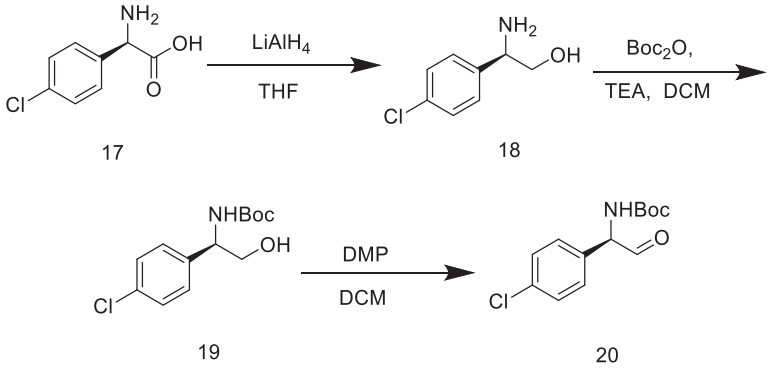

Entry	Yield %		
	18	19	20
1	72	75	71
2	80	70	92
3	80	75	98
4	83	68	95
5	83	70	97
6	99	82	95
8	96	23	92
9	80	34	91
10	80	75	82
11	72	76	96
12	90	72	98

In the next steps, N-Boc protected aldehyde was treated with 3-chlorophenylmagnesium bromide as reported by Gonzales et al. Altough they reported a very good yield for this step, our trials toward the preparation of N-Boc protected chiral aminoalcohol (22) were unsuccesful as summerized in Table 2. Many spots (at least 6 spots) were encountered in TLC at the step of adding chlorophenylmagnesium bromide (2 eq., then up to 5 eq.) to compound 20. While a 49% efficiency was reported for this experiment in the patents and publications of the relevant company, all the spots in the crude product were tried to be purified by column chromatography. At this point, the authors in the related source article stated that they did not carry out any purification process for this substance. One of the spots, obtained as a mixture in the purification process of the crude product obtained from the reaction by silica gel column chromatography (Hexane:Ethyl Acetate), is

very similar to the product in NMR. In the TLC study ($CHCl_3$ containing 2% MeOH), it was determined that this substance contains 2 different molecules. These were thought to be possible diastereomers, and in this solvent system, different attempts were made to separate these diastereomers, but they were not successful (Table 2.2).

Table 2.2. Addition of Grignard compound to N-Boc protected aldehyde (20)

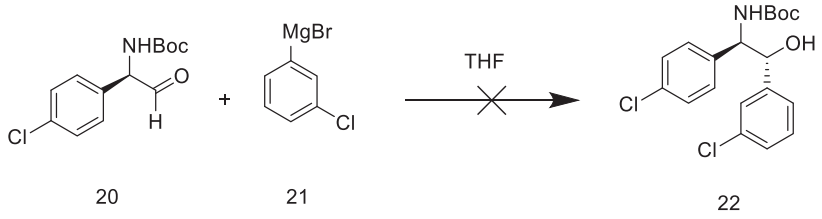

20 21 22

Entry	Grignard Eq.	Time	Temperature	Yield % 22
1	2	2 Hours	RT	38-45*
2	2	2 Hours	-40 ºC	31-50*
3	2.5	2 Hours	-40 ºC	42-50*
4	5	Overnight	RT	Not isolated

*Mixture yield

As a result of previous steps, it is desired to get rid of the impurities, if possible, in the next steps. Deprotection of N-Boc group was performed with the help of TFA as reported by Gonzales et al. Compound 24 was tried to be synthesized as shown in table 4. Each reaction conditions were reacted more than one time and same results were obtained. Even DTT and phenol were used as radical scevenger to minimize the side reactions and increase the yield of product, but similar results were obtained (Table 2.3 entires 4 and 5). As a result of these experiments there were many spots in TLC but none of these spots could be isolated purely (Table 3). In the following step, mixture from TFA treatments and trans-glutaconic acid (23) was tried to be reacted to form compound 1,4-oxazepan-5-one skeleton 101. Firstlly HATU was used to perform this cupling reaction and at the end of the several trials expected product (101) could not be obtained (Table 2.4). To be sure, another coupling reagent pyBOP, which is also can be used for sterically hindered amines, was used but expected product can not be obtained again. (Table 2.5)

Table 2.3. Attempts for the deprotection of N-Boc group by using TFA

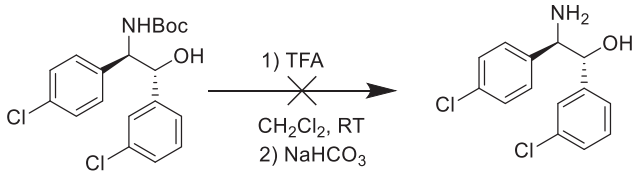

22 24

Entry	TFA Eq.	Time(Hour)	DTT Eq.	Phenol Eq.	Temperature	Yield % 24
1	16	1.5	-		RT	*
2	16	3	-	-	RT	*
3	16	2	-	-	RT	*
4	10	1.5	-	0.5	RT	*
5	4	3	0.5	-	RT	*

*Not isolated one crude NMR was checked and product was not obtained.

Table 2.4. Attempts for coupling of glutaconic acid (23) to TFA reaction mixture by using HATU

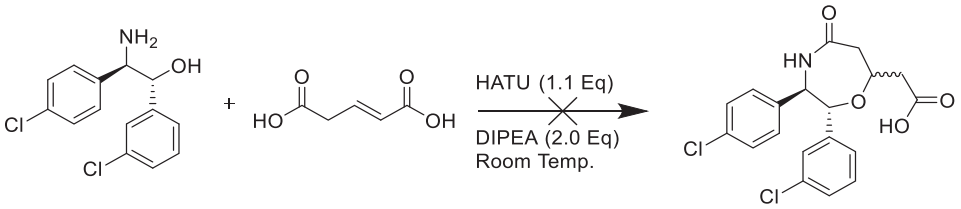

24 23 101

Entry	Solvent	Time (Hours)
1	DMF	Overnight
2	DMF	1.5

Table 2.5. Attempts for coupling of glutaconic acid (23) to TFA reaction mixture by using pyBOP

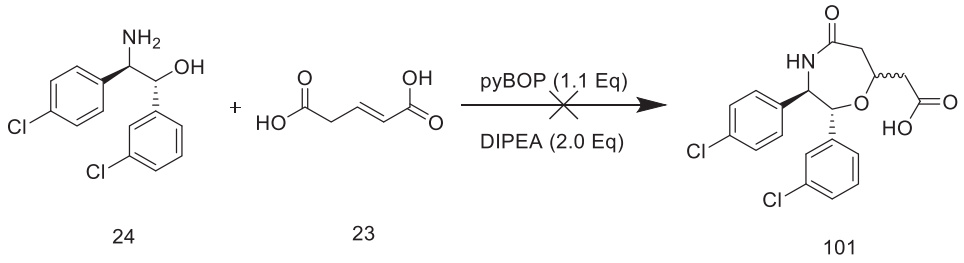

24 23 101

Entry	Solvent	Time(Hours)
1	DCM	1.5
2	DCM	5
3	DMF	5

2.2.Studies carried out by using N-Trt protected chiral aminoalcohol (105) and glutaconic acid (23) as precursors to prepare 1,4-oxazepan-5-one skeleton

Although Gonzales et al. (Gonzalez et al. 2014) reported that, Boc group can be used as a protective group in order to prepare the chiral aminol alcohol 24, it did not work in our hands. It seems that it is not stable enough during the addition of Grignard reagent.

Hence, in this part of the synthesis N-Trt protective group was used instead of N-Boc group. It is well known that N-Trt protective group is a quite stable against Grignard reagents. Synthesis were performed again starting from 4-chlorophenyl glycine 17 as shown in Table 2.6. Synthetic route is the same with the previous N-Boc protected amino alcohol 22. Synthetic route gave the expected chiral aminoalcohol 24 with good reproducibility (Table 2.6). The product of the first step was purified only once with 48% yield. In next trials the crude product was used in the next step. The yield of N-Trt protected aminoalcohol 103 quite well for two steps. Dess-Martin Periodinone oxidation of primary alcohol to corresponding chiral aldehyde 104 was also very good (75-100%).

During the addition of 3-chlorophenylmagnesium bromide to compound 104, formation of two diasteomers were observed. Purification of these two diasteomers were not so successful and two fractions were collected with varying ratios of the

diasteomers. At the last step diastereomerically rich fragment were reacted with TFA to produce chiral aminoalcohol 24. Interestingly second diasteomers could be purified in this step.

Table 2.6. Preparation of chiral aminoalcohol 24 by using trityl protecting group

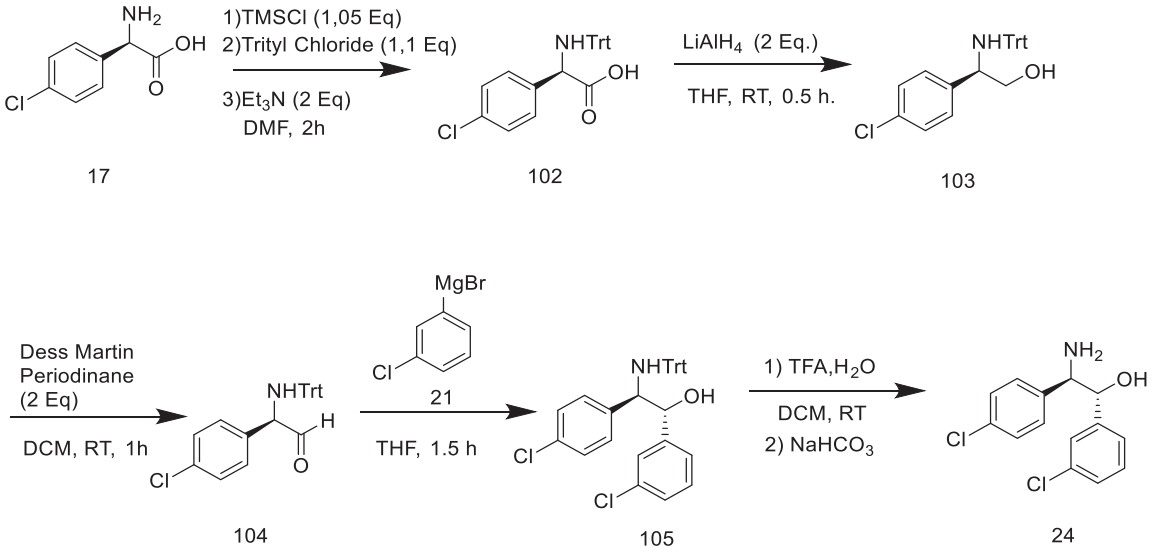

17 102 103 104 105 24

Entry	Yield %					
	102	103	104	105 Fraction 1	105 Fraction 2	24
1	48	95	85	42 (1:0,65)		-
2		73*	93	75 (1:0.15)		63
3		73*	94	43 (1:0.20)	47 (1:0.10)	70-
4		73*	94	23 (1:0.20)	25 (1:0.10)	
5		79*	92	20 (1:0.15)	25 (1:0.10)	24
6		65*	97	35 (1:0.50)		66
7		44*	93	26 (1:0.10)		65-
9		60*	85	35 (1:0.10)		50
10		55*	91	75 (1:0.15)		72
11		55*	94	79 (1:0,45)		-
12		42*	98	31 (1:0,40)	40 (1:1,40)	71
15		68*	100	26 (1:0,40)	36 (1:0,65)	55
16		42*	100	31 (1:0,40)	40 (1:1,40)	42
18		73*	93	19 (1:0,20)	12 (1:0,15)	70
19		77*	92	18 (1:0,40)	15 (1:0,12)	-
20		67*	93	14 (1:0,15)		68

*Overall yield for two steps.

In the next step of the synthesis, chiral aminoalcohol (24) should be coupled with trans-glutaconic acid (23) in order to form an amide group first then intramolecular Michael addition would give the 1,4-oxazepan-5-one derivative (101). For this purpose different coupling agents such as PyBOP (Figure 2.1), HATU (Figure 2.2) and DCC (Table 2.7) were used. Interestingly no product formation was observed in these reactions. H NMR analysis showed the lack of NMR signals belong to our expected chiral 1,4-oxazepan-5-one skeleton.

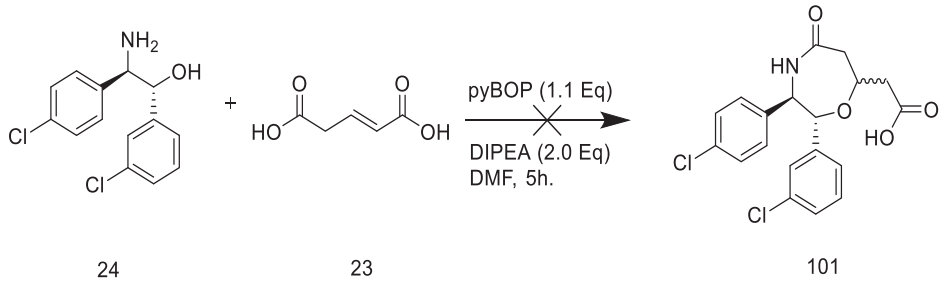

24 23 101

Figure 2.1. Trials for the coupling of chiral aminoalcohol (21) with t-glutaconic ACİD (23) in the prescence of PyBOP

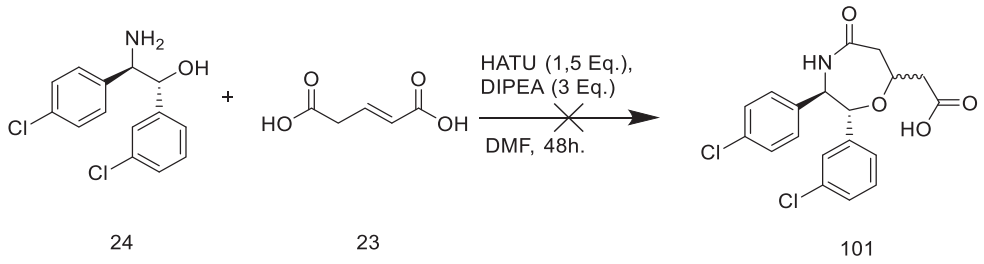

24 23 101

Figure 2.2. Trials for the coupling of chiral aminoalcohol (21) with t-glutaconic ACİD (23) in the prescence of HATU

Table 2.7. Trials for the coupling of chiral aminoalcohol (21) with t-glutaconic acid (23) in the prescence of DCC

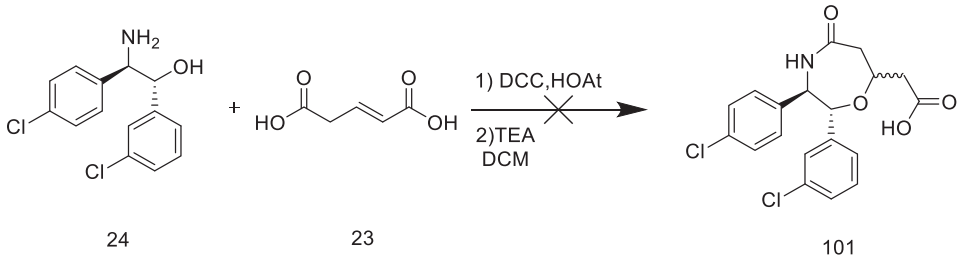

24 23 101

Entry	HOAt Eq.	DCC Eq.	TEA Eq.	Time(Hour)	Yield %23
1	2	2	2	2 h.	*
2	4	4	4	Overnight	*
3	4	4	4	Overnight	*

*NMR studies indicates the formation of unknown product.

As an alternative, stepwise approach was tried as shown in Figure 2.3. In here it was aimed to prepare OTBDMS protected chiral amino alcohol which can only form amide bond during coupling reactions. For this purpose, compound 105 was treated with TBDMSCl and base however no product formation was observed possibly because the prescence of sterically hindered N-Trt group close to the reaction center (Figure 2.3)

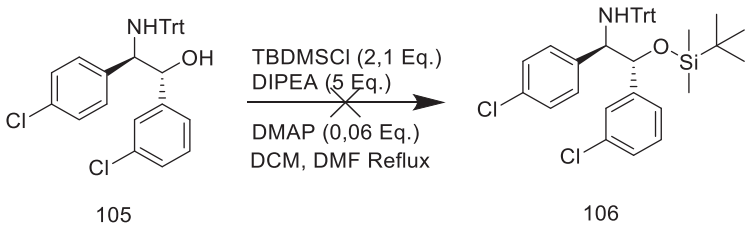

105 106

Figure 2.3. Trials for the TBDMS protection of OH group in chiral aminoalcohol 105

2.3.Studies carried by using glutaconic acid ester to modify the chiral aminoalcohol 24

In the next approach, possible Michael addition reaction of N-Trt protected chiral aminoalcohol 105 with dibenzylglutaconic acid ester 107 to produce compound 108, which can be directly transferred to 1,4-oxazepan-5-one structure

after removal of Trt group. For this purpose, various reaction conditions were tried as shown in Table 2.8. In the first two trials chiral aminoalcohol were recovered and no reaction formation was observed.

On the other hand, new product formations were observed in trials 3 and 4. ^{1}H NMR spectra of the products had new signals between 2-4 ppm. Especially NMR of the reaction performed with NaH was quite promising for the formation of the product with very low yield. In the NMR spectrum especially signals between 2.25 and 3.00 ppm indicates the prescence of glutaconic acid and derivative. This product was treated with TFA to release the amin group from Trt protection group and intramolecular cyclization reaction would gave seven membered ring system. However after treatment, doublet of doublets between 3-4 ppm in ^{1}H NMR for expected ring system could not be seen. Instead doublets coming from glutaconic acid remains unchanced (Figure 2.4).

Table 2.8. Attempts for the Michael addition of chiral aminoalcohol (105) to dibenzyl glutaconic acid ester (107)

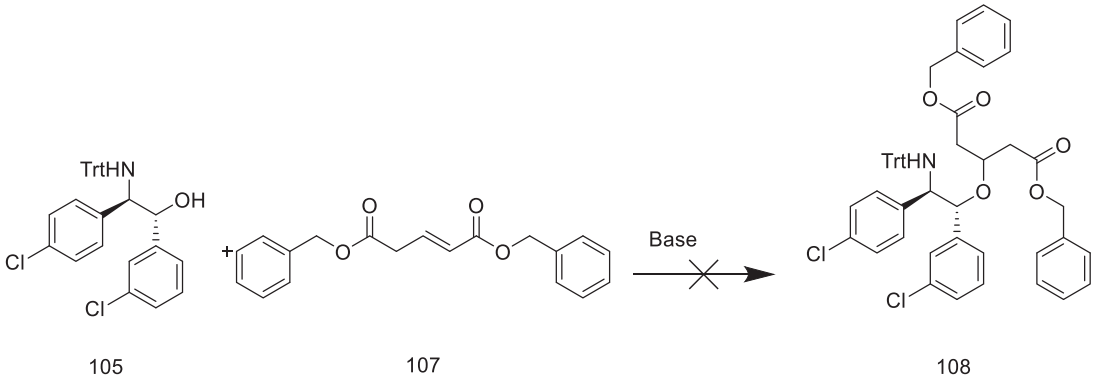

105 107 108

Entry	Solvent	Base (Eq)	Condition	Time(Hour)	Yield %
1	THF	$(CH_3)_3COK$ (1.5 Eq.) $(CH_3)_3COH$ (1.5 Eq.)	RT	Overnight	No Reaction
2	Toluene	Na_2CO_3 (1.5 Eq.) K_2CO_3 (1.5 Eq.)	RT	5	No Reaction
3	THF	NaH (4 Eq)	RT	6	Not expected product
4	DCM	DBU (1.1 Eq)	2 Hour RT 5 Hour Reflux	7	Not expected product

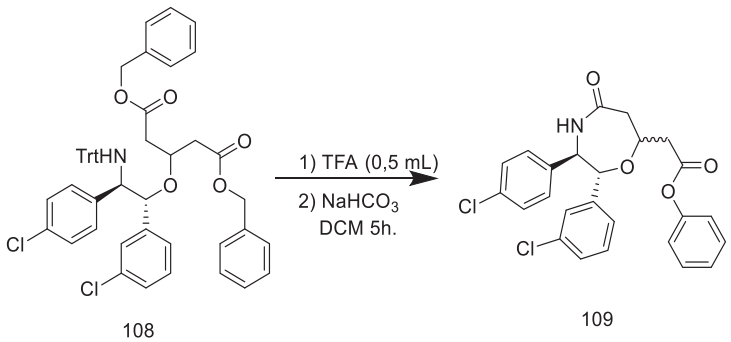

108 109

Figure 2.4. Attempts for the intramolecular cyclization of compounds 108

In the next synthetic plan, coupling of monobenzyl glutaconic acid ester to the chiral aminoalcohol (24) in the prescence of HATU then cyclization under basic condition to produce the diasteomers of 1,4-oxazepan-5-one skeleton as shown in Figure 2.5. For this purpose glutaconic acid (23) was reacted with benzylalcohol (110) by Mitsunobu reaction and two ester isomers (111a and 111b) were obtained as mixture. The yield of the product was better when the reaction was performed in DCM (Table 2.9).

Then the mixture was reacted with chiral aminoalcohol (24) in the prescence of HATU coupling agent. ^{1}HNMR of the products indicates the prescence of glutaconic acid in the structure. Glutaconic acid ester gave a doublet with 6.8 Hz coupling constants in the NMR around 2-3 ppm (Table 2.10). However in the next step it was expected to form a 1,4-oxazepan-5-one skeleton by intramolecular cyclization reaction Table 2.11. When the mixture is treated with K_2CO_3 base both compound should give the diasteomers. However ^{1}HNMR spectrum of the crude product of the loss of benzylic CH_2 signals around 5 ppm. Also doublet of doublet signals for the expected product could not be seen.

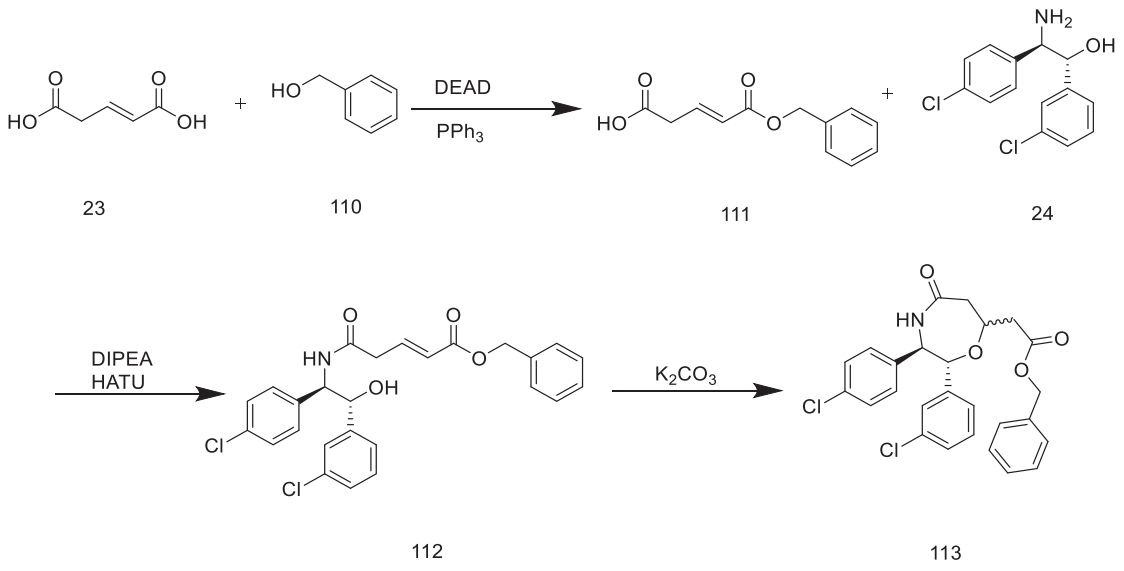

Figure 2.5. Proposed synthetic route for the stepwise preparation of diasteomeric mixtures of 1,4-oxazepan-5-one (113)

Table 2.9. Preparation of monobenzyl glutaconic acid ester (111a and 111b)

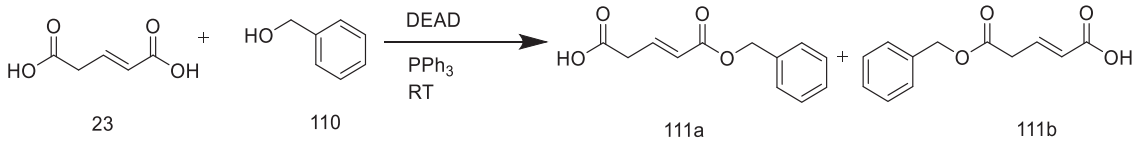

23 110 111a 111b

Entry	Solvent	Time(Hour)	Yield %
1	THF	6	8
2	DCM	Overnight	26

Table 2.10. Coupling of monobenzylglutaconic acid ester mixture to chiral aminoalcohol (24) by using HATU

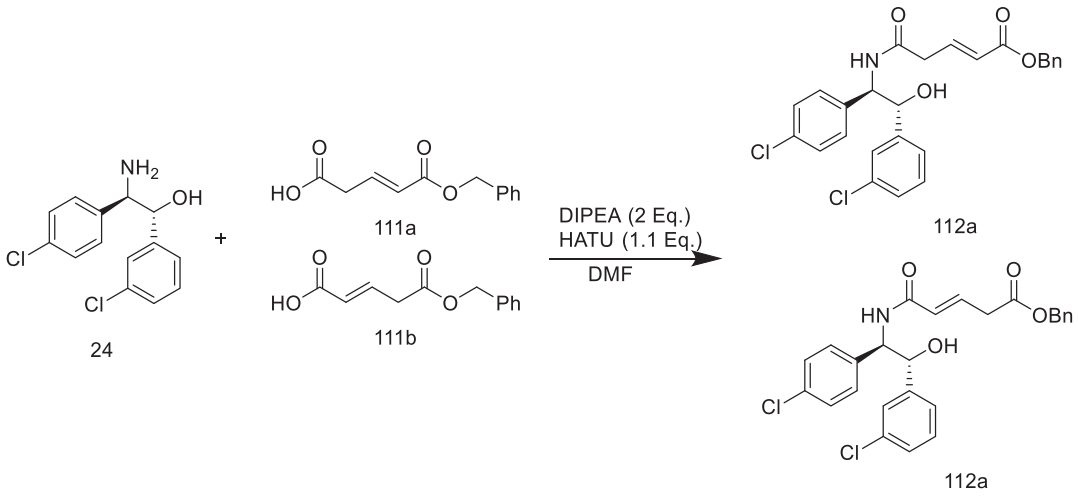

24 111a 111b 112a 112a

Entry	Compound 43 (Eq)	Time(Hour)	Yield 44%
1	1.1	1	66
2	1.1	1	48
3	1.1	1.5	59

Table 2.11. Attempts for the intramolecular cyclization reaction of 112a and 112b mixtures

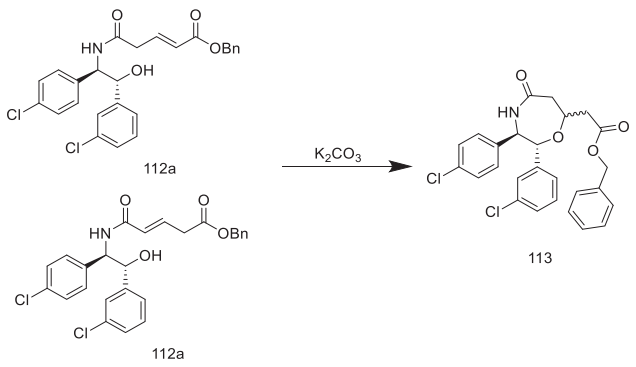

Entry	Solvent	Benzyl Alcohol (Eq.)	K_2CO_3 (Eq)	Time (Hour)	Yield %
1	CH_3OH	-	0,5	3	decomposition
2	DMF	4	2	3	decomposition
3	CH_3OH	-	0.5	3	decomposition

Due to the loss of benzylic CH_2 protons in the crude products ^1H NMR, monoesters of glutaconic acid (115a and 115b) were also prepared by using the synthetic procedure as shown in Figure 2.6. Then the mixture was coupled with aminoalcohol 24 by using HATU (Figure 2.7) to produce the corresponding amide mixtures. In this synthetic route, the glutaconic acid esters 39% yield. On the other hand, coupling reactions to aminoalcohol were not successful (Figure 2.7).

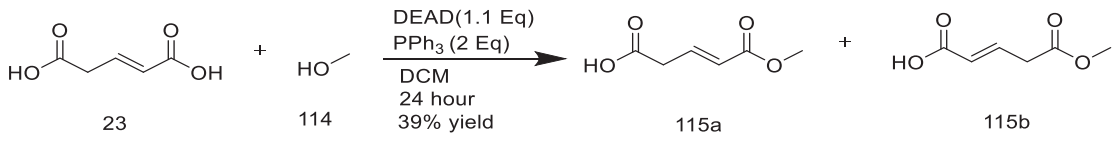

Figure 2.6. Preparation of the mixture of monomethyl glutaconic acid esters (115a and 115b)

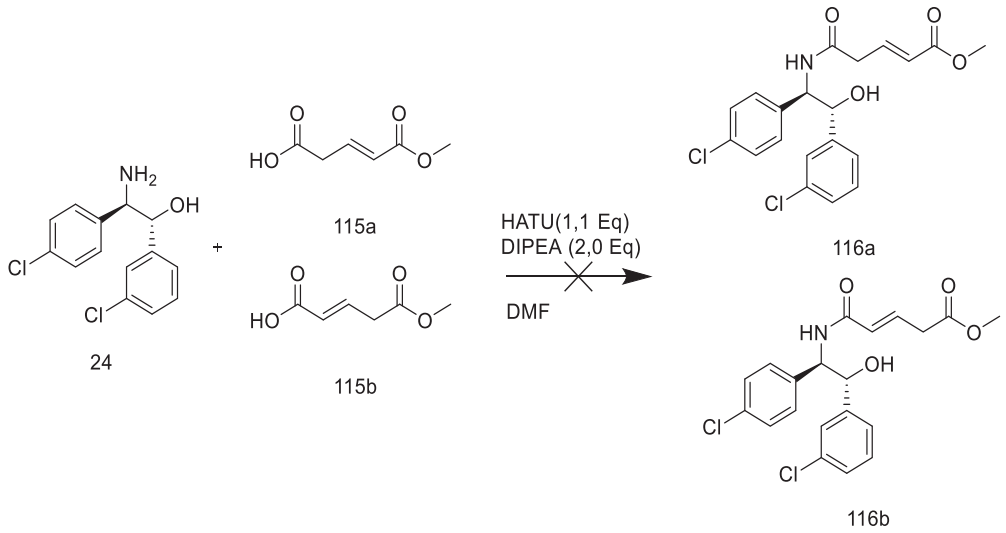

Figure 2.7. Preparation of the monomethylglutaconic acid amide mixtures starting from aminoalcohol 24

2.4.Studies carried out by using protected 5-hydroxy 2-pentanoic acid derivatives to modify the chiral aminoalcohol (34)

After all of the attempts toward the addition of glutaconic acid derivatives to chiral aminoalcohol (24) were failed, a new strategy was proposed on the base of formation and coupling of α,β-unsaturated 5-hydroxy pentanoic acid derivatives to the chiral aminoalcohol (24) (Figure 2.8). According to this strategy, TBDMS protected 1,3-propanediol was oxidized to corresponding aldehyde by using PCC and NaOAC. At the beginning of the trials, formation of the aldehyde could be monitored in the TLC but after purification process no product could be obtain. Then it was figured out that the boiling point of the aldehyde is very low and can be lost during solvent removal under reduced pressure.

Because of that in next trials aldehyde was prepared and used immediately in next step without completely concentrated under reduced pressure. In the next step aldehyde was reacted with the ylide of triethylphosphonate acetate to produce α,β-unsaturated ester 120 between 19-41% yields repeatedly (Table 2.12).

Hydrolysis of ester for this molecule was shown in the literature (Patent:T.Tetrasubstituted Alkene Compounds and Their use.US2018/141913,2018)

under basic conditions. Similarly, conversion of ester to carboxylic acid were tried many times but all attempts were failed (Table 2.13).

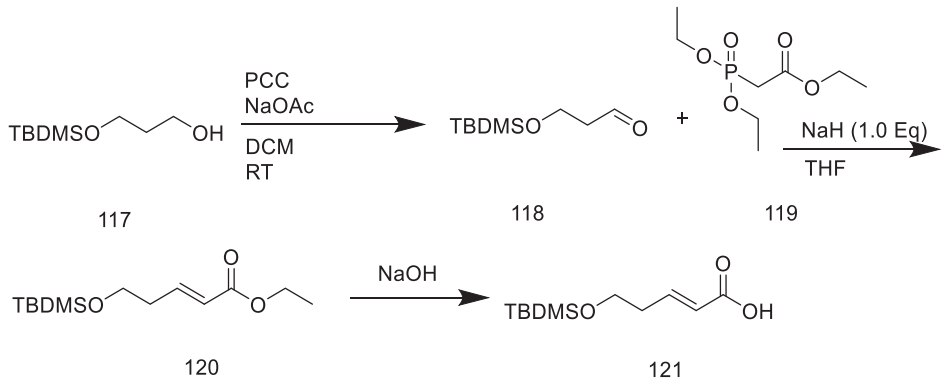

Figure 2.8. Proposed synthetic route fot the preparation of OTBDMS protected 5-hydroxy 2-pentanoic acid (121)

Table 2.12. Preparation of OTBDMS protected 5-hydroxy-2-pentanoic acid ethyl ester(120)

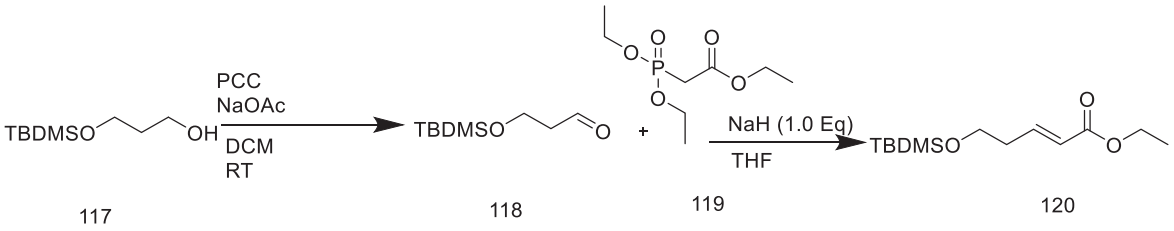

Entry	Yield % 118	Yield % 120
1	-	32*
2	-	38*
3	-	21*
4	-	27*
5	-	31*
6	-	19*
7	-	35*
8	-	40*
9	-	41*

*Overall yield for two steps

In this reaction, we encounter two important problems. The first one is OTBDMS is not stable at pH=14 and in the prescence acetic acid (our product is also a carboxylic acid). The second one is the formation of a transesterification product by reacting MeO^- ions. Relative amounts of acid and ester products can be detected from the ^1H NMR spectrum of crude product. As it can be seen from Table 2.13, it seems that more hydrolysis products were formed compared to the trans esterification product. In fact at longer reaction times, amount of total products were getting decreased. Overall recovery of the products were only 5-27 mg for these reactions. At last when K_2CO_3 was used as a base only 3% product was obtained. Due to the instability of the OTBDMS protective group, preparation of benzyl protected 5-hydroxy-2-pentanoic acid ester (126) was also studied.

Table 2.13. Synthesis of Compound 121

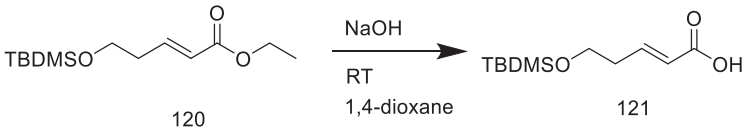

120 121

Entry	NaOH (Eq.)	Time (h)	Yield % 53
1	1.3	4	1:0.35 acid:ester mixture
2	2	8	1:0.35 acid:ester mixture
3	1.3	3	1:0.35 acid:ester mixture
4	1	8	1:0.4 acid:ester mixture
5	2	4	1:1 acid:ester mixture
6	K_2CO_3 (2.0 Eq)	4	3%

Conversion of 1,3-propanediol to monobenzyl ether was performed by addition of benzyl bromide under basic condition with 36% yield. Then primary alcohol oxidized to aldehyde and reacted with triethyl phosphonato acetate to produce benzyl protected ethyl 5-hydroxy-2-pentaoic acid (126) in 31% yield (Figure

2.9). Hydrolysis of ester with base gave the pentanoic acid derivative (127) in good yield (Figure 2.9).

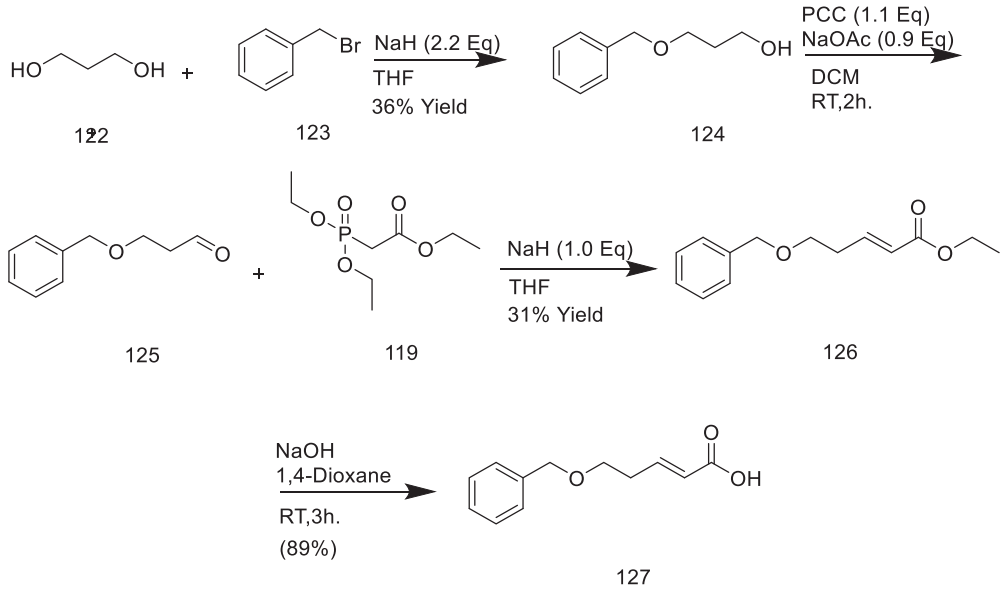

Figure 2.9. Conversion of 1,3-propanediol into benzyl protected 5-hydroxy-2-pentenoic acid (127)

Contrarly to the addition reactions of glutaconic acid monoesters to chiralaminoalcohol 24 were not successful, amide formation reaction between benzyl protected 5-hydroxy-2-pentenoic acid and aminoalcohol 24 could be carried out in moderate yields (16-63) as shown in Figure 2.10.

In the next step, intramolecular oxa-Michael reaction of compound 128 under basic conditions were failed in all of our trials (Table 19). In these trials, resin bond triphenylphosphine did not catalyzed the reaction, while all of the compound are consumed to form unexpected products under basic conditions (Table 2.14)

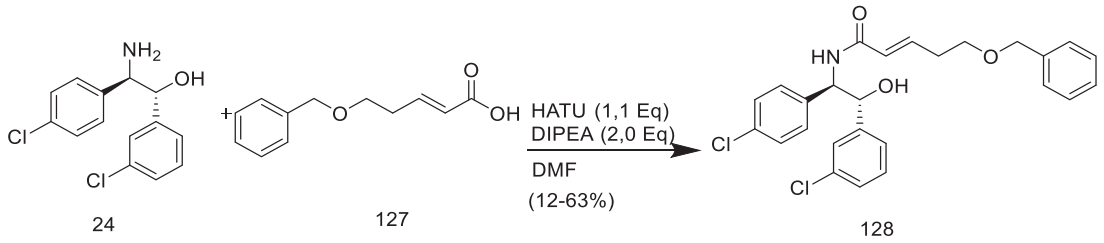

Figure 2.10. Coupling of benzyl protected 5-hydroxy-2-pentenoic acid with chiral aminoalcohol (24)

Table 2.14. Attempts for the intramolecular oxa-Michael cyclization reactions of compound (128)

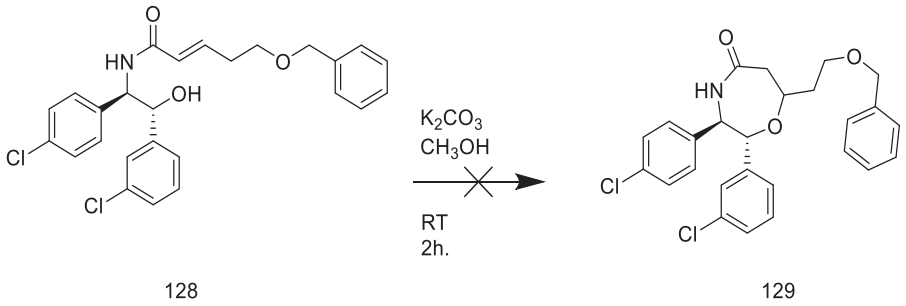

Entry	Catalayst	Solvent	Temperature (°C)	Time(hour)	Yield % 129
1	DBU	Toluene	90	Overnight	*
2	rPPh$_3$	THF	63	Overnight	No reaction
3	DMAP, DBU	Chloroform	RT-60	72	*
4	DBU	DMF	66-100	72	*

*Formation small amount of new compound was observed, but NMR studies indicate the lack of expected product.

The failure of the oxa-Michal reaction for compound 128 coluld be the prescence of acidic NH amide proton, whose deprotonation would give some polymerization reaction with α,β-unsaturated carbonyl. To test this possibility, N-Trt protected chiral aminoalcohol was treated with compound 127 in the perescence of HATU to form compound 128. All trials for this reaction were failed possibly due to the steric hinderance of the trityl group close to the reaction center. Alternatively the

same aminoalcohol (105) was treated with $rPPh_3$ to produce the Michael addition product 130, but again reactions were failed possibly due to the steric interactions (Figure 2.11).

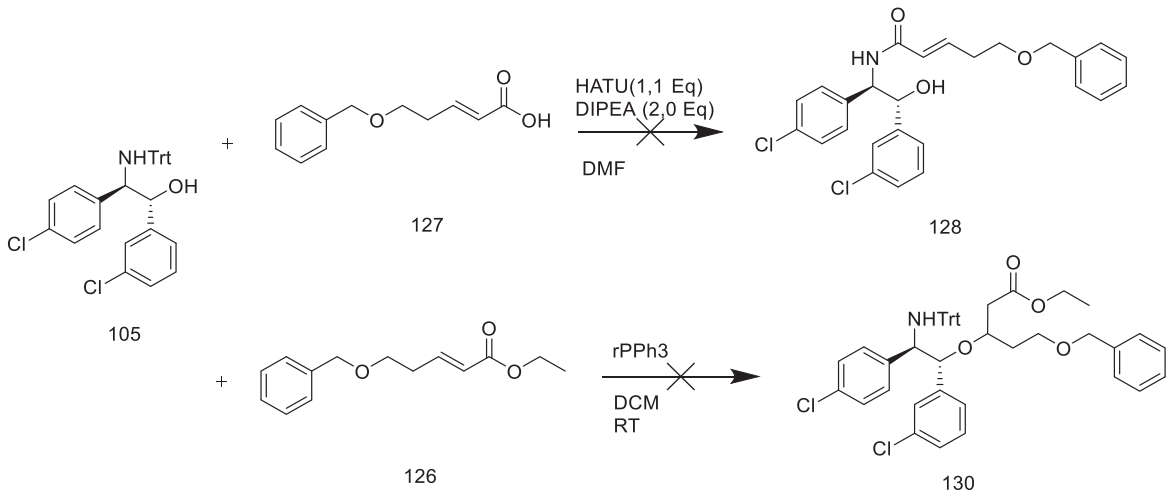

Figure 2.11. Synthesis of Compound 130

2.5.Installation of side chain first to eliminate the possible effect of acidic NH amide proton as an alternative strategy

To test the effect of the acidic NH proton, a new synthetic plan was proposed as shown in Figure 2.12. According to this, *R*-styrene oxide will be reacted with 3,4-dimethoxybenzyl alcohol (132) to produce compound (133). Then secondary alcohol can be converted to a good leaving group by adding Bs group under basic condition. Nucleophilic addition of chiral aminoalcohol 24 to benzylic position of compound 134.

Afterwards this secondary amine can be converted 1,3-dicarbonyl amide derivative (137), which can be further converted into triazol modfied 14-oxazepan-5-one derivative (Figure 2.12).

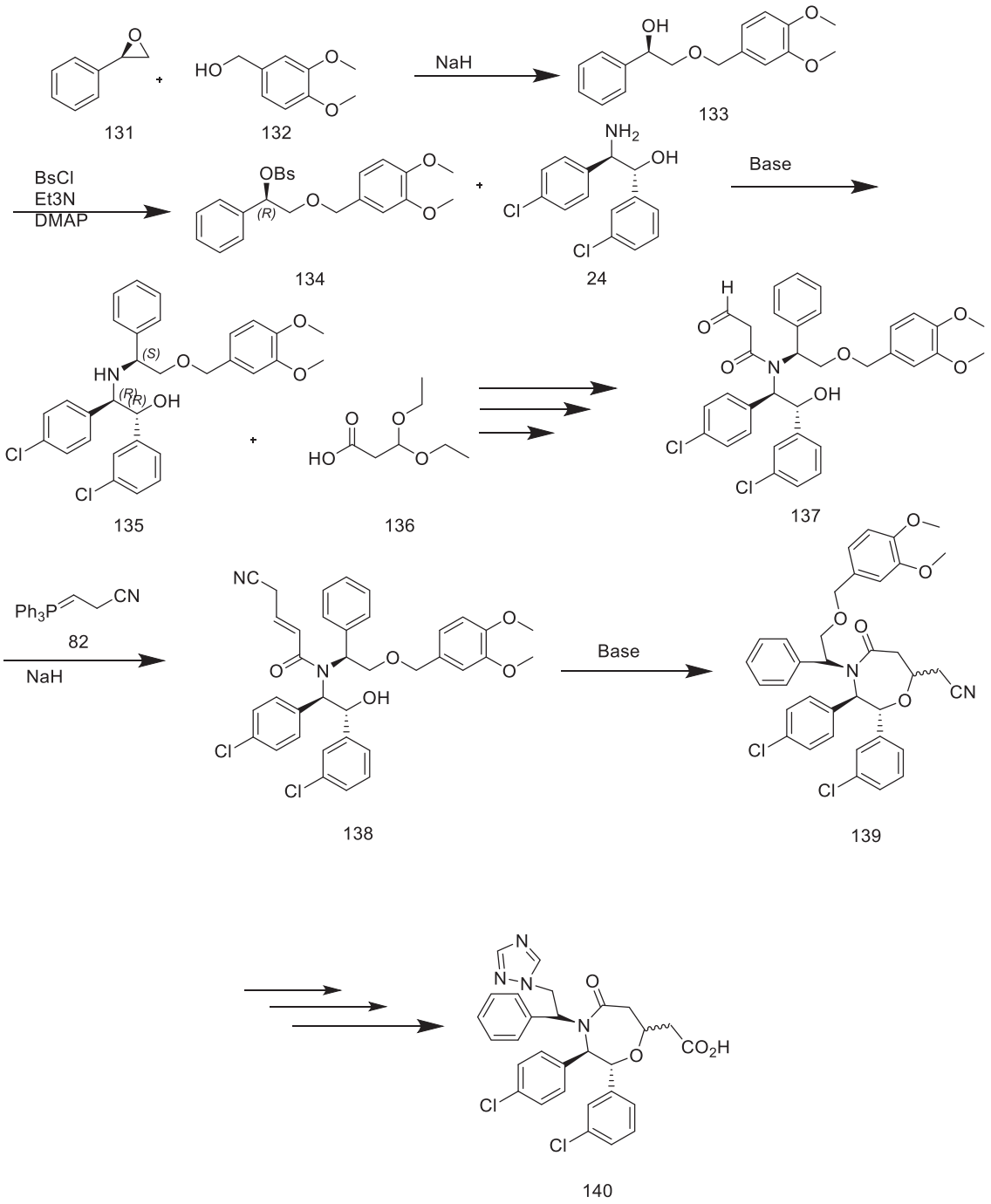

Figure 2.12. Synthesis plan of Compound 140

Compound 133 was successfully prepared starting from (*R*)-styreneoxide and 3,4-dimethoxy benzyl alcohol (132) in the prescence of NaH. This reaction was reproducible by 8-20% yields only (Figure 2.13). In the next step, generation of OBs leaving group was failed when one equivalent of BsCl was used at room temperature.

Interestingly, when 2 equivalent of BsCl was used formation of a intramolecular cyclization reaction occurred to produce compound 141 in 21% yield (Table 2.15)

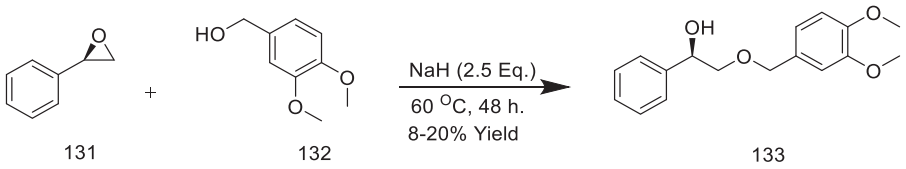

131 132 133

Figure 2.13. Addition of 3,4-dimethoxybenzyl alcohol to (*R*)-styrene oxide

Table 2.15. Attemts for the preparation of OBs leaving group

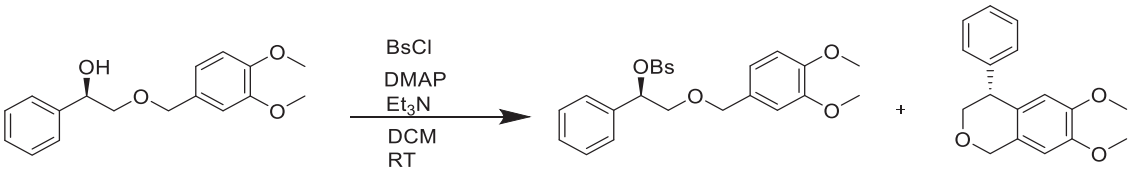

133 134 141

Entry	BsCl (Eq.)	Et_3N (Eq.)	DMAP(Eq.)	Time (h)	Yield % 134	Yield % 141
1	1	6	0.2	Overnight	-	-
2	2	4	0.1	3.5	-	21

Because of this intramolecular cyclization reaction installation of 1,2,4-triazole structure to side chain can be achieved by producing compound 144 starting from (*R*)-styreneoxide and 1,2,4-triazole under basic condition. This reaction gave a good yield (86%) of product formation (Figure 2.14). In the next step, conversion of alcohol to the OBs leaving group was tried. Although the formation of product was seen in TLC, by time it is started to give a side reaction and displacement of OBs group with chloride ion was observed (Table 2.16).

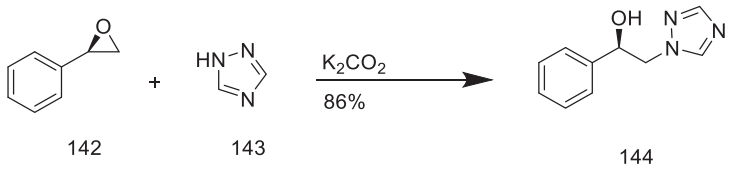

Figure 2.14. Addition of 1,2,4-triazole to (R)-styreneoxide

Table 2.16. Attemts toward the preparation of OBs leaving group triazol modified 1-phenyl ethanol 144

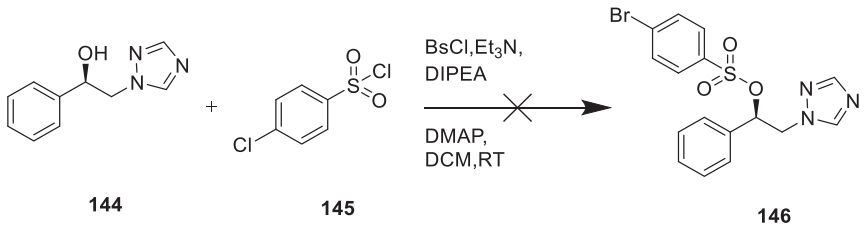

Entry	BsCl (Eq.)	Et_3N (Eq.)	DIPEA (Eq.)	DMAP(Eq.)	Time (h)	Yield % 146
1	2	2.5	-	-	Overnight	*
2	1.1	-	3	-	3	*
3	2	excess	-	0.1	12	*
4	1	excess	-	-	48	*
5	2	3	-	0.1	8	50% [a]
6	1	3	-	0.1	14	*

*Decomposition Product, [a] ^{1}H-NMR spectrum

To understand the effect of the aromatic ring system during the preparation of OBs leaving group, an isopropyl ether product (148) was produced starting from stryrene oxide (142) and isopropyl alcohol in the prescence of sodium hydride in 50% yield (Figure 2.15). Then formed secondary alcohol was reacted with BsCl as summarized in Table 2.17. The reaction only could be seen when three equivalent of DMAP to yield an unexpected product. It seems that installation of OBs group to a benzylic position is the main problem in these reactions. Because none of these leaving groups could be obtained this synthetic route was also aboundened.

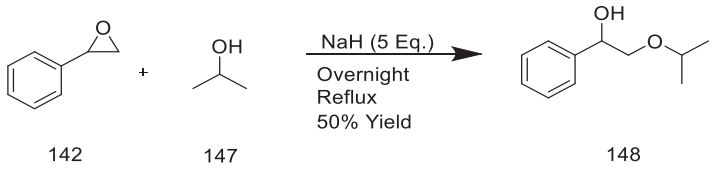

Figure 2.15. Addition of isopropyl alcohol to styrene oxide

Table 2.17. Synthesis of Compound 149

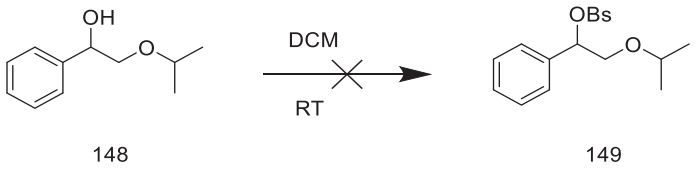

Entry	BsCl (Eq.)	DIPEA (Eq.)	DMAP(Eq.)	Time (h)	Yield % 92
1	2	3	0.1	24	No reaction
2	3	3	1.0	72	No reaction
3	5	-	3	30	Not expected product

2.6.Addition of 1,3-dicarbonyl species to chiral aminoalcohol (24) for a stepwise preparation of α,β-unsaturated ester derivatives

In this part of the thesis, medification of chiral aminoalcohol (24) with a 1,3-dioxo species then transformation into 1,4-oxazepan-5-one derivatives was aimed. As shown in Figure 2.16, acetal modified carboxylic acid (150) was successfully coupled with chiralamino alcohol in the perscence of HATU under basic condition. The yield of the reaction could be increased to 82% after 36 hours of stirring. In the next trials, all of the attempts for the conversion of acetal into aldehyde in the prescence of HCl, H_2SO_4 or I_2 in acetone were failed as shown in Figure 2.17. Interestingly, formation of aldehyde could be seen in ^{1}H-NMR of the crude product of the reaction in the prescence of H_3PO_4 (Figure 2.18). However aldehyde could not be purified from column chromatography.

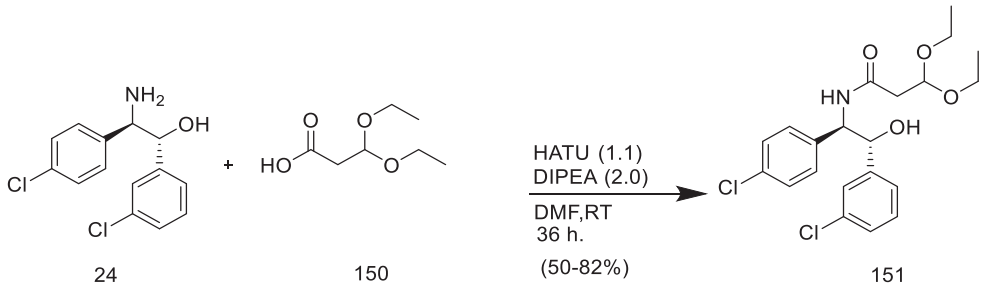

Figure 2.16. Coupling of acetal modified carboxylic acid (150) to aminoalcohol 24

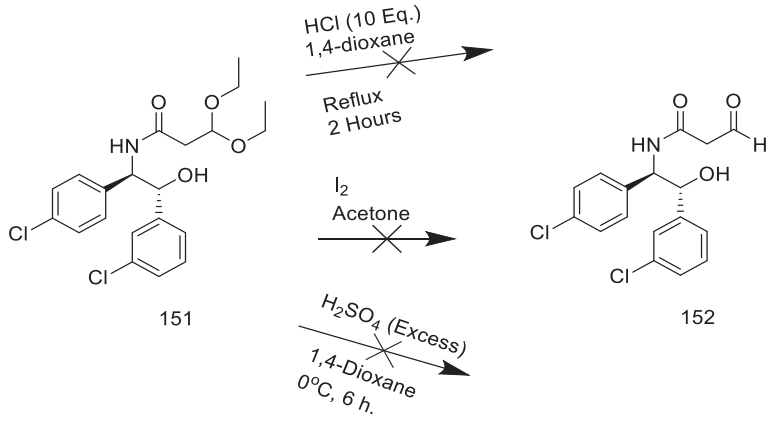

Figure 2.17. Attempts for the conversion of acetal to aldehyde by using HCl, I_2 and H_3PO_4

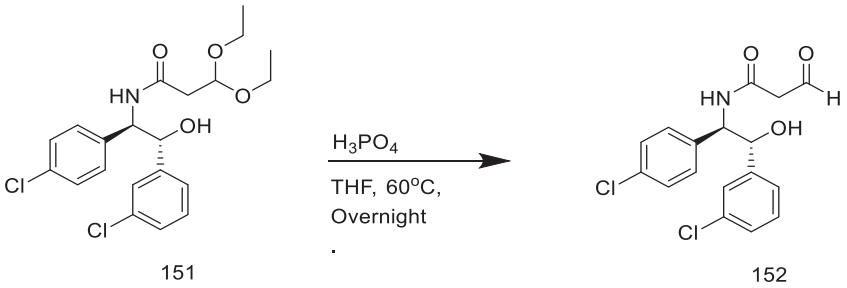

Figure 2.18. Attempts for the conversion of acetal to aldehyde by using H_3PO_4

Presence of activated methylene group between the two carbonyl groups in 1,3-dicarbonyl species or carbonyl α,β-unsaturated carbonyl in glutaconic acid derivatives may be the failure of pervious synthetic routes. To test this, 3-hydroxy-2,2-dimethyl propionic acid treated with PCC to form compound 154 (Figure 2.19).

All trials were failed and no aldehyde product could be purified from reaction mixture may be due to the possible decarboxylation reaction.

To eliminate such risk, compound 153 was coupled with amimoalcohol 24 by using HATU in 49-73% yields respectively (Figure 2.20). Later, different oxidizing agents were used to oxidize the primary alcohol to aldehyde. Although PCC did not give any product formation, DMP gave the corresponding aldehyde between 50-53% yiels respectively (Figure 2.21).

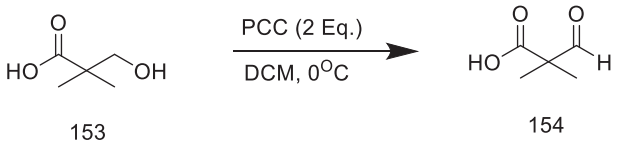

153 154

Figure 2.19. Attempts toward the oxidation of 3-hydroxy-2,2-dimethyl propanoic acid by PCC

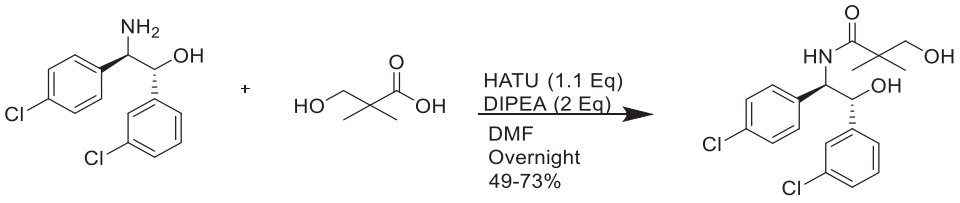

24 153 155

Figure 2.20. Addition of 3-hydroxy-2,2-dimethyl propanoic acid to chiral aminoalcohol (24)

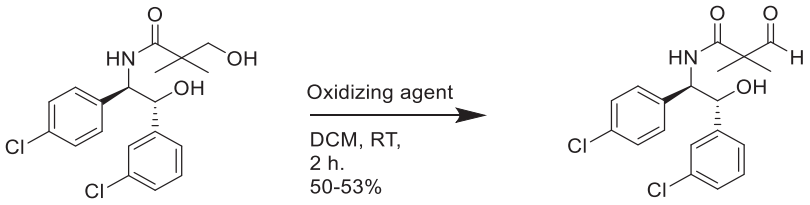

155 156

Figure 2.21. Formation of compound 156 by using DMP

Produced aldehyde (156) was reacted with the ylide of triethylphosphonato acetate to produce corresponding α,β-unsaturated ester (157), which is the dimethyl

substituted equivalent of glutaconic acid (Figure 2.22). At last, compound 157 was treated with different bases in order to form 1,4-oxazepan-5-one derivative (158). When similar reaction was performed for glutaconic acid derivatives mostly unwanted product formation or decomposition products were observed.

When the hydrogens of active methylene are excahanged with methyl groups, extra stability were seen for the α,β-unsaturated ester functional group in compound 157. This results implies that the prescence of acidic active methylene hydrogens are the main reason for the failure of the glutaconic acid derivatives.

On the other hand, formation of intramolecular oxa-Michael reaction for compound 157 could not be seen probably due to the prescence of a quaternary carbon next to β-carbon of α,β-unsaturated carbonyl. Prescence of steric interaction may block the reaction (Table 2.18).

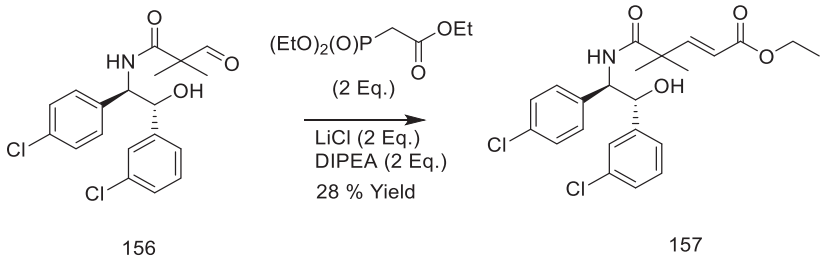

Figure 2.22. Synthesis of Compound 157

Table 2.18. Synthesis of Compound 158

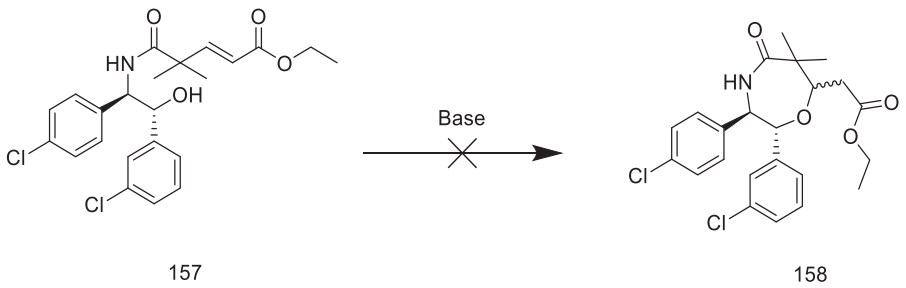

157 158

Entry	Base (Eq)	Temperature (^oC)	Time (Hour)	Solvent	% Yield
1	K_2CO_3 (0.5)	RT	5	EtOH	a
2	DBU (5)	RT	24	THF	a
3	DBU (5)	95	24	THF	b
4	Et_3N (3)	Reflux	5	THF	a
5	K_2CO_3	Reflux	5	EtOH	b

a:no product formation, b:decomposition products are formed room temperature

2.7.Preparation of novel 1,2,3 triazole substituted Coumarin derivatives

In this part of thesis, preparation of 1,4 disubstituted triazole modified coumarin structure was prepared. Acetyl salicylic acid was converted to its OAt ester (160) by reacting with HATU in the prescence of DIPEA. Reaction was monitored by TLC and whenever all starting materials are consumed, the crude product was treated with a mixture of NaH and dimethylmalonate to produce 4-OH coumarin ester (161). Then OH group at position 4- of coumarin was modified by reacting TsCl in the perscence of TEA to produce a pseudohalide OTs group (162). This syntetic route was quite reproducible and 4-OTf coumarin derivative was prepared in 69-92% yields (Table 2.19).

Table 2.19. Preparation of 4-OTs coumarin derivative (162)

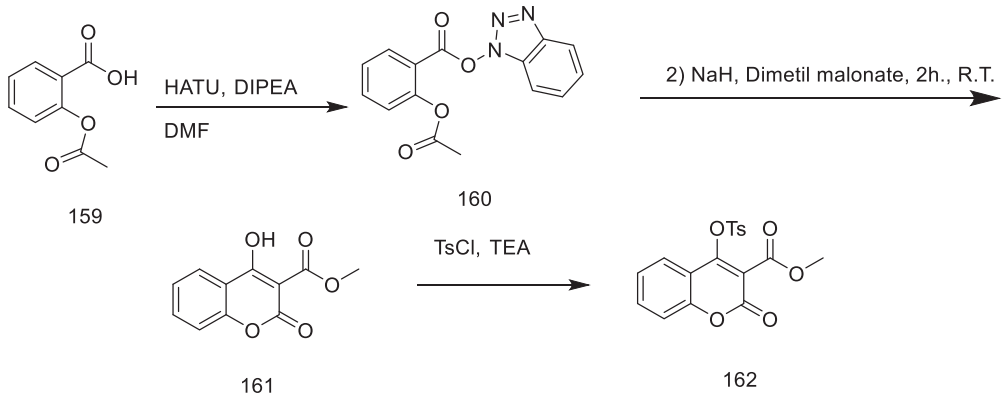

Entry	Yield % 160	Yield % 161	Yield % 162
1	-	-	92*
2	-	-	85*
3	-	-	77*
4	-	-	69*

*Overall yield for compound two steps

Next, 4-OTf coumarin derivative (162) was reacted with trimethylsilylacetylene by Sonagashira coupling in the prescence of $PdCl_2$ and CuI catalyst by 9-54% yields (Table 2.23). TBAF as used F^- source to remove the TMS group from compound 164, but the reaction. simply produced an unwanted dark brown side product (Figure 2.24). It seems that after formation of acetylenic carbonion, it reacts with ester to produce a mixture of oligomers and polymers. To overcome this problem ecetic acid was added to the reaction mixture and compound 165 was produced in 73% yield.

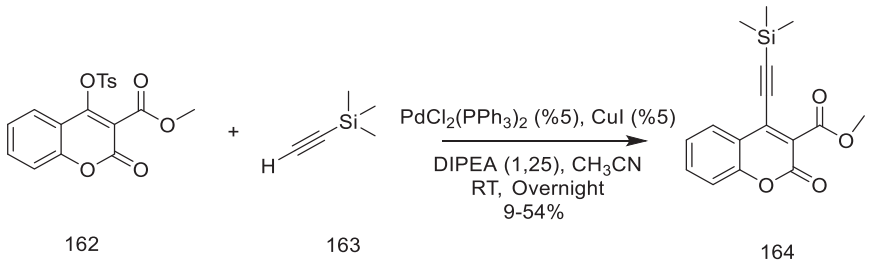

Figure 2.23. Sonagashira coupling of trimethylacetylene with 4-OTs coumarin (162)

164 165

Figure 2.24. Attempts to remove TMS group only by TBAF

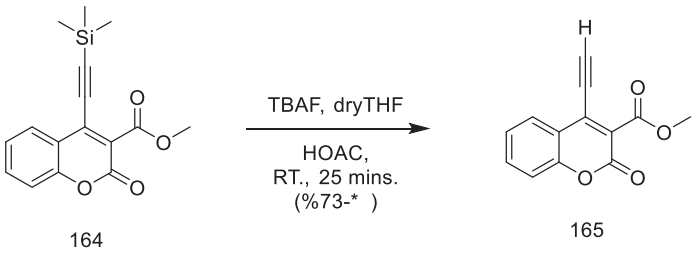

164 165

*Used without purification

Figure 2.25. Removal of TMS group by TBAF-HOAc mixture

Afterwards, click chemistry was used to generate 1,4-disubstituted 1,2,3-triazole functional group by reacting alkyne (165) and 4-chlorobenzyl azide (166) in the prescence of Cu(I) ion in DIPEA-HOAc mixture. In the last step of the synthesis, ester functional group was transformed to amide by simply heating with 2-(4-fluorophenyl)ethanamine (168) to produce the target product (169) in moderate yields.

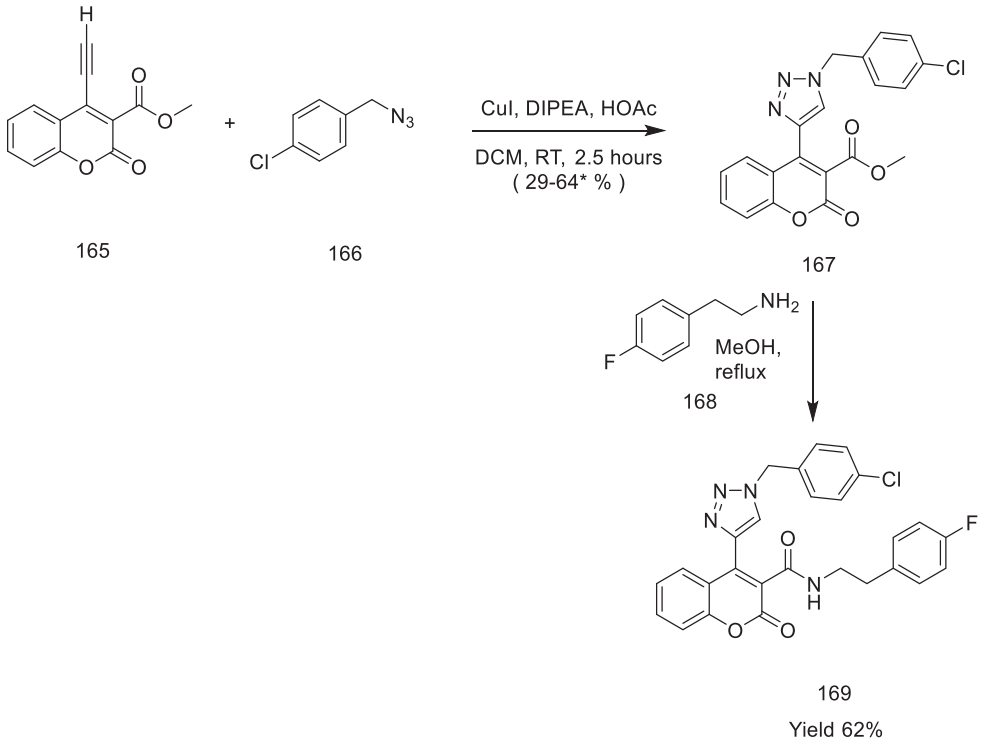

165 166 167 168 169

Yield 62%

*Overall yield for compound 121 and 123.

Figure 2.26. Preparation of target 1,4-disubstituted triazol modified coumarin derivative 169

CHAPTER 3

EXPERIMENTAL

3.1. General Methods

Purchased from Sigma-Aldrich and Riedel, reagents were used as supplies (Extra pure grade). Merck TLC plates were used for thin-layer chromatography monitoring of reactions (Silica gel 60 F254). Using column chromatography, substances were separated and isolated chromatographically. For column chromatography, 70-230 mesh silica gel was used. In addition, commercial-grade solvents were used as supplied. The spectrometer Varian 400-MR (400 MHz) collected ^{1}H NMR and ^{13}C NMR data. The ^{1}H-NMR and ^{13}C-NMR chemical shifts are given in (ppm). Reference peaks for ^{1}H-NMR (7.26 ppm) and ^{13}C-NMR (77.36 ppm) were the $CDCl_3$ peaks.

3.1.1. (R)-2-Amino-2-(4-chlorophenyl) ethanol (18)

A solution of 1 M $LiAlH_4$ in THF was dissolved in 5.0 mL of anhydrous THF and was heated up to 75 °C under a nitrogen atmosphere. (R)-2-amino-2-(4-chlorophenyl)acetic acid (17) (370 mg, 2.0 mmol) was added in several portions. The reaction mixture was heated up to reflux for about 3h, cooled to room temperature, and quenched by adding water (8.0 mL), aqueous 15% NaOH (8.0 mL), and water (25.6 mL), successively. The mixture was stirred vigorously for 30 min. The solids were filtered off, rinsed with THF and the combined organics were concentrated in vacuo and water phase extracted with EtOAc then combined organic phase was dried with $MgSO_4$ and evaporated under reduced pressure to provide compoud 18 as a yellow solid (96% yield, 327.3 mg). ^{1}H NMR (400 MHz, $CDCl_3$) δ 7.31− 7.35 (m, 2H), 7.29 (m, 2 H), 4.05 (br s, 1H), 3.69−3.78 (m, 1H), 3.53 (dd, J = 10.56 and 8.02 Hz, 1H), 2.48 (br s, 1H), 1.59 (br s, 2 H).

3.1.2. (R)-tert-Butyl 1-(4-Chlorophenyl)-2-hydroxyethylcarbamate (19)

A solution of di-tert-butyl dicarbonate (495.5 mg, 1.62 mmol) in DCM (8 mL) was added dropwise to a solution of compoud 18 (277 mg, 1.6 mmol) in DCM (10 mL) at 0 °C. After the addition was completed, the ice bath was removed and the reaction mixture was stirred at room temperature for 2 h. The reaction mixture was concentrated in vacuo and the crude material was purified with column chromatography (Hexane:EtOAc 4:1) (75% yield, 328.3 mg). ^{1}H NMR (400 MHz, DMSO-d_6) δ 7.33−7.39 (m, 2H), 7.27−7.32 (m, 2H), 7.24 (d, J = 8.02 Hz, 1H), 4.75−4.84 (m, 1H), 4.43−4.56 (m, 1H), 3.41 3.52 (m, 2), 1.36 (s, 9) $[\alpha]_D^{20}$= -250.0º (c=1.00, CH_2Cl_2)

3.1.3. (R)-tert-Butyl 1-(4-Chlorophenyl)-2-oxoethylcarbamate (20)

1,1,1-Tris(acetoxy)-1,1-dihydro-1,2-benziodoxol-3-(1H)-one(Dess−Martin periodinane) (852.1 mg, 2.0 mmol) was added in several portions to a stirred suspension of compound 19 (273 mg, 1.0 mmol) in wet DCM (8.0 mL of DCM/8.0 μL of water) at room temperature. The mixture was stirred for 1 h, diluted with diethyl ether (25.0 mL), and quenched by adding a solution of $Na_2S_2O_3$ (7 equiv) in saturated aqueous $NaHCO_3$ solution (25 mL) at room temperature. The mixture was stirred vigorously for 5 min, and the layers were separated. The aqueous layer was extracted with diethyl ether (40 mL). The organics were pooled, washed with saturated aqueous $NaHCO_3$ solution and brine, dried over $MgSO_4$, filtered, and the filtrate was concentrated. The crude material was used in the next step without further purification (98% yield, 265 mg) ^{1}H NMR (400 MHz, $CDCl_3$) δ 9.46 (br s, 1H), 7.31− 7.37 (m, 2H), 7.17−7.24 (m, 2H), 5.58−5.92 (m, 1H), 5.25 (d, J = 3.72 Hz, 1H), 5.14−5.34 (m, 1H), 1.27−1.45 (m, 9H).

3.1.4. tert-Butyl (1R,2R)-2-(3-Chlorophenyl)-1-(4-chlorophenyl)-2-hydroxyethyl carbamate (22).

Compound 20 (193 mg, 0,7 mmol) was dissolved at -40.0 ºC in 3 ml dry THF then 0,5 M 3-chlorobenzene magnesium bromide (21) (2,8 mL, 1,4 mmol) was added dropwise in two minutes. The mixture was stirred for an additional 2 h at -40.0 ºC. The reaction mixture was poured into 100 mL of a cold saturated aqueous NH_4Cl solution. The two layers were separated, and the aqueous layer was extracted with ethyl acetate

(3 × 30 mL). The combined organic layer was dried with $MgSO_4$, filtered, and the filtrate was concentrated under reduced pressure. The residue was purified with column chromatography (Hexane:EtOAc 8:1, 4:1 and 2:1) (50% yield obtained fron NMR , 134mg). Rf = 0.5 (Hexane:EtOAc, 4:1) $[\alpha]_D^{20}$= 30.0º (c=1.00, CH_3OH)

3.1.5. (1R,2R)-2-amino-1-(3-chlorophenyl)-2-(4-chlorophenyl)ethan-1-ol (24).

Compound 20 was dissolved with 2 ml dry DCM under nitrogen atmosphere. Then 320 µL TFA was added drop by drop at 0ºC. Ice bath was removed and reaction mixture was stirred at room temperature for 1.5 hours. Crude product's organic solvent was evaporated under reduced pressure and then $NaHCO_3$ X DCM (3X 30 mL) extraction was performed. The combined organic layer was dried with $MgSO_4$, filtered, and the filtrate was concentrated under reduced pressure. The residue was purified with column chromatography (Hexane:EtOAc 2:1 2-6% MeOH) (43% combined yield, 32mg). Rf = 0.07 (Hexane:EtOAc, 4:1 2% MeOH) ^{1}H NMR (400 MHz, CD_3OD) δ 7.87 – 7.83 (m, 1H), 7.49 – 7.45 (m, 1H), 7.24 – 7.20 (m, 2H), 7.18 – 7.14 (m, 4H), 4.62 (d, *J* = 7.9 Hz, 1H), 3.99 (d, *J* = 7.9 Hz, 1H) $[\alpha]_D^{20}$= +224º (c= 1,00, CH_2Cl_2)

3.1.6. (R)-2-(4-chlorophenyl)-2-(tritylamino)acetic acid (102).

(R)-2-amino-2-(4-chlorophenyl)acetic acid was dissolved with 4 mL of dry DMF 114.0 µL trimethylsilly chloride was added on the solution. Tis mixture was stirred until seeing a clear solution about 10 minutes. After observing clear solution 315.0 mg of trityl chloride was added then 301.0 µL triethylamine was added. Reaction mixture was stirred abour 2 hours, diluted with 20.0 mL diethyl ether and then 20.0 mL water. Reaction mixture was acidified with 1.0 M HCl until pH=3. The reaction mixture was extracted with (3X30 mL) diethyl ether then organic phase was washed with water and brine. The combined organic layer was dried with $MgSO_4$, filtered, and the filtrate was concentrated under reduced pressure. The residue was purified with column chromatography (Hexane:EtOAc 8:1 and 4:1) (48% combined yield, 222.0 mg). Rf = 0.22 (Hexane:EtOAc, 4:1) ^{1}H NMR (400 MHz, $CDCl_3$) δ 7.45 – 6.98 (m, 19H), 4.31 (s, 1H).

3.1.7. (R)-2-(4-chlorophenyl)-2-(tritylamino)ethan-1-ol (103).

(R)-2-(4-chlorophenyl)-2-(tritylamino)acetic acid 102 (200 mg, 0.46 mmol) was dissolved with 3.0 mL dry THF, $LiAlH_4$ (35.0 mg, 0,92 mmol) was dissolved with 2.0 mL of dry THF then added drop by drop on the solution at room temperature. Reaction was stirred about 30 minutes then cooled to 0 ^oC quenched with water and then 2.0 mL of sulfuric acid and 20.0 mL of diethyl ether was added. The reaction mixture was extracted with (3X30 mL) diethyl ether then organic phase was washed with saturated NaOH and brine. The combined organic layer was dried with $MgSO_4$, filtered, and the filtrate was concentrated under reduced pressure. The residue was used without purifiying. (95% yield, 181.0 mg). Rf = 0.47 (Hexane:EtOAc, 4:1) ^1H NMR (400 MHz, $CDCl_3$) δ 7.50 – 7.47 (m, 4H), 7.31 – 7.13 (m, 15H), 3.72 (t, J = 6.2 Hz, 2H), 3.20 (dd, J = 10.9, 4.4 Hz, 1H), 2.77 (dd, J = 10.9, 5.1 Hz, 1H) $[\alpha]_D^{20}$= -315^o (c= 1,00, CH_2Cl_2).

3.1.8. (R)-2-(4-chlorophenyl)-2-(tritylamino)acetaldehyde (104)

1,1,1-Tris(acetoxy)-1,1-dihydro-1,2-benziodoxol-3-(1H)-one (Dess−Martin periodinane) (323.0 mg, 0.80 mmol) was added in several portions to a stirred suspension of compound 103 (165.0 mg, 0.40 mmol) in wet DCM (8.0 mL of DCM/8.0 μL of water) at room temperature. The mixture was stirred for 1 h, diluted with diethyl ether (25.0 mL), and quenched by adding a solution of $Na_2S_2O_3$ (7 equivalent) in saturated aqueous $NaHCO_3$ solution (25 mL) at room temperature. The mixture was stirred vigorously for 5 min, and the layers were separated. The aqueous layer was extracted with diethyl ether (40 mL). The organics were pooled, washed with saturated aqueous $NaHCO_3$ solution and brine, dried over $MgSO_4$, filtered, and the filtrate was concentrated. The crude material was used in the next step without further purification (85% yield, 139.0 mg) ^1H NMR (400 MHz, $CDCl_3$) δ 9.04 (s, 1H), 7.34 – 7.15 (m, 19H), 4.41 (s, 1H).

3.1.9. (1R,2R)-1-(3-chlorophenyl)-2-(4-chlorophenyl)-2-(tritylamino)ethan-1-ol (105)

Compound 105 (139 mg, 0.35 mmol) was dissolved at -40.0 ^oC in 3 ml of dry THF then 0,5 M 3-chlorobenzene magnesium bromide (21) (1.8 mL, 0.88 mmol) was

added dropwise in two minutes. The mixture was stirred for an additional 1.5 h at -40.0 ^{o}C. The reaction mixture was poured into 100 mL of a cold saturated aqueous NH_4Cl solution. The two layers were separated, and the aqueous layer was extracted with ethyl acetate (3×30 mL). The combined organic layer was dried with $MgSO_4$, filtered, and the filtrate was concentrated under reduced pressure. The residue was purified with column chromatography (Hexane:EtOAc 10:1, 8:1 and 4:1) (42%, 77.0mg). Rf = 0.5 (Hexane:EtOAc, 4:1) $[\alpha]_D^{20}$=-416^{o} (c=1.00, CH_3OH) ^{1}H NMR (400 MHz, $CDCl_3$) δ 7.41 – 7.35 (m, 5H), 6.88 – 6.80 (m, 3H), 4.43 (d, J = 7.9 Hz, 1H), 3.93 (d, J = 7.9 Hz, 1H).

3.1.10. (E)-5-(benzyloxy)-5-oxopent-3-enoic acid (111)

Glutaconic acid 23 (100 mg, 0,77 mmol) and benzyl alcohol 110 (319 µL, 3.1 mmol) was dissolved in 2 mL of dry DCM at room temperature under nitrogen atmosphere DEAD (368.4 µL, 0,85 mmol) and $rPPh_3$ (282 mg, 0,85 mmol) was added and this mixture stirred for overnight. It was filtered with DCM organic solvent was evaporated under reduced pressure. The residue was purified with column chromatography compound 111a and 111b was obtained (Hexane:EtOAc 1:1-Hexane:EtOAc 1:1 5% Methanol 1% Acetic Acid) Rf = 0.6 (Hexane:EtOAc 1:4 5% Methanol 1% Acetic Acid) 26% yield ^{1}H NMR (400 MHz, $CDCl_3$) δ 7.39 – 7.29 (m, 10H), 7.17 – 7.00 (m, 2H), 6.04 – 5.89 (m, 2H), 5.18 (s, 2H), 5.16 (s, 2H), 3.30 (dd, *J* = 7.1, 1.2 Hz, 2H), 3.26 (d, *J* = 6.9 Hz, 2H).

3.1.11. benzyl (E)-5-(((1R,2R)-2-(3-chlorophenyl)-1-(4-chlorophenyl)-2-hydroxyethyl)amino)-5-oxopent-2-enoate (112)

Compound 111 (28 mg, 0,13 mmol), 2-(7-aza-*1H*-benzotriazole-1-yl)-1,1,3,3-tetramethyluronium hexafluorophosphate (HATU) (48 mg, 0,13 mmol) and N,N-diisopropylethylamine (DIPEA) (40 µL, 0,23 mmol) was dissolved in 1 mL dry DMF under nitrogen atmosphere. Compound 24 was dissolved with 1 mL dry DMF in a two necked flask under nitrogen atmosphere then compound 24, HATU and DIPEA mixture was added on it reaction was stirred for 1 hour. The reaction mixture was extracted with 100 mL 1M HCl X DCM (3X 30 mL). Combined organic phase was dried with $MgSO_4$

filtered and evaporated under reduced pressure. Product was used without purification. Rf = 0.48 (100 Chloroform:8 Methanol)

3.1.12. (*E*)-5-methoxy-5-oxopent-3-enoic acid (115)

Glutaconic acid 23 (200 mg, 1,52 mmol) was dissolved in 2 mL dry DCM at room temperature under nitrogen atmosphere and methanol 114 (250 uL, 6.1 mmol) was added on it. DEAD (740 µL, 1,67 mmol) and $rPPh_3$ (560 mg, 1,67 mmol) was added and this mixture stirred for 24 hours. It was filtered with DCM. Organic solvent was evaporated under reduced pressure. The residue was purified with SiO_2 column chromatography (Hexane:EtOAc 1:1- Hexane:EtOAc 1:1 2% Methanol 1% Acetic Acid) Rf = 0.48 (Hexane:EtOAc 1:4 5% Methanol, 1%Acetic Acid) 39% yield. ^1H NMR (400 MHz, $CDCl_3$) δ 7.18 – 6.95 (m, 1H), 5.96 (dd, J = 15.6 and 8.7 Hz, 1H), 3.74 (dd, J = 7.2 and 2.2 Hz, 2H), 3.29 (d, J = 7.0 Hz, 2H).

3.1.13. TBDMS protected 3-hydroxypropanol (118)

Sodium acetate (194.4 mg, 2.37mmol) was dissolved in 4 mL of dry DCM under nitrogen atmosphere 3-((tert-butyldimethylsilyl) oxy) propanol (560.0 µL, 2.63mmol) was added on it. PCC (625.0 mg, 2.9 mmol) was added on it in two portions at 0 ºC. The reaction mixture was stirred for 2 hours under nitrogen atmosphere at room temperature and diluted with 100 mL diethyl ether and stirred for a further 10 minutes. The reaction mixture was filtered through a (silica gel- magnesium sulfate) mixture column with 300 mL diethyl ether. The resulting organic phase was extracted with 10% NaOH solution and brine solution. Combined organic phase was dried with $MgSO_4$ filtered and evaporated under reduced pressure until left about 20 mL diethl ether. Product was used without purification. Rf= 0.6 (EtOAc: Hexane 1: 4) ^1H NMR (400 MHz, $CDCl_3$) δ 9.78 (t, J = 2.1 Hz, 1H), 3.97 (t, J = 6.0 Hz, 2H), 2.58 (td, J = 6.0 and 2.1 Hz, 2H), 0.86 (s, 9H), 0.05 (s, 6H).

3.1.14. Ethyl (*E*)-5-((tert-butyldimethylsilyl)oxy)pent-2-enoate (120)

Sodium hydride (158.0 mg, 3.9 mmol) was dissolved in 6 mL of dry THF under nitrogen atmosphere at 0 °C and triethyl phosphonoacetate (783.0 µL, 3.9 mmol) was

added over 20 minutes to the solution. The reaction mixture was stirred at 0 °C for 40 minutes and the mixture was cooled to -78 °C and compound 118 solution in diethyl ether was added to the reaction mixture over 30 minutes. The reaction was slowly heated to 0 °C and stirred at 0 °C for 30 minutes. It was extracted with ammonium chloride solution the organic phase was washed with water (4x20 mL) and brine solution. The combined organic layer was dried with $MgSO_4$, filtered, and the filtrate was concentrated under reduced pressure. The residue was purified with SiO_2 column chromatography (EtOAc: Hexane 1:20) Rf = 0.70 (EtOAc: Hexane 1: 4) (28% yield, 260 mg) ^{1}H NMR (400 MHz, $CDCl_3$) δ 6.94 (dt, *J* = 14.2 ve 7.1 Hz, 1H), 5.84 (dd, *J* = 15.7 ve 1.6 Hz, 1H), 4.16 (q, *J* = 7.1 Hz, 2H), 3.70 (t, *J* = 6.5 Hz, 2H), 2.39 (dt, *J* = 8.0 and 6.1 Hz, 2H), 1.26 (t, *J* = 7.1 Hz, 4H), 0.87 (s, 9H), 0.03 (s, 6H).

3.1.15. (*E*)-5-((tert-butyldimethylsilyl)oxy)pent-2-enoic acid (121)

Ethyl (*E*)-5-((tert-butyldimethylsilyl)oxy)pent-2-enoate 120 (90 mg, 0.35 mmol) was dissolved in 3mL of methanol under nitrogen atmosphere and 1M NaOH solution (1.75 mL, 1.75 mmol) was added to the solution at 0 ºC. The reaction mixture was stirred under nitrogen atmosphere for 2 hours at 0 °C. The reaction mixture was neutralized with 0.5 M H_2SO_4 and the mixture was extracted with (3x 50mL) DCM. The combined organic layer was dried with $MgSO_4$, filtered, and the filtrate was concentrated under reduced pressure. The material was purified by SiO_2 column chromatography (EtOAc: Hexane: Acetic acid, 1: 4: 1%) Rf = 0.57 (EtOAc: Hexane: Acetic acid, 1: 4: 1%). NMR data showed the formation of transesterification product. ^{1}H NMR (400 MHz, $CDCl_3$) δ 6.96 (dt, J = 15.7, 7.1 Hz, 1H), 5.87 (dt, J = 15.7, 1.5 Hz, 1H), 3.72 (s, 1H), 3.71 (t, J = 6.5 Hz, 1H), 2.40 (ddd) , J = 13.6, 6.5, 1.5 Hz, 1H), 0.88 (s, 9H), 0.04 (s, 6H).

3.1.16. 3-(Benzyloxy)propan-1-ol (124)

Sodium hydride (1156.0 mg, 28.91 mmol) was dissolved in 6mL of dry THF under nitrogen atmosphere at 0°C and 1,3-propanediol (122**)** (950.0 µL, 13.14 mmol) was added slowly to the solution. The reaction mixture was stirred at 0 °C for 10 minutes and compound 123 (950.0 µL, 13.14 mmol) was added to the solution over 10 minutes. The reaction mixture was warmed to room temperature and stirred for 18 hours

and extracted with water and EtOAc (3x50mL) the organic phase was washed with water (4x20 mL). The combined organic layer was dried with $MgSO_4$, filtered, and the filtrate was concentrated under reduced pressure. The residue was purified with SiO_2 column chromatography (EtOAc: Hexane 1:3) Rf= 0.22 (EtOAc:Hexane,1:3) (36% yield, 788 mg) ^{1}H NMR (400 MHz, $CDCl_3$) δ 7.31 (s, 5H), 4.48 (s, 2H), 3.72 (td, *J* = 5.9 and 2.0 Hz, 2H), 3.61 (td, *J* = 5.9 and 2.2 Hz, 2H), 1.86 – 1.78 (m, 2H).

3.1.17. 3-(Benzyloxy)propanal (125)

Sodium acetate (350mg, 4.67mmol) was dissolved in 4mL dry DCM under nitrogen atmosphere 3-(benzyloxy)propan-1-ol 124 (788 mg, 4.74 mmol) was added on it. PCC (1121 mg, 5.2 mmol) was added on it in two portions at 0 ºC. The reaction mixture was stirred for 2 hours under nitrogen atmosphere at room temperature and diluted with 100 mL diethyl ether and stirred for a further 5 minutes. The reaction mixture was filtered through a (silica- magnesium sulfate and silica) mixture column with 300 mL diethyl ether. The resulting organic phase was extracted with 10% NaOH solution and brine solution. Combined organic phase was dried with $MgSO_4$ filtered and evaporated under reduced pressure until left about 20 mL of diethl ether. Product was used without purification. Rf= 0.57 (EtOAc: Hexane 1: 4)

3.1.18. Ethyl (*E*)-5-(benzyloxy)pent-2-enoate (126)

Sodium hydride (284 mg, 7.11 mmol) was dissolved in 6 mL of dry THF under nitrogen atmosphere at 0 °C and triethyl phosphonoacetate (1410 µL, 7.11 mmol) was added over 20 minutes to the solution. The reaction mixture was stirred at 0 °C for 40 minutes and the mixture was cooled to -78 °C and 3-(benzyloxy)propanal 119 solution in diethyl ether was added to the reaction mixture over 30 minutes. The reaction was slowly heated to 0 °C and stirred at 0 °C for 30 minutes. It was extracted with ammonium chloride solution the organic phase was washed with water (4x20 mL) and brine solution. The combined organic layer was dried with $MgSO_4$, filtered, and the filtrate was concentrated under reduced pressure. The residue was purified with SiO_2 column chromatography (EtOAc: Hexane 1:8) Rf = 0.54 (EtOAc: Hexane 1: 4) (31% yield, 344 mg) ^{1}H NMR (400 MHz, $CDCl_3$) δ .31 (s, 5H), 6.97 (dt, J = 15.7 ve 6.9 Hz,

1H), 5.88 (dt, J = 15.7 and 1.6 Hz, 1H), 4.49 (s, 2H), 4.16 (q, J = 7.1 Hz, 2H), 3.55 (t, J = 6.5 Hz, 2H), 2.49 (qd, J = 6.5 and 1.6 Hz, 2H), 1.26 (t, J = 7.1 Hz, 3H).

3.1.19. (*E*)-5-(benzyloxy)pent-2-enoic acid (127)

Ethyl (E)-5-(benzyloxy)pent-2-enoate 126 (344mg, 1.47mmol) was dissolved in 3 mL of dioxane under nitrogen atmosphere and 1M NaOH solution (2.94 mL, 2.94 mmol) was added to the solution at room temperature. The reaction mixture was stirred under nitrogen atmosphere for 3 hours at room temperature. The reaction mixture was concentrated under reduced pressure and extracted with water and diethyl ether (2 x 50mL). Water layer was acidified to pH 1.5 then extracted with diethyl ether (2 x 50mL). Both organic phases was washed with water and brine dried with $MgSO_4$, filtered, and the filtrate was concentrated under reduced pressure. Rf = 0.23 (EtOAc:Hexane:Acetic acid, 1:4:1%) (89% yield, 270 mg) ^{1}H NMR (400 MHz, $CDCl_3$) δ 7.36 (s, 5H), 7.12 (dt, J = 15.7 and 6.9 Hz, 1H), 5.92 (dt, J = 15.7 and 1.5 Hz, 1H), 4.54 (s, 2H), 3.61 (t, J = 6.4 Hz, 2H), 2.56 (qd, J = 6.5 and 1.5 Hz, 2H).

3.1.20. 1-Phenyl-2-(*1H*-1,2,4-triazol-1-yl)ethan-1-ol (144)

(R)-Styrene oxide was dissolved with dry THF then 1,2,4-triazole and K_2CO_3 was added on the reaction mixture at room temperature under nitrogen atmosphere.Then reaction mixture was heated up to 100 °C and stirred overnight. It was cooled to room temperature and 50 mL of cold water and EtOAc (3x50 mL) extraction was performed. Organic phase was washed with brine solution and dried with $MgSO_4$, filtered, and the filtrate was concentrated under reduced pressure. Rf = 0.43 (Chloroform:Methanol, 100:4) (86% yield, 405 mg) ^{1}H NMR (400 MHz, $CDCl_3$) δ 8.07 (s, 1H), 7.90 (s, 1H), 7.41 – 7.28 (m, 5H), 5.09 (dd, J = 8.5 and 3.3 Hz, 1H), 4.43 – 4.34 (m, 1H), 4.35 – 4.22 (m, 1H).

3.1.21. N-((1R,2R)-2-(3-chlorophenyl)-1-(4-chlorophenyl)-2-hydroxyethyl)-3,3-diethoxypropanamide (151)

Compound 150 (23 mg, 0,20 mmol), 2-(7-aza-*1H*-benzotriazole-1-yl)-1,1,3,3-tetramethyluronium hexafluorophosphate (HATU) (75 mg, 0,20 mmol) and N,N-

diisopropylethylamine (DIPEA) (61 µL, 0,36 mmol) was dissolved in 1 mL of dry DMF under nitrogen atmosphere. Compound 24 was dissolved with 1 mL of dry DMF in a two necked flask under nitrogen atmosphere then compound 150, HATU and DIPEA mixture was added over it. The reaction mixture was stirred for overnight. The reaction mixture was extracted with 100 mL of saturated $NaHCO_3$ X DCM (3X 30mL). Collected organic phase was extracted with 100 mL water whose pH arranged to 5 with 0.05 M H_2SO_4 solution. Combined organic phase was dried with $MgSO_4$ filtered and evaporated under reduced pressure. Rf = 0.59 (Chloroform:Methanol 100:4) (73% yield, 73 mg) ^{1}H NMR (400 MHz, $CDCl_3$) δ 7.56 – 6.68 (m, 8H), 5.17 (dd, J = 8.0, 3.9 Hz, 1H), 5.06 (dd, J = 8.0, 4.0 Hz, 1H), 4.95 (d, J = 3.8 Hz, 1H), 4.86 (d, J = 3.9 Hz, 1H), 3.51 – 3.47 (m, 1H), 3.41 (s, 1H), 1.07 (s, 3H), 1.03 (s, 3H).

3.1.22. N-((*1R,2R*)-2-(3-chlorophenyl)-1-(4-chlorophenyl)-2-hydroxyethyl)-2,2-dimethyl-3-oxopropanamide (156)

1,1,1-Tris(acetoxy)-1,1-dihydro-1,2-benziodoxol-3-(1H)-one (Dess−Martin periodinane) (49 mg, 0.12 mmol) was added in several portions to a stirred suspension of 155 (44 mg, 0.12 mmol) in wet DCM (4.0 mL of DCM/4.0 µL of water) at room temperature. The mixture was stirred for 2 h, diluted with diethyl ether (25.0 mL), and quenched by adding a solution of $Na_2S_2O_3$ (7 equiv) in saturated aqueous $NaHCO_3$ solution (25 mL) at room temperature. The mixture was stirred vigorously for 5 min, and the layers were separated. The aqueous layer was extracted with diethyl ether (40 mL). The organics were pooled, washed with saturated aqueous $NaHCO_3$ solution and brine, dried over $MgSO_4$, filtered, and the filtrate was concentrated. The crude material was used in the next step without further purification (50% yield, 22 mg) ^{1}H NMR (400 MHz, $CDCl_3$) δ 7.27 – 7.23 (m, 8H), 5.13 – 5.07 (m, 1H), 4.94 (s, 1H), 1.36 (dd, J = 4.4, 1.8 Hz, 6H).

3.1.23. Ethyl (*E*)-5-(((*1R,2R*)-2-(3-chlorophenyl)-1-(4-chlorophenyl)-2-hydroxyethyl)amino)-4,4-dimethyl-5-oxopent-2-enoate (157)

Lithium Chloride (52.8 mg, 0.47 mmol) was dissolved in 2 mL of dry acetonitrile under nitrogen gas at room temperature, then triethyl phosphonoacetate (83 µL, 0.42 mmol) , diisopropylethylamine (73 µL, 0.42 mmol) , and compound 156 was

added to this mixture. while dissolving in 2 mL of dry acetonitrile. The reaction mixture was stirred at room temperature overnight, then extracted with Ethyl Acetate (3x20 mL) and pH= 4 water. Combined organic phase was dried with $MgSO_4$ filtered and evaporated under reduced pressure. The organic layer was purified by SiO_2 column chromatography (1 Ethyl Acetate: 2 Hexane). Rf = 0.50 (1 Ethyl Acetate: 2 Hexane) ^1H NMR check was done compound is not pure but some of the signals could be belong the these compound so it was used next step.

3.1.24. *1H*-benzo[d][1,2,3]triazol-1-yl 2-acetoxybenzoate (160)

Compound 159 (300 mg, 116 mmol) was sissolved in 1 mL of dry DMF, then 2-(7-aza-*1H*-benzotriazole-1-yl)-1,1,3,3-tetramethyluronium hexafluorophosphate (HATU) (700 mg, 1,84 mmol) and N,N-diisopropylethylamine (DIPEA) (318 µL, 1,84 mmol) was added on the reaction mixture The reaction mixture was stirred for 2 hours under nitrogen atmosphere. The reaction mixture was extracted with 100 mL of 1.0 M HCl solution while tuning pH=7 and EtOAc (3X 30mL). Collected organic phase was extracted with 3x100 mL water. Combined organic phase was dried with $MgSO_4$ filtered and evaporated under reduced pressure. Rf = 0.47 (EtOAc: Hexane 1:1) The reaction mixture was used without purification.

3.1.25. Methyl 4-hydroxy-2-oxo-2H-chromene-3-carboxylate (161)

NaH (98,4 mg, 2,46 mmol,) was dissolved with 5.0 mL dry THF and dimethyl malonate (141 µl, 1,23 mmol) was added on it. Crude product of compound 160 was dissolved with 2.0 mL dry THF and added on the reaction mixture. The reaction mixture is stirred under nitrogen atmosphere for 2 hours at room temperature. Then THF was evaporated under reduced pressure yellowish solid was observed. It is washed with 100 ml of distilled water and taken into a separatory funnel. Acidify with 10 ml of concentrated HCL and extract with 75 ml of chloroform (25x3 ml). The collected organic phase is first washed with brian solution, then separated and dried with dry MgSO4. Collected organic phase was used in next step without evaporatio. Rf = 0.40 (Chloroform:Methanol 100:4) ^1H NMR (400 MHz, $CDCl_3$) δ 14.62 (s, 1H), 8.01 (dd, J = 8.0, 1.7 Hz, 1H), 7.69 (ddd, J = 8.4, 7.3, 1.6 Hz, 1H), 7.37 – 7.28 (m, 2H), 4.05 (s, 3H).

3.1.26. Methyl 2-oxo-4-(tosyloxy)-2H-chromene-3-carboxylate (162)

Compound 161 which was in the chlorofrm from previous step was used without evaporation. Firstly pTsCl (214 mg, 1.12 mmol) was added and then triethylamine was added (468 µl, 3,36 mmol) over the reaction mixture. Reaction mixture was stirred for about 48 hours. Then solvent was evaporated under reduced pressure. Residue was added on the SiO_2 column while attaching SiO_2. (EtOAc: Hexane 1:3) Rf = 0.40 (EtOAc: Hexane 1:1) (73% yield) ^{1}H NMR (400 MHz, $CDCl_3$) δ 7.85 (d, J = 8.3 Hz, 2H), 7.63 – 7.55 (m, 2H), 7.38 (d, J = 8.4Hz, 2H), 7.32 (d, J = 8.3 Hz, 1H), 7.23 (t, J = 7.4 Hz, 1H), 3.72 (s, 3H), 2.46 (s, 3H).

3.1.27. Methyl 2-oxo-4-((trimethylsilyl)ethynyl)-2H-chromene-3-carboxylate(164)

In a screw sealed tube, 6 mL of acetonitrile was degassed and then compound 162 (100.0 mg, 0.27 mmol) was dissolved in the solvent at room temperature. After that, Bis(triphenylphosphine)palladium dichloride (9.4 mg, 0.013 mmol), copper iodide (2.5 mg, 0.013 mmol), ethynyltrimethylsilane (45.0 µL, 0.324 mmol) and N,N-diisopropylethylamine (58.0 µL, 0.34 mmol) is added to the flask and mixed overnight. The reaction mixture is filtered through a column (10-15 cm) prepared with a silica gel-celite mixture with the help of ethyl acetate. The removed ethyl acetate layer was purified by column chromatography by removing the solvent under vacuum. (Hexane: EtOAc 1:3) Rf= 0.71 (Hexane: EtOAc 1:1) (28% Yield) ^{1}H NMR (400 MHz, $CDCl_3$) δ 7.89 (dd, J = 7.9, 1.6 Hz, 1H), 7.62 – 7.55 (m, 1H), 7.39 – 7.29 (m, 2H), 3.94 (s, 3H), 0.31 (s, 9H). ^{13}C NMR (400 MHz, $CDCl_3$) δ 163.84, 157.24, 153.20, 135.37, 133.38, 127.68, 124.92, 123.98, 117.45, 116.92, 115.82, 95.39, 52.91, 29.68, -0.58.

3.1.28. Methyl 4-ethynyl-2-oxo-2H-chromene-3-carboxylate (165)

Compound 164 (38.0 mg, 0.77 mmol) and acetic acid (300 µL, 5.24 mmol) are dissolved in 2 mL of dry THF at room temperature, then 1.0 M molar solution of tetrabutylammonium fluoride (TBAF) (39.6 µL, 0.132 mmol) in THF is added and the reaction is monitored with TLC and stirred for 25 minutes. The reaction mixture is extracted with 50 mL of saturated $NaHCO_3$ solution and 3x30 mL of ethyl acetate. After

the combined ethyl acetate layer was dried with $MgSO_4$, the solvent was removed under vacuum and purified by column chromatography (Hexane: EtOAc 1:3). Rf = 0.32 (Hexane: EtOAc 1:4) (73% Yield) ^{1}H NMR (400 MHz, $CDCl_3$) δ 7.95 – 7.92 (m, 1H), 7.61 (ddd, J = 8.2, 7.4, 1.6 Hz, 1H), 7.39 – 7.31 (m, 2H), 4.04 – 4.03 (m, 1H), 3.97 – 3.95 (s, 3H). ^{13}C NMR (400 MHz, $CDCl_3$) δ 163.69, 156.92, 153.19, 134.82, 133.63, 127.60, 125.06, 124.98, 117.40, 116.99, 95.03, 53.19.

3.1.29. Methyl 4-(1-(4-chlorobenzyl)-1H-1,2,3-triazol-4-yl)-2-oxo-2H-chromene-3-carboxylate (167)

Compound 165 (21.0 mg, 0.93 mmol) is dissolved in 2 mL dry DCM at room temperature, then 4-chlorobenzyl azide (16.29 mg, 0.097 mmol), copper iodide (0.35 mg, 0.0019 mmol)), N,N-diisopropylethylamine (1.30 mg, 0.00744 mmol) and acetic acid (0.52 μL, 0.0074 mmol) are added and the reaction is controlled with TLC and stirred for 2.5 hours. The reaction mixture is extracted with water and 3x30 mL of ethyl acetate, and the combined organic layers are washed with 50 mL of saturated $NaHCO_3$ solution. After the combined ethyl acetate layer was dried with $MgSO_4$, the solvent was removed under vacuum and purified by column chromatography. (Hexane: EtOAc 1:1) Rf= 0.64 (Hexane: EtOAc 1:4) (29% Yield) ^{1}H NMR (400 MHz, $CDCl_3$) δ 7.88 (dd, J = 8.1, 1.4 Hz, 1H), 7.84 (s, 1H), 7.63 – 7.56 (m, 1H), 7.40 – 7.35 (m, 3H), 7.31 – 7.23 (m, 3H), 5.60 (s, 2H), 3.64 (s, 3H). ^{13}C NMR (400 MHz, $CDCl_3$) δ 164.96, 157.82, 153.45, 141.11, 139.97, 135.22, 133.18, 132.48, 129.52, 129.40, 128.17, 125.17, 124.93, 121.14, 117.18, 117.12, 53.73, 53.00.

3.1.30. 4-(1-(4-chlorobenzyl)-1H-1,2,3-triazol-4-yl)-N-(4-fluorophenethyl)-2-oxo-2H-chromene-3-carboxamide (169)

Compound 167 (22.0 mg, 0.057 mmol) is dissolved in 3 mL of methanol at room temperature, then 4-fluorophenethylamine (9.0 μL, 0.068 mmol) is added and the reaction stirred overnight. The solvent of the reaction mixture is removed under vacuum and extracted with water and 3x30 mL of ethyl acetate. The combined ethyl acetate layer was dried with $MgSO_4$, the solvent was removed under vacuum and purified by column chromatography. (Hexane: EtOAc 2:1-1:1-1:2) Rf =0.20 (Hexane: EtOAc 1:2) (62% Yield) ^{1}H NMR (400 MHz, DMSO) δ 8.47 (d, J = 3.6 Hz, 1H), 7.92 (dd, J = 8.1,

1.5 Hz, 1H), 7.67 (ddd, J = 8.8, 6.3, 1.6 Hz, 1H), 7.48 (dd, J = 8.4, 1.0 Hz, 1H), 7.39 – 7.30 (m, 4H), 7.02 (d, J = 7.6 Hz, 3H), 5.72 (s, 2H), 3.32 (s, 3H). ^{13}C NMR (400 MHz, DMSO) δ 163.67, 163.58, 162.40, 160.00, 158.37, 153.19, 139.44, 139.27, 135.54, 135.02, 133.46, 133.09, 130.74, 130.66, 130.38, 129.18, 128.59, 127.25, 125.23, 124.98, 117.84, 117.15, 115.45, 115.24, 52.51, 34.13.

CHAPTER 4

CONCLUCISION

As the most commonly mutated gene in cancer, the tumor suppressor p53 gene is of great importance to cancer research. The MDM2 protein inhibits the transcriptional activation of the p53 protein expressed by the p53 gene in healthy cells. This control is essential for maintaining adequate p53 protein levels and cell survival in cells to enable normal cell cycle progression. Due to the fact that this equilibrium is disturbed and tumor growth develops when MDM2 protein is overexpressed as a result of mutation, studies on the design of compounds that are effective at inhibiting MDM2 protein are essential for the development of new anti-cancer target molecules.

The purpose of this project is to synthesize a new MDM2 inhibitor with a 1,4-oxazepan-5-one structure. As a starting material, (R)-(4-chlorophenyl)glycine was utilized for this purpose. This was reduced using $LiAlH_4$ and the amine was protected with a Trt group. After oxidation to aldehyde, direct or stepwise installation of glutaconic to the structure by either Michael type addition or coupling with amine by using HATU was rather difficult, and all attempts to create this skeleton were unsuccessful.

Additionally, coupling of protected 5-hydroxy-2-pentanoic acid to the chiral aminoalcohol and then cyclization via intramolecular oxa-Michael addition was also studied. However this route is also failed.

The objective of the second section of this thesis was to synthesize several 1,2,3-triazole-substituted coumarin in order to evaluate their potential antiproliferative effects on cancer cells. In these synthesis, acetylsalicylic acid was employed as the starting material. As crucial intermediates, they were converted to 4-acetylene-substituted coumarin derivatives, which were subsequently converted to the respective end products by 14% overall yield.

REFERENCES

Akkol, Esra Küpeli, Yasin Genç, Büşra Karpuz, Eduardo Sobarzo-Sánchez, and Raffaele Capasso. 2020. "Coumarins and Coumarin-Related Compounds in Pharmacotherapy of Cancer." *Cancers* 12 (7): 1–25. https://doi.org/10.3390/cancers12071959.

An, Ran, Zhuang Hou, Jian Teng Li, Hao Nan Yu, Yan Hua Mou, and Chun Guo. 2018. "Design, Synthesis and Biological Evaluation of Novel 4-Substituted Coumarin Derivatives as Antitumor Agents." *Molecules* 23 (9): 1–12. https://doi.org/10.3390/molecules23092281.

Binaschi, Monica, Andrea Boldetti, Maurizio Gianni, Carlo Alberto Maggi, Martina Gensini, Mario Bigioni, Massimo Parlani, et al. 2010. "Antiproliferative and Differentiating Activities of a Novel Series of Histone Deacetylase Inhibitors." *ACS Medicinal Chemistry Letters* 1 (8): 411–15. https://doi.org/10.1021/ml1001163.

Chunyuan Guo1, Guie Dong1, Xinling Liang2, Zheng Dong1, 1Department. 2017. "乳鼠心肌提取 HHS Public Access." *Physiology & Behavior* 176 (12): 139–48. https://doi.org/10.1002/cmdc.201500487.How.

Cochran, Brian M., Michael T. Corbett, Tiffany L. Correll, Yuan Qing Fang, Tawnya G. Flick, Siân C. Jones, Maria V. Silva Elipe, et al. 2019. "Development of a Commercial Process to Prepare AMG 232 Using a Green Ozonolysis-Pinnick Tandem Transformation." *Journal of Organic Chemistry* 84 (8): 4763–79. https://doi.org/10.1021/acs.joc.8b02390.

Ding, Qingjie, Zhuming Zhang, Jin Jun Liu, Nan Jiang, Jing Zhang, Tina M. Ross, Xin Jie Chu, et al. 2013. "Discovery of RG7388, a Potent and Selective P53-MDM2 Inhibitor in Clinical Development." *Journal of Medicinal Chemistry* 56 (14): 5979–83. https://doi.org/10.1021/jm400487c.

Elinos-Báez, C. M., F. León, and E. Santos. 2005. “Effects of Coumarin and 7OH-Coumarin on Bcl-2 and Bax Expression in Two Human Lung Cancer Cell Lines in Vitro.” *Cell Biology International* 29 (8): 703–8. https://doi.org/10.1016/j.cellbi.2005.04.003.

Emami, Saeed, and Sakineh Dadashpour. 2015. “Current Developments of Coumarin-Based Anti-Cancer Agents in Medicinal Chemistry.” *European Journal of Medicinal Chemistry* 102: 611–30. https://doi.org/10.1016/j.ejmech.2015.08.033.

Fang, Song Chwan, Chin Lin Hsu, Yu Shen Yu, and Gow Chin Yen. 2008. “Cytotoxic Effects of New Geranyl Chalcone Derivatives Isolated from the Leaves of Artocarpus Communis in SW 872 Human Liposarcoma Cells.” *Journal of Agricultural and Food Chemistry* 56 (19): 8859–68. https://doi.org/10.1021/jf8017436.

Fetzer, Damian E.L., Luis Ricardo S. Kanda, Lorenna Alves Xavier, Pollyanna Nogueira da Cruz, Massimiliano Errico, and Marcos L. Corazza. 2022. “Lipids and Coumarin Extraction from Cumaru Seeds (Dipteryx Odorata) Using Sequential Supercritical CO2+solvent and Pressurized Ethanol.” *Journal of Supercritical Fluids* 188 (July): 105688. https://doi.org/10.1016/j.supflu.2022.105688.

Gonzalez, Ana Z., John Eksterowicz, Michael D. Bartberger, Hilary P. Beck, Jude Canon, Ada Chen, David Chow, et al. 2014. “Selective and Potent Morpholinone Inhibitors of the MDM2-P53 Protein-Protein Interaction.” *Journal of Medicinal Chemistry* 57 (6): 2472–88. https://doi.org/10.1021/jm401767k.

Graves, Bradford, Thelma Thompson, Mingxuan Xia, Cheryl Janson, Christine Lukacs, Dayanand Deo, Paola Di Lello, et al. 2012. “Activation of the P53 Pathway by Small-Molecule-Induced MDM2 and MDMX Dimerization.” *Proceedings of the National Academy of Sciences of the United States of America* 109 (29): 11788–93. https://doi.org/10.1073/pnas.1203789109.

Haque, Ashanul, Ming Fa Hsieh, Syed Imran Hassan, Md Serajul Haque Faizi, Anannya Saha, Necmi Dege, Jahangir Ahmad Rather, and Muhammad S. Khan. 2017.

"Synthesis, Characterization, and Pharmacological Studies of Ferrocene-1H-1,2,3-Triazole Hybrids." *Journal of Molecular Structure* 1146: 536–45. https://doi.org/10.1016/j.molstruc.2017.06.027.

Hsieh, Jung Kuang, Florence S.G. Chan, Daniel J. O'Connor, Sibylle Mittnacht, Shan Zhong, and Lu Xin. 1999. "RB Regulates the Stability and the Apoptotic Function of P53 via MDM2." *Molecular Cell* 3 (2): 181–93. https://doi.org/10.1016/S1097-2765(00)80309-3.

Hu, Chunqi, Xin Li, Weisi Wang, Lei Zhang, Lulu Tao, Xiaowu Dong, Rong Sheng, Bo Yang, and Yongzhou Hu. 2011. "Design, Synthesis, and Biological Evaluation of Imidazoline Derivatives as P53-MDM2 Binding Inhibitors." *Bioorganic and Medicinal Chemistry* 19 (18): 5454–61. https://doi.org/10.1016/j.bmc.2011.07.050.

Kim, Do Hee, Ji Eun Park, In Gyeong Chae, Geumi Park, Soo Yeun Lee, and Kyung Soo Chun. 2017. "Isoliquiritigenin Inhibits the Proliferation of Human Renal Carcinoma Caki Cells through the ROS-Mediated Regulation of the Jak2/STAT3 Pathway." *Oncology Reports* 38 (1): 575–83. https://doi.org/10.3892/or.2017.5677.

Klein, C., and L. T. Vassilev. 2004. "Targeting the P53-MDM2 Interaction to Treat Cancer." *British Journal of Cancer* 91 (8): 1415–19. https://doi.org/10.1038/sj.bjc.6602164.

Kumar, K Ajay, Renuka Nagamallu, and Vasanth Kumar Govindappa. 2015. "Comprehensive Review on Coumarins : Molecules of Potential Chemical and Pharmacological Interest Comprehensive Review on Coumarins : Molecules of Potential Chemical and Pharmacological Interest." *Journal of Chemical and Pharmaceutical Research* 7 (9): 67–81.

Li, Xin Yu, Yuan Yuan Zu, Wei Ning, Ming Xu Tang, Chi Gong, Sheng Li Niu, and Hui Ming Hua. 2020. "A New Xanthyletin-Type Coumarin from the Roots of Peucedanum Praeruptorum." *Journal of Asian Natural Products Research* 22 (3): 287–94. https://doi.org/10.1080/10286020.2018.1551887.

Lin, Duoru, Jianhao Xiong, Congxin Liu, Lanqin Zhao, Zhongwen Li, Shanshan Yu, Xiaohang Wu, et al. 2021. “Application of Comprehensive Artificial Intelligence Retinal Expert (CARE) System: A National Real-World Evidence Study.” *The Lancet Digital Health* 3 (8): e486–95. https://doi.org/10.1016/S2589-7500(21)00086-8.

Liu, Yanli, Chunxiao Chu, Aiping Huang, Chunjing Zhan, Ying Ma, and Chen Ma. 2011. “Regioselective Synthesis of Fused Oxazepinone Scaffolds through One-Pot Smiles Rearrangement Tandem Reaction.” *ACS Combinatorial Science* 13 (5): 547–53. https://doi.org/10.1021/co2001058.

Lu, Shui Ming, and Howard Alper. 2005. “Intramolecular Carbonylation Reactions with Recyclable Palladium-Complexed Dendrimers on Silica: Synthesis of Oxygen, Nitrogen, or Sulfur-Containing Medium Ring Fused Heterocycles.” *Journal of the American Chemical Society* 127 (42): 14776–84. https://doi.org/10.1021/ja053650h.

Luthar, Suniya, Dante Cicchetti, and Bronwyn Becker. 2000. “基因的改变NIH Public Access.” *Child Development* 73 (3): 543–562. https://doi.org/10.1146/annurev.pharmtox.48.113006.094723.Small-Molecule.

Malini, B., A. Purohit, D. Ganeshapillai, L. W.L. Woo, B. V.L. Potter, and M. J. Reed. 2000. “Inhibition of Steroid Sulphatase Activity by Tricyclic Coumarin Sulphamates.” *Journal of Steroid Biochemistry and Molecular Biology* 75 (4–5): 253–58. https://doi.org/10.1016/S0960-0760(00)00178-3.

Molnar, Maja, Melita Lončarić, and Marija Kovač. 2020. *Green Chemistry Approaches to the Synthesis of Coumarin Derivatives*. *Current Organic Chemistry*. Vol. 24. https://doi.org/10.2174/1385272824666200120144305.

Moreira, Joana, Joana Almeida, Lucília Saraiva, Honorina Cidade, and Madalena Pinto. 2021. “Chalcones as Promising Antitumor Agents by Targeting the P53 Pathway: An Overview and New Insights in Drug-Likeness.” *Molecules* 26 (12).

https://doi.org/10.3390/molecules26123737.

Mugunthan, Kayalvili, Treasure Mcguire, and Paul Glasziou. 2011. “Minimal Interventions to Decrease Long-Term Use of Benzodiazepines in Primary Care.” *British Journal of General Practice*, no. September: 573–78. https://doi.org/10.3399/bjgp11X593857.Conclusion.

Nahmany, Moshe, and Artem Melman. 2001. “Facile Acylation of Sterically Hindered Alcohols through Ketene Intermediates.” *Organic Letters* 3 (23): 3733–35. https://doi.org/10.1021/ol0166855.

Nemallapudi, Bakthavatchala Reddy, Dinneswara Reddy Guda, Nagarjuna Ummadi, Balakrishna Avula, Grigory V. Zyryanov, Cirandur Suresh Reddy, and Sravya Gundala. 2020. “New Methods for Synthesis of 1,2,3-Triazoles: A Review.” *Polycyclic Aromatic Compounds* 0 (0): 1–19. https://doi.org/10.1080/10406638.2020.1866038.

Odlo, Kristin, Jean Hentzen, Jérémie Fournier dit Chabert, Sylvie Ducki, Osman A.B.S.M. Gani, Ingebrigt Sylte, Martina Skrede, Vivi Ann Flørenes, and Trond Vidar Hansen. 2008. “1,5-Disubstituted 1,2,3-Triazoles as Cis-Restricted Analogues of Combretastatin A-4: Synthesis, Molecular Modeling and Evaluation as Cytotoxic Agents and Inhibitors of Tubulin.” *Bioorganic and Medicinal Chemistry* 16 (9): 4829–38. https://doi.org/10.1016/j.bmc.2008.03.049.

Ouellet, G, Danny Gauvreau, Mark Cameron, Sarah Dolman, Louis-charles Campeau, Gregory Hughes, Paul D O Shea, and Ian W Davies. 2012. “Convergent, Fit-For-Purpose, Kilogram-Scale Synthesis of a 5-Lipoxygenase Inhibitor,” 4–9.

Peterson, Laura B., and Brian S.J. Blagg. 2010. “Click Chemistry to Probe Hsp90: Synthesis and Evaluation of a Series of Triazole-Containing Novobiocin Analogues.” *Bioorganic and Medicinal Chemistry Letters* 20 (13): 3957–60. https://doi.org/10.1016/j.bmcl.2010.04.140.

Rew, Yosup, and Daqing Sun. 2014. “Discovery of a Small Molecule MDM2 Inhibitor

(AMG 232) for Treating Cancer." *Journal of Medicinal Chemistry* 57 (15): 6332–41. https://doi.org/10.1021/jm500627s.

Rew, Yosup, Daqing Sun, Felix Gonzalez-Lopez De Turiso, Michael D. Bartberger, Hilary P. Beck, Jude Canon, Ada Chen, et al. 2012. "Structure-Based Design of Novel Inhibitors of the MDM2-P53 Interaction." *Journal of Medicinal Chemistry* 55 (11): 4936–54. https://doi.org/10.1021/jm300354j.

Shinohara, Tokuyuki, and Motonari Uesugi. 2007. "In-Vivo Activation of the P53 Pathway by Small-Molecule Antagonists of MDM2." *Tanpakushitsu Kakusan Koso. Protein, Nucleic Acid, Enzyme* 52 (13 Suppl): 1816–17.

Silva, Jerson L., Carolina G.S. Lima, Luciana P. Rangel, Giulia D.S. Ferretti, Fernanda P. Pauli, Ruan C.B. Ribeiro, Thais De B. Da Silva, Fernando C. Da Silva, and Vitor F. Ferreira. 2020. *Recent Synthetic Approaches towards Small Molecule Reactivators of P53*. *Biomolecules*. Vol. 10. https://doi.org/10.3390/biom10040635.

Sławińska-Brych, Adrianna, Barbara Zdzisińska, Magdalena Dmoszyńska-Graniczka, Witold Jeleniewicz, Jacek Kurzepa, Mariusz Gagoś, and Andrzej Stepulak. 2016. "Xanthohumol Inhibits the Extracellular Signal Regulated Kinase (ERK) Signalling Pathway and Suppresses Cell Growth of Lung Adenocarcinoma Cells." *Toxicology* 357–358: 65–73. https://doi.org/10.1016/j.tox.2016.06.008.

Smits, Rogier A., Herman D. Lim, Bart Stegink, Remko A. Bakker, Iwan J.P. De Esch, and Rob Leurs. 2006. "Characterization of the Histamine H4 Receptor Binding Site. Part 1. Synthesis and Pharmacological Evaluation of Dibenzodiazepine Derivatives." *Journal of Medicinal Chemistry* 49 (15): 4512–16. https://doi.org/10.1021/jm051008s.

Soto-Ortega, Deborah D., Brandon P. Murphy, Francisco J. Gonzalez-Velasquez, Kelly A. Wilson, Fang Xie, Qian Wang, and Melissa A. Moss. 2011. "Inhibition of Amyloid-β Aggregation by Coumarin Analogs Can Be Manipulated by Functionalization of the Aromatic Center." *Bioorganic and Medicinal Chemistry*

19 (8): 2596–2602. https://doi.org/10.1016/j.bmc.2011.03.010.

Sun, Daqing, Zhihong Li, Yosup Rew, Michael Gribble, Michael D. Bartberger, Hilary P. Beck, Jude Canon, et al. 2014. "Discovery of AMG 232, a Potent, Selective, and Orally Bioavailable MDM2-P53 Inhibitor in Clinical Development." *Journal of Medicinal Chemistry* 57 (4): 1454–72. https://doi.org/10.1021/jm401753e.

Synthesis, Metal-free. 2022. "N. T. Pokhodylo" 58 (2): 209–18.

Urbagarova, Bayarma M., Elvira E. Shults, Vasilii V. Taraskin, Larisa D. Radnaeva, Tatyana N. Petrova, Tatyana V. Rybalova, Tatyana S. Frolova, Andrey G. Pokrovskii, and Jamsranjav Ganbaatar. 2020. "Chromones and Coumarins from Saposhnikovia Divaricata (Turcz.) Schischk. Growing in Buryatia and Mongolia and Their Cytotoxicity." *Journal of Ethnopharmacology* 261 (December 2019): 112517. https://doi.org/10.1016/j.jep.2019.112517.

Valizadeh, Hassan, and Sevil Vaghefi. 2009. "One-Pot Wittig and Knoevenagel Reactions in Ionic Liquid as Convenient Methods for the Synthesis of Coumarin Derivatives." *Synthetic Communications* 39 (9): 1666–78. https://doi.org/10.1080/00397910802573163.

Vekariya, Rajesh H., and Hitesh D. Patel. 2014. "Recent Advances in the Synthesis of Coumarin Derivatives via Knoevenagel Condensation: A Review." *Synthetic Communications* 44 (19): 2756–88. https://doi.org/10.1080/00397911.2014.926374.

Vu, Binh, Peter Wovkulich, Giacomo Pizzolato, Allen Lovey, Qingjie Ding, Nan Jiang, Jin Jun Liu, et al. 2013. "Discovery of RG7112: A Small-Molecule MDM2 Inhibitor in Clinical Development." *ACS Medicinal Chemistry Letters* 4 (5): 466–69. https://doi.org/10.1021/ml4000657.

Wade, Mark, Yao Cheng Li, and Geoffrey M. Wahl. 2013. "MDM2, MDMX and P53 in Oncogenesis and Cancer Therapy." *Nature Reviews Cancer*. https://doi.org/10.1038/nrc3430.

Wang, Hongbo, and Chunhong Yan. 2011. “A Small-Molecule P53 Activato Induces Apoptosis through Inhibiting MDMX Expression in Breast Cancer Cells1,2.” *Neoplasia* 13 (7): 611–19. https://doi.org/10.1593/neo.11438.

Wang, Shaomeng, Yujun Zhao, Angelo Aguilar, Denzil Bernard, and Chao Yie Yang. 2017. “Targeting the MDM2-P53 Protein-Protein Interaction for New Cancer Therapy: Progress and Challenges.” *Cold Spring Harbor Perspectives in Medicine* 7 (5): 1–10. https://doi.org/10.1101/cshperspect.a026245.

Wang, Siyu, Kai Jia, Jiajia Cheng, Yu Chen, and Yaofeng Yuan. 2017. “Dual Roles of Substituted Thiourea as Reductant and Ligand in CuAAC Reaction.” *Tetrahedron Letters* 58 (38): 3717–21. https://doi.org/10.1016/j.tetlet.2017.08.029.

Wang, Ziyu, Xuejie Zhu, Shengnan Zuo, Ming Chen, Cong Zhang, Chenyu Wang, Xiaodong Ren, et al. 2020. “27%-Efficiency Four-Terminal Perovskite/Silicon Tandem Solar Cells by Sandwiched Gold Nanomesh.” *Advanced Functional Materials* 30 (4). https://doi.org/10.1002/adfm.201908298.

Yang, Qian, Hong Cao, Al Robertson, and Howard Alper. 2010. “Synthesis of Dibenzo[b, f][1,4]Oxazepin-11(10 H)-Ones via Intramolecular Cyclocarbonylation Reactions Using PdI2/Cytop 292 as the Catalytic System.” *Journal of Organic Chemistry* 75 (18): 6297–99. https://doi.org/10.1021/jo101312z.

Yao, Dahong, Dabo Pan, Yongqi Zhen, Jian Huang, Jinhui Wang, Jin Zhang, and Zhendan He. 2020. “Ferulin C Triggers Potent PAK1 and P21-Mediated Anti-Tumor Effects in Breast Cancer by Inhibiting Tubulin Polymerization in Vitro and in Vivo.” *Pharmacological Research* 152 (December 2019): 104605. https://doi.org/10.1016/j.phrs.2019.104605.

Zhang, Wenjuan, Zhi Li, Meng Zhou, Feng Wu, Xueyan Hou, Hao Luo, Hao Liu, et al. 2014. “Synthesis and Biological Evaluation of 4-(1,2,3-Triazol-1-Yl)Coumarin Derivatives as Potential Antitumor Agents.” *Bioorganic and Medicinal Chemistry Letters* 24 (3): 799–807. https://doi.org/10.1016/j.bmcl.2013.12.095.

VITA

Tuğçe Akbaş

Education:

2015-2023 Izmir Institute of Technology, Chemistry Ph.D

2013-2016 Izmir Institute of Technology, Chemistry M.Sc

2010-2011 Universitat Rovira i Virgili, Chemistry B.Sc (Erasmus)

2007-2012 Izmir Institute of Technology, Chemistry B.Sc

Work Experineces:

Teaching and Research Assistant at Izmir Institute of Technology, Department of Chemistry (2014- continue)

Internship at Izmir Criminal Laboratory (July 2011-August 2011)

Internship at Balıkesir University, Science and Technology Application and Research Center (July 2010-August 2010)

Publications

Tuğçe Kanbur, Murat Kara, Meltem Kutluer, Ayhan Şen, Murat Delman, Aylin Alkan, Hasan Ozan Otaş, İsmail Akçok, Ali Çağır, CRM1 inhibitory and antiproliferative activities of novel 4′-alkyl substituted klavuzon derivatives, Bioorganic & Medicinal Chemistry **2017**, Volume 25, Issue 16, Pages 4444-4451, ISSN 0968-0896,

Murat Delman, Sanem Tercan Avcı, İsmail Akçok, Tuğçe Kanbur, Esra Erdal, Ali Çağır,Antiproliferative activity of (R)-4′-methylklavuzon on hepatocellular carcinoma cells and EpCAM+/CD133+ cancer stem cells via SIRT1 and Exportin-1 (CRM1) inhibition, European Journal of Medicinal Chemistry **2019**, Volume 180, 2019,Pages 224-237, ISSN 0223-5234,

H.Y. Khan, Y. Li, A. Aboukameel, G. Mpilla, R. Sexton, T. Kanbur, H. Cetinkaya, A. Cagir, M.N. Al-Hallak, A. Sukari, A.S. Azmi, M. Nagasaka, A10 A Novel Inhibitor for KRASG12C Mutant Lung Carcinoma, Journal of Thoracic Oncology **2020**, Volume 15, Issue 2, Supplement,2020,Page S15, ISSN 1556-0864,

Academic Activities:

Kanbur, T., Çağır, A., (2016, July). Syntheses Of Novel 4'-Alkyl Substıtuted Klavuzon Derivatives. Poster Presentation, 7th European Colloquium on Heterocyclic Chemistry Amsterdam, The Netherlands.

Kanbur, T., (2015, September). Participant, Turkey Symposium Series: Catalysis and Sensing for Health Symposium at Izmir Institute of Technology, Izmir, Turkey.

Kanbur, T., (2014, March). Participant, International Drug Chemistry Conference, Antalya.,Turkey.

Kanbur, T., (2013, September). Participant, Advanced Materials World Congress, İzmir, Turkey.